

UNIVERSITA' DEGLI STUDI DI PALERMO

Dipartimento di Scienze della Terra e del Mare

FACIES HETEROGENEITY AND SEDIMENTARY
PROCESSES ALONG A TECTONICALLY-CONTROLLED
CARBONATE SLOPE: A CASE STUDY FROM THE
CRETACEOUS OF WESTERN SICILY (ITALY)

Vincenzo Randazzo

Ph.D. thesis

Palermo, Italy
February 27, 2020



UNIVERSITÀ DEGLI STUDI DI PALERMO

Dipartimento di Scienze della Terra e del Mare (DiSTeM)

Dottorato di Ricerca in Scienze della Terra e del Mare

FACIES HETEROGENEITY AND SEDIMENTARY
PROCESSES ALONG A TECTONICALLY-CONTROLLED
CARBONATE SLOPE: A CASE STUDY FROM THE
CRETACEOUS OF WESTERN SICILY (ITALY)

DOTTORANDO
Dr. Vincenzo Randazzo

TUTOR
Prof. Pietro Di Stefano

XXXII CICLO - ANNO ACCADEMICO 2018 - 2019

DOTTORATO



*Little by little,
one travels far.*

J.R.R. Tolkien

Table of Content

Extended abstract	4
1. Introduction	8
1. Carbonate slopes.....	8
2. Carbonate VS siliciclastic slopes	9
3. Sediment gravity-flow deposits and transport mechanisms	12
4. The Cretaceous of Sicily	17
5. Structure of the PhD thesis	19
2. Carbonate slope re-sedimentation in a tectonically-active setting (Western Sicily Cretaceous Escarpment, Italy).....	21
1. Introduction	23
2. Geological and stratigraphic setting	25
3. Methodology	28
4. Facies Analysis	30
4.1. <i>FA - Facies Association A (FA)</i>	32
4.2. <i>Facies Association B (FB)</i>	32
4.3. <i>Facies Association C (FC)</i>	37
4.4. <i>Facies Association D (FD)</i>	46
5. Facies stacking.....	49
5.1. <i>Western Mount Sparagio</i>	52
5.2. <i>Eastern Mount Sparagio</i>	54
5.3. <i>Mount Monaco</i>	55
5.4. <i>Custonaci</i>	56
6. Discussion.....	57
6.1 <i>Volcanic intercalations</i>	57
6.2. <i>Physiography of the Western Sicily Cretaceous Escarpment</i>	58
6.3. <i>Source area and evolution of the Western Sicily Cretaceous Escarpment</i>	60
6.4. <i>Comparison with other tectonically-controlled carbonate margins</i>	66
6.5 <i>Palaeogeographic and geodynamic scenario</i>	67
7. Conclusions	70
References	72

3. A Cretaceous Carbonate Escarpment from Western Sicily (Italy): biostratigraphy and tectono-sedimentary evolution	88
1. Introduction	90
2. Geological setting	92
3. Material and methods	94
4. Lithostratigraphy.....	95
4.1 Unit A [<i>Calpionellid/Crescentiella</i> limestones (Tithonian-lowermost Cretaceous p.p.)]....	95
4.2 Unit B [<i>Ellipsactinia breccias</i> (Lower Cretaceous p.p.)]	96
4.3 Unit C [<i>Rudist breccias</i> (Lower Cretaceous p.p.-Upper Cretaceous p.p.)]	97
4.4 Unit D [<i>Scaglia-type calcilutites interbedded with calcidebrites</i> (Senonian)]	99
5. Biostratigraphy and microfacies analysis	100
5.1 Biozone 1.....	102
5.2 Biozone 2.....	102
5.3 Biozone 3.....	105
5.4 Biozone 4.....	106
5.5 Biozone 5.....	106
5.6 Biozone 6.....	108
5.7 Biozone 7.....	109
5.8 Biozone 8.....	109
6. Discussion.....	111
6.1 Biozone 1 (Kimmeridgian-Berriasian)	111
6.2 Biozone 2 (Valanginian-Aptian?).....	112
6.3 Biozone 3 (lower Albian)	113
6.4 Biozone 4 (upper Cenomanian p.p.).....	113
6.5 Biozone 5 (uppermost Cenomanian/lowermost Turonian)	114
6.6 Biozone 6 (Coniacian)	114
6.7 Biozone 7 (Santonian).....	115
6.8 Biozone 8 (Campanian-Maastrichtian)	115
6.9 Age of extraclasts occurring in the allochthonous carbonate deposits	116
7. Conclusions	121
References	123
4. General conclusions.....	127
References	130

Acknowledgments

I would like to sincerely thank all those people, who supported me during the last three years in so many different ways. It's impossible to mention everyone and summarize my gratitude within a few lines, but I'll try to do my best.

I am thankful to my fiancée Viviana, to my mom and dad and to all those people who are my friends or who just were there for me during the last three years. I'll mention just some of them: Marcella, Salvatore, Ambra, Francesco V., Francesco P., Eleonora, Andrea, Alessandra, Mauro, Simona T., Elisabetta, Nicolò, Walter, Simona P., Noemi, Massimo, Sabrina and Zio Filippo. Thanks to all the rest and please forgive me if you are not mentioned explicitly.

Many thanks to Professor Dr. John Reijmer, Dr. Alex Hairabian, Dr. Arnoud Sloodman, Dr. Jalel Jaballah and Dr. Johan Le Goff from the College of Petroleum and Minerals at the King Fahd University of Dhahran (Saudi Arabia) for treating me as a staff member and never as a guest. This outstanding research group made a decisive contribution to my work and to my personal growth. Thanks also to Ghazi and all the KFUPM staff for their hospitality. I will never forget my stay in Middle-East.

Thanks to Professor Dr. Andrea Mindszenty, Dr. Gianni Mallarino and Dr. Szilvia Kövér for their hospitality during the three months stage at Eötvös Loránd University of Budapest (Hungary) and for their stimulating comments and criticism on my work.

Many thanks to the owners and the staff members of the quarries and marble sawmills and in particular Pellegrino, Bova, Maiorana, Santoro, Bellanova and Miceli industries of the Custonaci area for their permission to access the properties and facilities.

Due thanks are also given to the staff of the Department of Earth and Marine Sciences (DiSTeM) of the University of Palermo and, in particular, to Maria Cannilla and Mattia Butera.

I am thankful to Dr. Simona Todaro (DiSTeM) and Dr. Simona Cacciatore (ENI) for always being ready to help and advise and for being examples to follow.

Last but not least, my biggest thanks go to my supervisor Professor Pietro Di Stefano who gave me the opportunity to initiate this research project and write this thesis. I am indebted to him for his continuous help, support, and invaluable scientific input. He pushed me beyond my limits leading me to grow up and achieving personal and professional results that I would never have dreamed to. I know this can't be enough, but thanks.

Extended abstract

The PhD study focuses on the sedimentological and biostratigraphic characterization of Cretaceous slope limestones cropping out in the Capo San Vito Peninsula (north-westernmost Sicily). The collected data allow to reconstruct the sedimentary evolution of a debris-dominated escarpment (Western Sicily Cretaceous Escarpment, WSCE) and to assess the main trigger mechanisms of the gravity-flow sediments. At present the original escarpment is dismembered in several tectonic units in the Maghrebian Chain and the Tertiary deformations have obscured the relationships of the slope with the original source area. Nevertheless, a tight correlation exists between the evolution of the Cretaceous Panormide Platform and the studied slope allowing to put forward an interpretation of the evolutionary history of this carbonate system.

The topic of this PhD study was selected on the basis of three main objectives: (i) several contributions have shown that sea-level variations and tectonic processes are major mechanisms influencing the development of carbonate platforms, sediment production and sediment export. Nevertheless, it is still challenging to assess the influence of sea-level variations and tectonics when dealing with carbonate systems. The presence of submarine volcanic intercalations along the WSCE succession is a strong evidence of a dominant tectonic control, although the influence of sea-level fluctuations is not ruled out totally. In this respect, the study provides new insights in understanding sedimentary dynamics along tectonically-controlled carbonate slopes. (ii) The Cretaceous slope carbonates have a great economic significance for the oil industry, since they are considered as excellent carbonate reservoirs. In particular, the Cretaceous slope limestones are typically rich in rudist aragonite fragments determining high percentages of porosity. The detailed study of outcrop analogues of these depositional systems can offer examples for the prediction of the geometry and distribution of the most productive facies types. As far as Italy, the outcrop examples of the Maiella and Gargano Cretaceous escarpments have been fully described by many authors representing

“training areas” for generations of petroleum geologists. In this respect, the studied depositional system represents a further and new detailed outcrop analogue for carbonate slope reservoir. (iii) Last but not least, although these rocks are mentioned in several papers dealing with regional geology or geological mapping of Sicily, this PhD thesis provides an original sedimentological and biostratigraphic contribution concerning the Cretaceous slope limestones from the Capo San Vito Peninsula (Western Sicily) and their meaning in the frame of the palaeogeographic evolution of the central Mediterranean area.

The resedimented carbonates from the WSCE are intensely exploited as ornamental stones since the past century and commercially known as “Perlato di Sicilia”. The wire-cut walls of a number of quarries in the study area allowed to study in detail the facies architecture along the slope. The outstanding exposure of the studied outcrops allowed also to observe and describe carefully many sedimentary structures such as metre-scale slump scars and pinch-out geometries. Despite tertiary tectonics, these sedimentary structures as well as several synsedimentary faults enabled to put forward a well-constrained hypothesis about the palaeoslope direction.

A new 3D comparative slope model based on the observed facies and their distribution along the studied sedimentary system is among the main outputs of the PhD study. Eleven different facies types grouped in four facies associations have been differentiated along the WSCE through detailed logs and correlations of selected sections cropping out in different tectonic units of the study area. The facies associations allowed to define the sedimentary evolution of the slope throughout the Cretaceous, thus reflecting in turn specific depositional settings: from platform margin/slope transition, talus, toe of slope and basin, while the oldest Cretaceous facies are indicative of a carbonate ramp. Most common facies types mainly consist of well-bedded or massive and chaotic megabreccia bodies whose matrix consists of skeletal packstone to rudstone mainly made of rudist fragments. These calciclastic deposits have been interpreted as Mass Transport Deposits (MTDs). Moreover, a genetic link to

specific resedimentation processes has been proposed. Well-bedded megabreccias often exhibit an evident inverse to normal gradation. Finer grained levels on the top are interpreted as the result of the deposition of the turbid cloud generated by the movement of the debris flow along the slope. Conversely, neither bedding nor gradation have been observed within massive bodies of chaotic megabreccias. The most evident feature of this facies is the high heterogeneity of the grain size spanning from few centimetres to some metres. Moreover, the chaotic megabreccias are usually located above or below the volcanic outcrops suggesting a tight relation between this facies type and seismo-tectonic processes.

Besides the description and interpretation of the sedimentary features of the Cretaceous carbonate slope, a consistent part of the PhD study focuses on the bio-chronostratigraphic characterization of the facies successions representing the whole depositional system. Eight informal biozones have been defined that provide a confident chronostratigraphic frame that allows to define the different steps of the evolution of the slope throughout the Cretaceous. Moreover, the reconstruction of the sedimentary evolution of this depositional system provided important insights about the geodynamic and paleogeographic frame of the western Tethys during Cretaceous times.

A sharp contact between calpionellid wackestone and the overlying *Ellipsactinia* breccias characterized the lowermost part of the WSCE. Such an abrupt stratigraphic boundary is interpreted as a result of the conversion from a gentle ramp to a steep escarpment and it has been referred to the Berriasian/Valanginian. Upward, the *Ellipsactinia* calcidebrites show a gradual transition to rudist calcidebrites. The repeated emplacement of thick chaotic megabreccia bodies followed during the Aptian-Cenomanian interval. A major downslope shedding of skeletal debris occurred in the upper part of the same interval. The resulting facies consists of floatstones/rudstones bearing orbitolinids and rudists. The widespread occurrence of such facies is interpreted as the response, in slope setting, to the high productivity rate of the adjacent Panormide carbonate platform at that time. On the other hand, chaotic

megabreccia bodies could account for periods of major tectonic instability tied to the activation of crustal faults as suggested by the occurrence of volcanic intercalations. The latter mainly consist of pillow basalts and tuffites that have been constrained to the Albian-Cenomanian interval. The volcanic activity, along with the other evidences of tectonic deformations, points out to an intense extensional phase experienced by the WSCE as well as by the Panormide Platform, during Cretaceous times. These extensional phenomena are interpreted as being the northern expression of the coeval tectonic subsidence experienced by the Sirt Basin. The Panormide Platform has been interpreted as a continental bridge linking Africa and Adria during the Cretaceous. Therefore, the events recorded by the study area are fundamental to the understanding of the geodynamic evolution of this sector of the western Tethys. In particular, the oldest volcanic eruption documented in the WSCE, could indicate the beginning of the dismemberment and the progressive drowning of discrete sectors of the Panormide Platform. From the latest Cenomanian onward, the overlap of coarse gravity-flow deposits on facies typical of platform margin suggests a severe phase of tectonic dismantling of the WSCE source area. This stratigraphic evidence, coupled with the clastic and intrabasinal carbonate supply recorded in the uppermost Senonian may account for a severe tectonic backstepping of the platform taking place during the Late Cretaceous. Notwithstanding, the resedimentation pulses lasted at least up to the Maastrichtian thus indicating the ongoing carbonate production in small isolated patches.

1. Introduction

1. Carbonate slopes

Thick sequences of sediment gravity-flow deposits form carbonate slopes extending from the shelf margin tens of kilometres out into the basin (Cook and Mullins, 1983; Enos and Moore, 1983; Mullins and Cook, 1986). These sedimentary systems are the subject of several contributions from present-day (e.g. Bahamas, see Fig. 1 - Hine and Neumann, 1971; Schlager and Ginsburg, 1981; Reijmer et al., 2009; Jo et al., 2015; Principaud et al., 2015; Tournadour et al., 2015; Wunsch et al., 2016; Mulder et al., 2017 among others) and ancient examples from different regions of the world, such as the Cambrian and Silurian in Greenland (Surlyk and Ineson, 1987; Surlyk and Ineson, 1992; Ineson and Surlyk, 1995), the Frasnian in the Canadian Rocky Mountains (McLean and Mountjoy, 1993; Mountjoy and Becker, 2000; Whalen et al., 2000), the Carboniferous of the Pre-Caspian Basin (Weber et al., 2003; Kenter et al., 2005) and the Cretaceous of Albany (Le Goff et al., 2015; Le Goff et al., 2019) and Italy (Maiella and Gargano, Eberli et al., 1993; Neri, 1993; Neri and Luciani, 1994; Vecsei, 1998; Graziano, 2000; Morsilli et al., 2004; Rusciadelli et al., 2003; Rusciadelli, 2005; Hairabian et al., 2015; Rustichelli et al., 2017). Carbonate slopes are the result of many interacting processes (e.g. climate, sea-level changes, exposure with respect to the dominant winds, oceanic circulation, lateral continuity of the reef barrier, earthquakes) influencing the production of sediment on the source area and the export toward the basin (Cook et al., 1972; Haak and Schlager, 1989; Reijmer et al., 1992, 2012, 2015a, 2015b; Tournadour et al., 2017). It is therefore by no means surprising that gravity-flow deposits may provide a wealth of information about the growth, evolution, and depositional conditions of the carbonate platform (Crevello and Schlager, 1980; Everts, 1991; Playton et al., 2010). However, academic attention for carbonate slopes revolves around the interests of oil industries (Payros and Pujalte, 2008). In particular, Cretaceous slope successions are known to host giant hydrocarbon reservoirs such as the Poza

Rica field in Mexico (Enos, 1977; 1985; Enos and Stephens; 1993; Loucks et al., 2010) and the Apulian oilfields in Italy (Beckett et al., 1996; Jagiello et al., 1996; Casabianca et al., 2002).

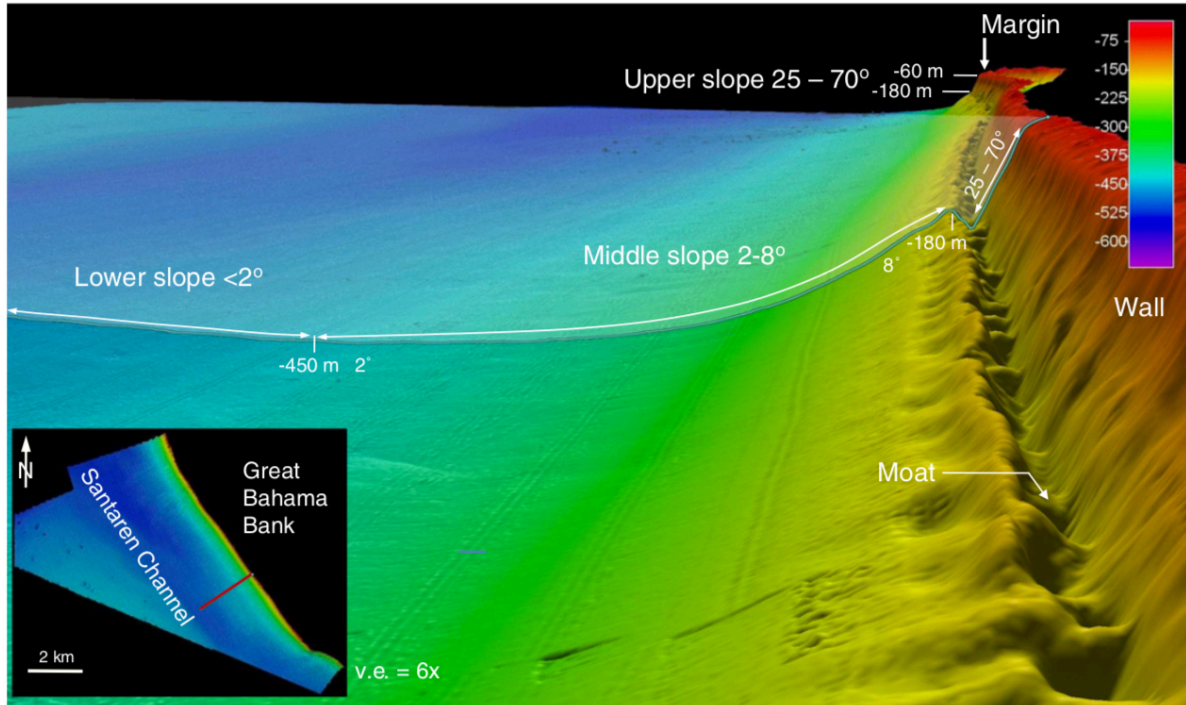


Fig. 1. 3D view along southwestern Great Bahama Bank displaying the slope morphology. V.E. stands for Vertical Exaggeration (from Jo et al., 2015).

2. Carbonate VS siliciclastic slopes

A comparison between carbonate slopes and their siliciclastic counterparts has been attempted by several authors (Schlager and Camber, 1986; Schlager, 1991, 1992; Bosellini, 1992; Spence and Tucker, 1997; Adams and Kenter, 2013 among others). Playton et al. (2010) provide an exhaustive tabled summary of the main features differentiating carbonate and siliciclastic slopes. Both carbonate and siliciclastic systems may exhibit similar slope curvatures (linear, exponential, and Gaussian profiles) as well as the predominance of specific grain-size classes building mud-, grain- and debris-dominated slopes (Adams and Kenter, 2013). However, the location of sediment generation and supply is a fundamental difference between carbonate and siliciclastic slopes, affecting the general morphologies of such depositional

systems (Spence and Tucker, 1997). Accordingly, two main different models have been proposed: a fan model for siliciclastic slopes (Walker, 1966; Mutti and Ricci Lucchi, 1972) and an apron model for carbonate counterparts (Mullins and Cook, 1986). The former is characterized by channelized flows (Nelson, 1983), while the latter mainly results from unchannelized sheet-flows originating parallel to and along the adjacent platform margins (linear source) (Mullins and Cook, 1986). Therefore, an alignment of small submarine canyons acting as source points characterizes carbonate systems (Schlager and Chermak, 1979; Mullins et al., 1984), thus contrasting with siliciclastic fans in which a single main source is located seaward of large rivers and/or large submarine canyons (Gorsline, 1978; Bates and Jackson, 1980). However, it is worth noting that calciclastic slopes may develop fan-type morphologies, though *bona fide* examples are rare in the geological record and lacking nowadays (Payros and Pujalte, 2008). Another important difference between siliciclastic and carbonate systems lies in their slope angles. Sediments of different nature have specific physical characteristics, resulting in different slope architectures. In particular, siliciclastic slopes display a lower and narrower range of depositional angles of repose when compared with carbonate examples (Schlager and Camber, 1986). Electrostatic attraction of clay minerals provides the matrix strength within clay-rich flows differentiating siliciclastic flows from carbonate flows (Marr et al., 2001). Further, shear strength in carbonates is inversely proportional with the lime-mud content, with a progressive increase in shear strength from mudstone to grainstone as a consequence of the higher grain-grain interlock of grain-supported fabrics (Spence and Tucker, 1997). Therefore, unlithified granular carbonate sediments have higher shear strength than siliciclastic grains, thus resulting in higher slope angles (Cook and Mullins, 1983; Kenter and Schlager, 1989; Kenter, 1990; Adams and Kenter, 2013). A further distinction concerns the slope architecture of carbonate systems, being differentiated in slope aprons and base-of-slope aprons. The latter are steeper ($>4^\circ$) as sediment gravity flows travel downslope through a by-pass zone separating the platform margin from the toe-of-slope. The

occurrence of several slightly incised canyons, namely gullies, characterizes the by-pass zone. Conversely, slope aprons show lower acclivities ($<4^\circ$) and the by-pass zone is absent (Crevello and Schlager, 1980; Mullins et al., 1984; Mullins and Cook, 1986; Ginsburg et al., 1991). Slope architectures also depends on the controlling factors of sediment shedding. Transport processes along carbonate platform slopes can be triggered by various mechanisms (Spence and Tucker, 1997). Among these, eustatic and tectonic processes are major mechanisms influencing the production and the export of carbonate sediments from the platform (Hine et al., 1981; Schlager and Ginsburg, 1981; Eberli and Ginsburg, 1989; Floquet and Hennuy, 2003; Hennuy, 2003; Floquet et al., 2005; Reijmer et al., 2012; 2015a; 2015b; Wunsch et al., 2016; Mulder et al., 2017). Carbonate and siliciclastic systems respond in exactly the opposite way during a cycle of relative sea-level change (Mullins, 1983). While external subaerial sources provide most of the supplies in siliciclastic systems, carbonate sediment is produced *in situ* being mostly biogenic and chemically precipitated. Consequently, carbonate systems are much more sensitive to climate and sea-level changes when compared with siliciclastic analogues (Spence and Tucker, 1997). In siliciclastic systems, sea-level lowstands favour the sediment export in response to the increase of erosion and fluvial sediment supply (Haq et al., 1987, 1988; Posamentier and Vail, 1988; Vail et al., 1991). Conversely in carbonate systems, a peak of sediment export occurs during sea-level highstand (highstand shedding), when the platform is flooded and carbonate production is at its maximum (Hine et al., 1981; Mullins, 1983; Mullins et al., 1984; Droxler and Schlager, 1985; Schlager, 1991; Schlager et al., 1994; Reijmer et al., 2012; Reijmer et al., 2015a, 2015b).

Table 1. Comparison of carbonate and siliciclastic slope features (from Playton et al., 2010).

	Carbonate Slopes	Siliciclastic Slopes
Dominant Sediment Grain Size Range	mud to boulders (μms to 10s m)	mud to sand (μms to mms)
Sand Grain Characteristics	irregular to spherical shapes, primary intragranular and microporosity common	angular to spherical shapes, primary intragranular and microporosity uncommon
Mud Characteristics	aragonite needles, planktonic skeletal forms, less cohesive	platy micaceous forms, more cohesive
Dominant Sediment Sources	platform top, margin, slope, water column	hinterland, water column
Dominant Re-sedimentation/ Flow Processes	bedload and suspended load: rockfall, debris flow, (hyper) concentrated flow, turbidity flow, suspension	primarily suspended load: turbidity flow, suspension, lesser debris flow and concentrated flow
Early Lithification	common: submarine cementation and biological binding	uncommon
Potential for Brittle Failure and Gravitational Collapse	high: early lithification and high gradients, coarse debris common	low: lack of lithification and common regrading, coarse debris uncommon
Common Maximum Slope Declivities	re-sedimented: 35-40° autochthonous: 90°	all re-sedimented: 3-6°
Sediment Dispersal	inherently line-fed, requires sediment focusing mechanism for downslope point source	inherently point-sourced with modification from strike reworking
Depositional Patterns	strike-continuous fine- to coarse-grained aprons on slope or at toe-of-slope; fan-channel complexes less common	strike-discontinuous toe-of-slope or basinal fan-channel complexes and fine-grained bypass slopes common

3. Sediment gravity-flow deposits and transport mechanisms

Sediment gravity-flow studies mainly concern siliciclastic systems, (Bouma, 1962; Mutti, 1992; Mulder and Alexander, 2001; Posamentier and Kolla, 2003). However same classifications are frequently applied to their carbonate counterparts (e.g. Mulder and Alexander, 2001, see Fig. 2). Sediment gravity flows are flows of sediments or mixtures of sediments and fluids that move downslope under the action of gravity (Middleton and Hampton, 1973). Contrary to fluid gravity flows in which the fluid is displaced by gravity and

drives the sediment along, in sediment gravity flows the action of gravity moves the particles and the displacement of the interstitial fluid results from the sediment motion (Middleton and Hampton, 1973). Mulder and Alexander (2001) prefer the term “density flow”, considering these underwater flows as mainly driven by their excess density. Despite these different approaches, “sediment gravity flows” and “density flows” are often used as synonyms when generically referring to the transport processes acting along slopes (Allen, 1985; Dasgupta, 2003). Debris flows and turbidity currents are the most common density flows operating along clastic slope systems. The product of laminar debris flows are debrites (either clast or matrix-supported), while turbidites are the deposits of both high- and low-density turbulent turbidity flows (Payros and Pujalte, 2008). In debris flows, the matrix strength allows to support and transport boulders up to several metres across (Hampton, 1972; Nardin et al., 1979; Lowe, 1982), while in turbidity currents, the excess of density forces the downslope flow of the sediment-laden emulsions (Kuenen and Migliorini, 1950). Therefore, while debrites are built up by *en masse* deposition (Lowe, 1982; Postma, 1986), resulting in the typical chaotic arrangement of these deposits (Mulder and Alexander, 2001), both high- and low-density turbidity flows result in sedimentary bodies featured by a layer-by-layer incremental structure, though rates of bed aggradation are more rapid in high-density turbidity currents. A number of processes (grain to grain interactions, development of excess pore pressure, reduced density difference between particles and surrounding fluid, increased fluid viscosity) other than fluid turbulence, contribute in supporting sediment within high-density turbidity currents (Talling et al., 2012 and references therein). Furthermore, downflow transformations can occur from one flow type to another since a single flow event typically comprises several different types of flow mechanisms (Hampton, 1972; Weirich, 1988; Talling et al., 2007). These issues point to the high variability of gravity-flow deposits, suggesting they actually cover a much wider spectrum than previously believed (see Fig. 2 for a comprehensive review).

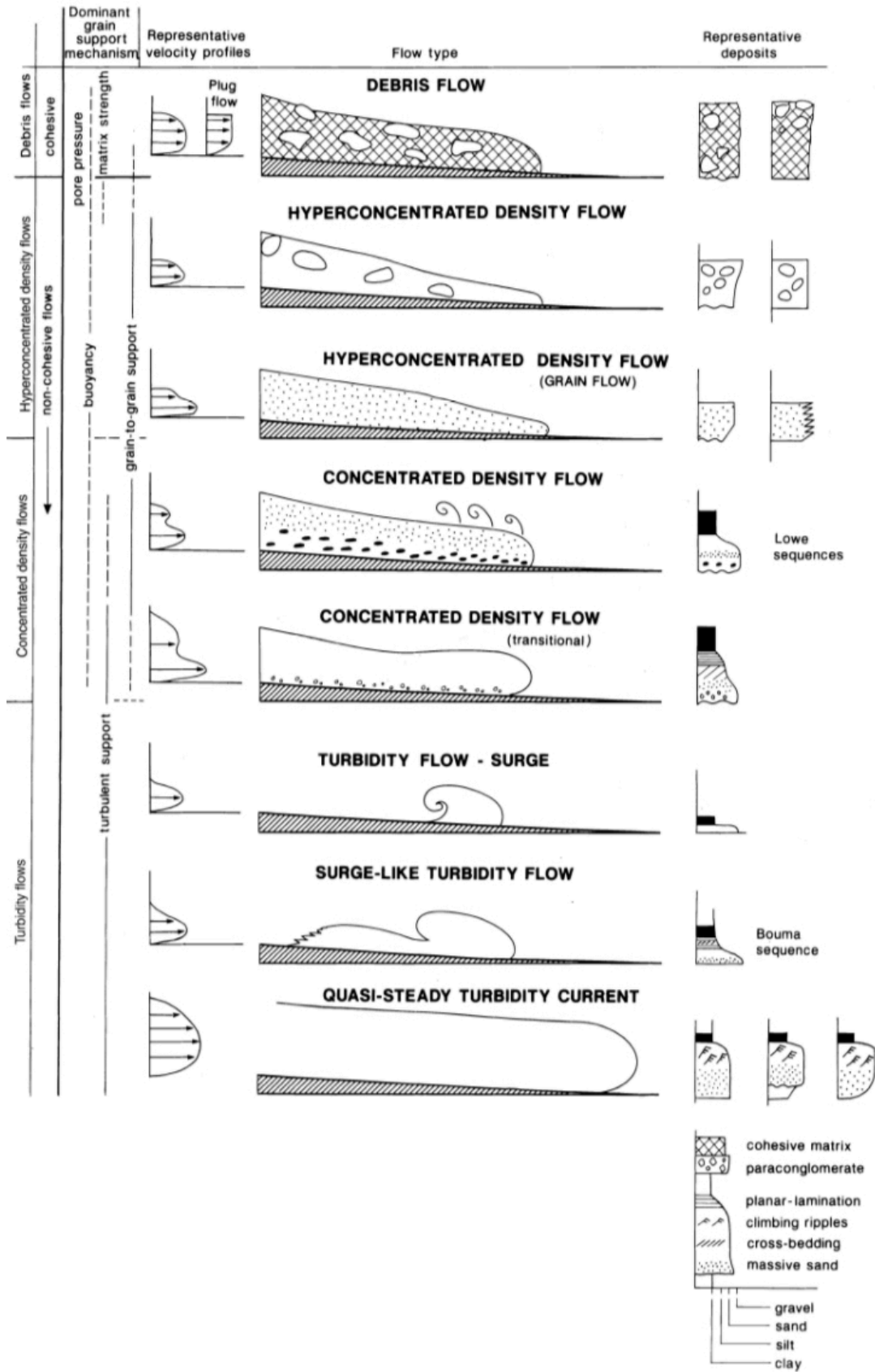
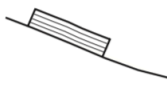

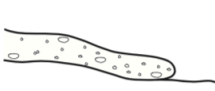



Fig. 2. Schematic definition diagram for subaqueous sedimentary density flows (from Mulder and Alexander, 2001).

Including different types of gravity-flow deposits, the term “Mass Transport Deposits” (MTDs) allows to simplify the high heterogeneity of such sedimentary bodies. These sedimentary bodies can originate both from single slope failure events and multistage events, and they are usually composed of different types of mass-wasting deposits (Fischer et al., 2005; Minisini et al., 2007) reflecting their broad diversity of morphological features (Mulder and Cochonat, 1996; Locat, 2001; Locat and Lee, 2002; Wilson et al., 2004; Gamberi et al., 2011). However, the term “MTDs” or “MTCs” (Mass Transport Complexes, the two terms are often used as synonyms) remains ambiguous due to its inconsistent use made by different authors (Nardin et al., 1979; Cook and Mullins, 1983; Mulder and Cochonat, 1996; Spence and Tucker, 1997; Principaud et al., 2015). It may take on a broad and generic meaning used to describe chaotic bodies related to “mass transport processes” that include turbidity currents (Hampton, 1972; Cook and Enos, 1977; Artoni et al., 2010). Conversely, an exhaustive definition proposed by Meckel (2010) holds MTDs as “sedimentary, stratigraphic successions that were remobilized after initial deposition but prior to substantial lithification and transported downslope by gravitational processes as non-Newtonian rheological units”. Similarly, according to Meckel III (2011) MTDs cannot include turbidites due to differences concerning seismic morphology, core-scale sand-body architecture, and petrophysical properties. Moscardelli and Wood (2008) provide a simplified scheme showing the main differences which separate MTDs/MTCs from turbidites (Table 3). In agreement with this rheological distinction, MTDs and turbidites are discussed separately in this PhD thesis, being considered as the products of different sedimentary processes. With respect to grain size, MTDs can also embed large megablocks or olistoliths ranging from less than a meter to several hundred meters in size (Mountjoy et al., 1972). Therefore, MTDs also include the term “megabreccia” according to the definition put forward by Bates and Jackson (1984), who describe megabreccias as deposits having an abundance of meter-scale (or larger) boulders.

Besides these academic issues, sediment gravity flows have a great economic significance. Slope deposits are widely considered prone to the development of petroleum systems, in particular in generating traps and seals and in defining key hydrocarbon reservoir features (e.g. location and geometry, facies distributions, development of stratigraphic traps and integrity of seal intervals) (Casabianca et al., 2002; Lamarche, 2016). However, the economic significance of such sedimentary bodies is not only related to the oil industry. Sediment gravity flows may indeed trigger - directly or indirectly - industrial, environmental and human disasters (Principaud et al. 2015; Artoni et al., 2019). As an example, destructive tsunamis may follow massive water displacement associated with these phenomena, (e.g. Nice 1979 - Gennesaux et al., 1980; Kopf et al. 2011; Papua Nuova Guinea 1998 - Tappin et al. 2001). Further, sediment gravity flows often bring serious hazards to pipelines or cables (e.g. Strait of Messina - Platania, 1909; Ryan and Heezen, 1965; south of Taiwan 2009 - Carter et al. 2012). In this respect, annual cost of damages to pipelines caused by submarine landslides is about \$400 million, as reported by the Society for Underwater Technology (Mosher et al. 2010). Finally, the geopolitical impact of these phenomena shouldn't be underestimated since the extent of submarine mass-wasting deposits defines the distal toe of the continental slope determining the border of the ECS - Extended Continental Shelf (Mosher et al. 2016). These direct social and economic issues should encourage further studies concerning gravity-flow deposits in order to enhance our understanding of parent processes and risk prediction.

Table 2. Classification of gravity-flow deposits showing the main differences between Mass Transport Complexes/Deposits and turbidites (from Moscardelli and Wood, 2008).

GRAVITY INDUCED DEPOSITS		Genetic Classification Transport Mechanism	Descriptive Classification Sedimentary Structures	Seismically Recognizable Features (Moscardelli et al., 2006; this work)
Mass Transport Complex	Slide 	Shear failure along discrete shear planes with little or no internal deformation or rotation	Essentially undeformed, continuous bedding	Continuous blocks without apparent internal deformation. High-amplitude, continuous reflections.
	Slump 	Shear failure accompanied by rotation along discrete shear surfaces with various degrees of internal deformation	Plastic deformation particularly at the toe or base. Plow structures, folds, tension faults, joints, slickensides, grooves, rotational blocks	Compressional ridges, imbricate slides, irregular upper bedding contacts, duplex structures, contorted layers. Low- and high-amplitude reflections geometrically arranged as though deformed through compressive stresses.
	Debris Flow 	Shear distributed throughout the sediment mass. Strength is principally from cohesion due to clay content. Additional matrix support may come from buoyancy. Plastic rheology and laminar state.	Matrix supported, random fabric, clast size variable, matrix variable. Rip ups, rafts, inverse grading and flow structures possible.	Mega rafted and/or detached blocks, irregular upper bedding contacts, lateral pinch-out geometries, oriented ridges and scours. Low-amplitude, semitransparent chaotic reflections.
Turbidity Current	Turbidite 	Supported by fluid turbulence (newtonian rheology)	Normal size grading, sharp basal contacts, gradational upper contacts.	Lobate features Laterally continuous

4. The Cretaceous of Sicily

As a consequence of the transtensional processes related to the opening of Western Tethys, most of the Sicilian palaeodomains were drowned during the Cretaceous (Catalano and D'Argenio, 1982). Therefore, thick sequences of pelagic/hemipelagic limestones and marly limestones were emplaced during this period. Cretaceous pelagic carbonates from Sicily have been subdivided into three main lithostratigraphic units (Patacca et al., 1979; Catalano and D'Argenio, 1982): Lattimusa Fm. (Maiolica-type calcipionellid calcilutites, Tithonian to lowermost Cretaceous), Hybla Fm. (Aptychus marls and calcilutites, Lower Cretaceous) and Amerillo Fm. (Scaglia-type cherty calcilutites, Cenomanian to Eocene). Such deep-water limestones are widespread in the whole Island, however the very first contributions to the knowledge of the Cretaceous system in Sicily concerned shallow-water limestones. A paleontological approach characterized these studies, being focused on rudist associations (Gemmellaro, 1860, 1865, 1868-1876; Ciofalo, 1869, 1878; Di Stefano, 1888, 1889, 1908).

Afterwards, several stratigraphic and sedimentological studies followed (De Stefani, 1949; Montanari, 1964, 1966; Camoin, 1982; Di Stefano and Ruberti, 2000 among the others). Well-studied rudist lithosomes of Campanian-Maastrichtian age, belonging to the Hyblean domain, are located in the foreland of the Maghrebian chain and in the southernmost sector of the Island (Capo Passero; Camoin, 1982; Grasso and Lentini, 1982; Grasso et al., 1983; Amore et al., 1988). However, most of the Cretaceous shallow-water limestones crop out in northern Sicily and are involved in the tectonic units of the Maghrebian thrust-and-fold belt. These limestones are referred to the Panormide Platform and its remnants occur in the Madonie and Palermo Mountains (Caflish, 1966, 1967; Broquet, 1968; Ogniben, 1960; Catalano and D'Argenio, 1982; Di Stefano and Ruberti, 2000) and in the Nebrodi Mountains on the basis of borehole data (Bianchi et al., 1987). Furthermore, seismic lines (D'Argenio, 1999; Pepe et al., 2004; Finetti, 2005) and tomographic images (Gattacceca and Speranza, 2002) suggested that sliced crustal blocks of the Panormide Platform were rifted off towards the Tyrrhenian Sea. An anomalous subsidence history characterized this carbonate platform during the Mesozoic Era (Zarcone, 2008; Zarcone and Di Stefano, 2008), causing the onset of intraplatform basins and a scalloped-margin morphology (Basilone et al., 2016). In particular, a tectonic subsidence trend affected the Panormide Platform from the Late Aptian to the end of the Early Cretaceous and a tectonic uplift trend followed during the Late Cretaceous (Basilone and Sulli, 2018). This notwithstanding, a number of authors put forward the role of the Panormide Platform as a continental bridge between Africa and Adria during the Jurassic-Cretaceous interval (Turco et al., 2007; Zarcone and Di Stefano, 2007; 2008; Canudo et al., 2009; Zarcone et al., 2010) on the basis of (i) the dinosaur ichnocoenosis and bones of central-southern Italy (Petti, 2006; Nicosia et al., 2007; Garilli et al., 2009; Pereda-Superbiola, 2009) and Croatia (Mezga et al., 2007); (ii) comparable patterns in the subsidence curves of the Panormide Platforms and Apennine and Apulian platforms (Corrado, 1996; Stampfli and Mosar, 1999; Zarcone and Di Stefano, 2010; Basilone et al., 2016; Basilone and Sulli, 2018);

(iii) and the interpretation of seismic lines (Finetti, 2005) and tomographic images (Gattacceca and Speranza, 2002; 2007). In analogy with modern carbonate systems, the Panormide platform fed the the adjacent slope-to-basin domains. Well-studied examples documenting the relationship between the source area and the Imerese slope-to-basin domain are found in the Madonie Mountains, in north-eastern Sicily (Ogniben, 1960; Broquet, 1968; Broquet and Mascle, 1972; Grasso et al., 1978; Abate et al., 1982; Catalano and D'Argenio, 1982) and in the Termini Imerese area (Camoin; 1982). In particular, calciclastic deposits mainly made of breccias and megabreccias with abundant rudists and Orbitolinidae occur as thick carbonate prisms interbedded with siliceous deep-water sediments (Crisanti Fm., Schmidt di Friedberg et al., 1960; Montanari, 1964). In the north-western sector of Sicily, several authors mentioned the Cretaceous slope carbonates from the Capo San Vito Peninsula (Broquet and Mascle, 1972; Giunta and Liguori, 1972, 1973; Abate et al., 1991, 1993; Catalano et al., 2011). However, owing to the Maghrebian orogeny and the Plio-Pleistocene transtensional processes, the source area of these slope limestones is debated and is attributed to different palaeodomains (Intermediate Platform *sensu* Giunta and Liguori, 1972; 1973; Hyblean-Pelagian block *sensu* Nigro and Renda, 1999; Panormide Platform *sensu* Abate et al., 1991; 1993; Di Stefano and Ruberti, 2000; Catalano et al., 2011).

5. Structure of the PhD thesis

This chapter aims to introduce the issues addressed by two papers that constitute the core of the thesis. A section intended for the general concluding remarks to the PhD study follows. Each paper describes the adopted methodologies to carry out this PhD study, thus they will be not repeated in the present chapter. The reference lists follow each paper, while the contributions cited in the present chapter are enlisted at the end of the thesis. The manuscript entitled "Carbonate slope re-sedimentation in a tectonically-active setting (Western Sicily Cretaceous Escarpment, Italy)" (DOI: 10.1111/sed.12705) was submitted to the journal

“Sedimentology” in June 2019 and, after minor revisions, definitely accepted for publication last January. This contribution is the result of the fruitful cooperation between our Department, the sedimentological group of the KFUPM and ENI. While this paper mainly concerns the sedimentological part of the PhD study, the paper entitled “A Cretaceous Carbonate Escarpment from Western Sicily (Italy): biostratigraphy and tectono-sedimentary evolution” (ID: YCRES_2019_397) concerns the biostratigraphic part. This manuscript was submitted to “Cretaceous Research” last November and accepted with moderate revisions at the end of December.

2. Carbonate slope re-sedimentation in a tectonically-active setting (Western Sicily Cretaceous Escarpment, Italy)

Randazzo, V. (1); Le Goff, J (2); Di Stefano, P (1); Reijmer, J.J.G. (2); Todaro, S. (1); Cacciatore, M.S. (3)

(1) University of Palermo - Department of Earth and Marine Sciences, Palermo, Italy.

Corresponding author: vincenzo.randazzo04@unipa.it

(2) College of Petroleum Engineering and Geosciences, King Fahd University of Petroleum and Minerals, Dhahran, Saudi Arabia.

(3) Eni S.p.A. Upstream and Technical Services, Italy.

Abstract

Tectonic processes are widely considered as a mechanism causing carbonate platform margin instabilities leading to the emplacement of mass transport deposits and calciturbidites. However, only few examples establishing a clear link between tectonics and re-sedimentation processes are known from the literature. The two-dimensional and three-dimensional wire-cut walls of hundreds of quarries extracting ornamental limestones (for example, *Perlato di Sicilia*) from the Western Sicily Cretaceous Escarpment in Italy expose a series of mass transport deposits. The depositional architecture, spatial facies distribution and sedimentary features of these deposits were studied in detail. Thin section analysis was used to define the microfacies characteristics and to determine the age of the re-sedimented limestones. Eleven facies types grouped into four facies associations were recognized that defined specific depositional processes and environments. The stratigraphic architecture of the slope was reconstructed using four composite facies successions based on the detailed analysis and correlation of the field sections. The palaeoslope orientation was reconstructed based on the

analysis of synsedimentary faults, slump scars and pinch-out geometries. The Western Sicily Cretaceous Escarpment was strongly influenced by synsedimentary transtensional tectonics in combination with magmatic processes, as suggested by the presence of tuffites and pillow lava intercalations within the re-sedimented carbonate series. These volcanics point to a major role of crustal shear as a trigger for mass transport deposit emplacement. The facies distribution along the Western Sicily Cretaceous Escarpment delivers new insights into the deformation processes accompanying the crustal extension of the Cretaceous western Tethys realm.

Keywords: Carbonate slope, Cretaceous, mass transport deposits, re-deposited facies, tectonics.

1. Introduction

The diversity of sediment-transport mechanisms acting along carbonate slopes such as turbulence, grain to grain interactions or matrix support (Mulder and Alexander, 2001), as well as the wide range of grain sizes and fabrics (Kenter, 1990) induce depositional and stratigraphic heterogeneities of slope architectures (Playton et al., 2010). Subsurface seismics provided valuable insights into the architecture of both modern and ancient slope architectures (Hine et al., 1992; Eberli et al., 2004; Bull et al., 2009; Jo et al., 2015; Principaud et al., 2015; Tournadour et al., 2015; Mulder et al., 2018). Outcrop analogues, however, are critical to further detail the high-resolution architecture of carbonate slope facies (Janson et al., 2010; Heubeck et al., 2013). A series of studies addressed the key role played by mass transport deposits (MTDs) in governing the slope architecture of both modern (Playton et al., 2010, and references therein; Mulder et al., 2017) and ancient carbonate slope systems (Crevello and Schlager, 1980; Spence and Tucker, 1997; Hairabian et al., 2015; Reijmer et al., 2015a,b; Playton and Kerans, 2018) as well as providing information on the source area (Mullins et al., 1986, 1991; Mullins and Hine, 1989; Ross et al., 1994; Borgomano, 2000; Posamentier and Kolla, 2003). The terminology of MTDs remains ambiguous due to the disparate definitions and its variable usages (Cook and Mullins, 1983; Mulder and Cochonat, 1996; Artoni et al., 2010; Meckel, 2011). In this study, MTDs refer to the product of mass movement transport processes as defined in Posamentier and Martinsen (2011), resulting as the downslope displacement of poorly lithified strata. Slope architecture also depends on the controlling factors of sediment shedding occurring on platform top and/or their adjacent slopes (Spence and Tucker, 1997; Playton et al., 2010; Reijmer et al., 2015a). Controlling factors of slope architecture include: (i) sea-level fluctuations (for example, Bahamas: Hine et al., 1981; Schlager and Ginsburg, 1981; Eberli and Ginsburg, 1989; Reijmer et al., 2002, 2012, 2015a; Wunsch et al., 2016; Mulder et al., 2017; Great Barrier Reef: Webster et al., 2012, 2016; Puga-Bernabeu et al., 2013, 2017; Maldives: Betzler et al., 2016); (ii) tectonics (for example,

Southern Provence: Floquet and Hennuy, 2003; Hennuy, 2003; Floquet et al., 2005; Reijmer et al., 2015b; Pyrenees: Drzewiecki and Simo, 2002; general reviews: Payros and Pujalte, 2008, and references therein; Playton et al., 2010, and references therein); and (iii) the system growth itself (Canning Basin: Playton and Kerans, 2015a,b; Delaware Basin: Playton and Kerans, 2018). In addition, the downslope movement of sediment-laden flows covers a variety of processes that may coexist within a single gravity flow event. For instance, matrix-supported, non-Newtonian types of flows (i.e. cohesive) and turbulence-supported, Newtonian flows (i.e. non-cohesive) give rise to hybrid events and linked deposits (Hampton, 1972; Krause and Oldershaw, 1979; Haughton et al., 2009; Talling et al., 2012). This variability makes it difficult to develop both depositional and stratigraphic models for hydrocarbon evaluation and hinders the enhancement of an accurate terminology to describe deposits in outcrop. In siliciclastic systems, MTDs are considered as good traps and seals, thus presenting an important reservoir feature (Beaubouef and Abreu, 2010; Kneller et al., 2016; Lamarche et al., 2016). In carbonate systems, giant hydrocarbon reservoirs have been discovered in Cretaceous slope successions worldwide (Borgomano, 2000), for example, the Poza Rica trend in Mexico (e.g. Enos, 1977; Janson et al., 2011; Loucks et al., 2011) and the Ruby field in the Makassar Straits of Indonesia (Pireno et al., 2009; Tanos et al., 2012). Tethyan outcrop examples of reservoir analogues include the Maiella and Gargano escarpments in Italy (Eberli et al., 1993; Neri, 1993; Neri and Luciani, 1994; Vecsei et al., 1998; Graziano, 2000; Rusciadelli et al., 2003; Rusciadelli, 2005; Hairabian et al., 2015; Rustichelli et al., 2017). Tectonic processes resulted in the emplacement of the thick volumes of re-sedimented carbonates constituting these Cretaceous escarpments (Borgomano, 2000; Morsilli et al., 2004). In north-western Sicily Cretaceous slope system series are well-exposed along the wirecut walls of a large number of quarries. These outcrops allow for the detailed study of facies heterogeneity characterizing the

carbonate slope system, and the comprehensive documentation of numerous syndimentary features.

The aim of this paper is to reconstruct the facies architecture of the carbonate slope of the Western Sicily Cretaceous Escarpment (WSCE) and to document the re-sedimentation processes within a coarse-grained dominated system in response to eustatic and tectonic processes. The assessment of the genetic relationships between the carbonate deposits and the volcanic submarine effusions will provide new insights into the tectonic evolution of the WSCE and its palaeogeographic significance in the western Tethyan realm during Cretaceous times.

2. Geological and stratigraphic setting

The Capo San Vito Peninsula is situated in north-western Sicily and constitutes a segment of the inner zone of the Maghrebian fold and thrust belt (Fig. 1A and B). The lithostratigraphic setting of the peninsula has been the subject of several studies (Giunta and Liguori, 1972, 1973; Abate et al., 1993; Catalano et al., 2011, among others). However, only the facies stacking of the Upper Triassic–Lower Jurassic peritidal limestones has been analyzed in detail so far (Todaro et al., 2017, 2018). Other studies concentrated on the Cretaceous magmatic intrusions exposed in the south-western sector of the peninsula (western part of the Mt Sparagio ridge; see Fig. 1C; Bellia et al., 1981; Catalano et al., 1984; Speziale, 1997). The nappe emplacement occurred during the late Miocene–earliest Pliocene (Nigro and Renda, 1999) and was accompanied by a clockwise rotation (up to 90°) of the thrust sheets (Oldow et al., 1990; Speranza et al., 2000). During the late Pliocene and Pleistocene, the thrust stack was affected by extensional and transtensional faults (NNW–SSE) related to the evolution of the Tyrrhenian margin and to the opening of the Castellammare Basin (Mauz and Renda, 1991; Nigro and Renda, 1999; Giunta et al., 2002; Agate et al., 2005). The structural setting of the area was discussed by several authors (Broquet and Mascle, 1972; Giunta and Liguori,

1972, 1973; Abate et al., 1993; Catalano et al., 2011) and resulted in different interpretations and nomenclatures (Table 1). In this study, three main tectonic units were distinguished, namely: (i) the Acci Unit; (ii) the Monaco-Sparagio Unit (subdivided in three subunits); and (iii) the Ramalloro Unit (Fig. 1C and D). This subdivision partially agrees with Giunta and Liguori (1972, 1973). The tectonic units in the study area comprise a Triassic to Miocene carbonate succession (Fig. 2; Abate et al., 1991, 1993). The lower part of the succession shows a 1000 m thick series of Upper Triassic–Lower Jurassic peritidal limestones that is overlain by condensed pelagic limestones (Rosso Ammonitico) covering the Middle to Upper Jurassic. A gradual transition upward to Calpionellid and Tubiphytes limestones corresponds to the uppermost Jurassic–lowermost Cretaceous interval. The Mt Monaco–Mt Sparagio tectonic unit reveals carbonate slope deposits such as the Cretaceous Ellipsactinia and rudist breccias. The calciclastic carbonate succession is interrupted by three main volcanic intervals, mainly tuffites and basalts (Bellia et al., 1981). The downslope transition of these slope deposits shows interfingering with Lower Cretaceous marls (Hybla Formation) and Upper Cretaceous lime mudstones (Amerillo Formation). Upsection, patches of Oligocene nummulitid limestones, Miocene calcarenites and clay deposits occur. In places, an angular unconformity marked by a deep erosional truncation separates the Miocene deposits and the Cretaceous limestones.

Relicts of the Panormide Platform, the source of Cretaceous slope sediments, crop out in the Palermo and Madonie Mountains (Fig. 1B; see also stratigraphy in Fig. 2; Di Stefano and Ruberti, 2000). The transition between the carbonate platform and the adjacent slope is not preserved due to the compressional Maghrebian deformation and subsequent development of Plio-Quaternary extensional and transtensional faults (Abate et al., 1991, 1993).

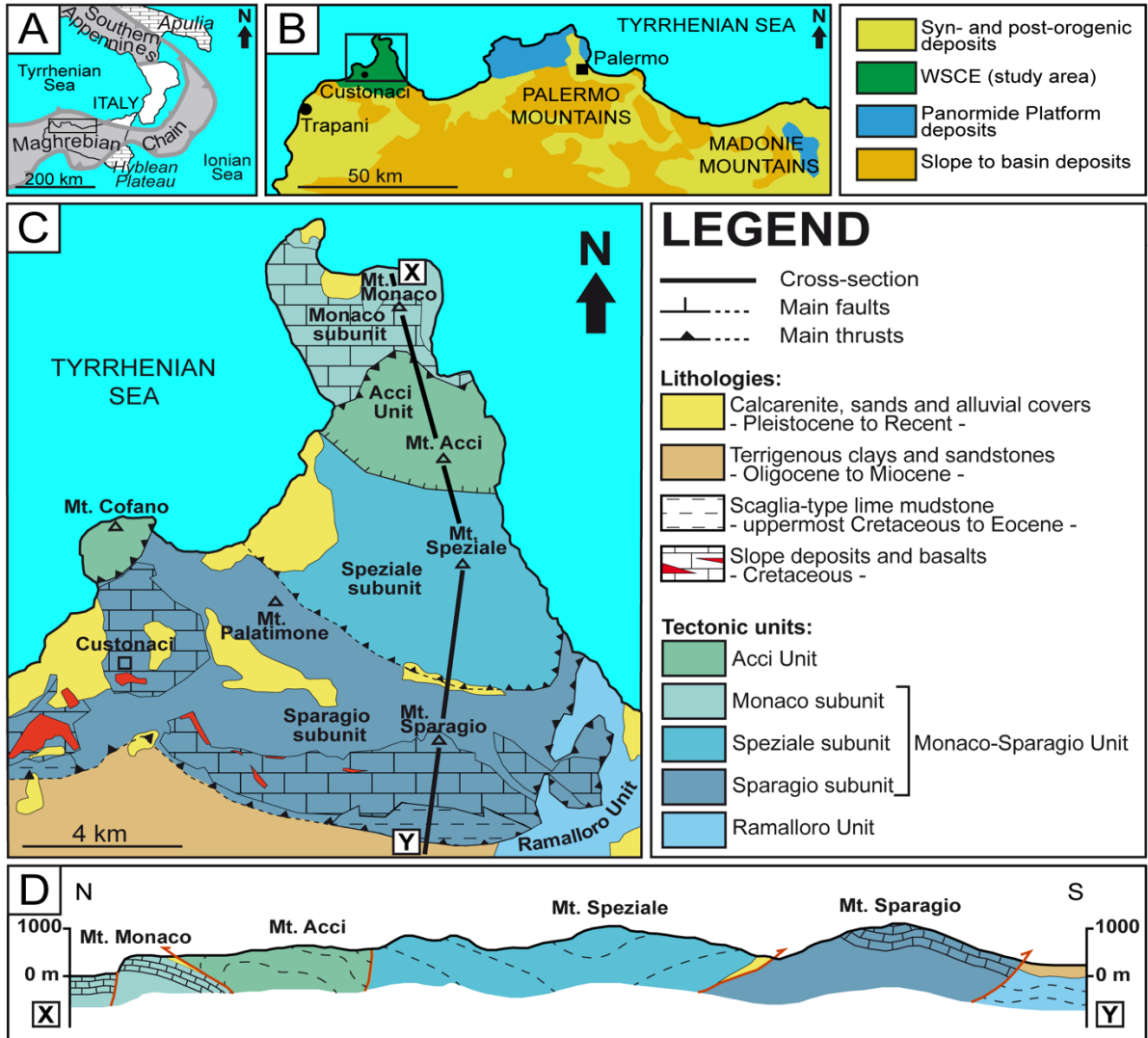


Fig. 1. (A) Tectonic sketch of the Central Mediterranean. Outline shows location of study area. (B) Tectonic map of north-western Sicily with location of the Capo San Vito Peninsula (black rectangle) and the tectonic units of the Panormide Platform. (C) Structural map of the Capo San Vito Peninsula (modified after Abate et al., 1991) and associated legend. (D) North-south cross-section of the study area, see (C) for location.

Table 1: Comparison of the structural interpretations for the Capo San Vito Peninsula.

<i>Broquet and Masclé, 1972</i>	<i>Giunta and Liguori, 1973</i>	<i>Catalano and D'Argenio, 1982</i>	<i>Abate et al., 1991</i>	<i>Catalano et al., 2011</i>	<i>This Work</i>
Mt. Cofano - Mt. Acci "Series"	Mt. Acci - Egadi Unit	Mt. Acci - Mt. Monaco - Mt. Sparagio Unit	Mt. Le Curcie Unit	Busetto Palizzolo Unit	
Mt. Sparagio - Mt. Monaco "Series"	Mt. Monaco - Mt. Sparagio Unit	Mt. Luziano Unit	Mt. Sparagio - Mt. Cofano Unit	Acci Unit	Acci Unit
Mt. Erice "Series"	Mt. Erice Unit		Mt. Speziale - Mt. Palatimone Unit	Sparagio - Monaco Unit	Monaco - Sparagio Unit
			Mt. Acci - Pizzo di Sella Unit		
			Mt. Monaco Unit		
Mt. Ramalloro - Mt. Inici "Series"	Mt. Inici - Montagna Grande Unit	Mt. Inici - Montagna Grande Unit		Inici - Ramalloro Unit	Ramalloro Unit
			Mt. Ramalloro Unit		

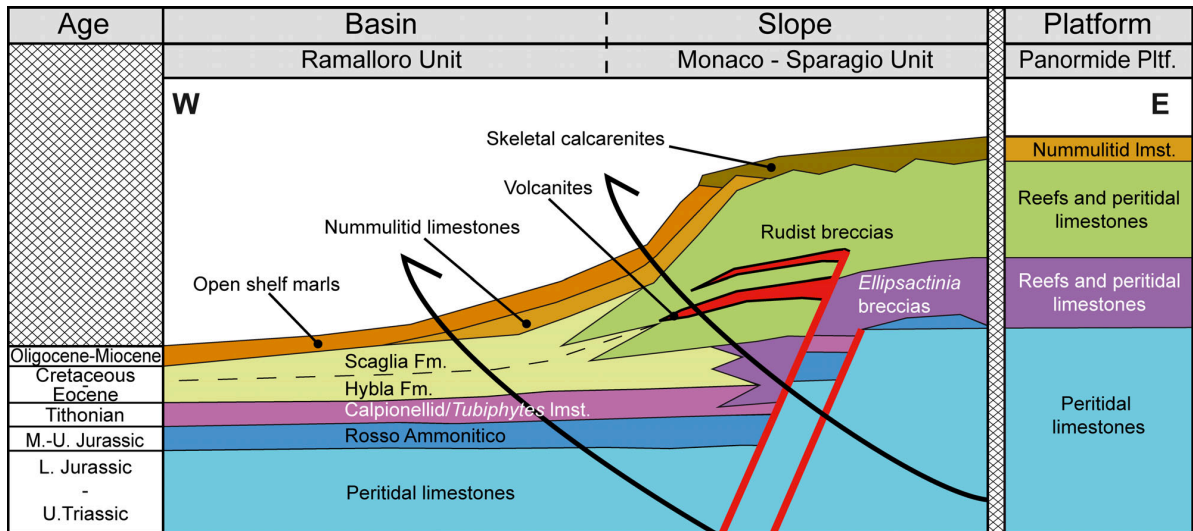


Fig. 2. Lithostratigraphy of Panormide Platform and the adjacent slope and basin deposits of the Western Sicily Cretaceous Escarpment (WSCE). Red lines are Mesozoic extensional faults while black lines represent Neogene thrust faults. Fm., formation; lmst., limestones; Pltf., platform.

3. Methodology

This study relies on the description of the microfacies types and their vertical organization along 18 measured sections selected out of a vast number of outcrops and quarries (Fig. 3). Four composite sections were acquired, each of them corresponding to a cartographic sector. Restricted access areas along sub-vertical quarry walls were investigated by drone imaging to analyze the sedimentary features and to determine the vertical and lateral relationships between the individual sedimentary bodies. The facies classification used textural characteristics (Dunham, 1962; Embry and Klovan, 1971), constituents (Flügel, 2004), bed thickness (Table 2; McKee and Weir, 1953), grain sizes (Table 2; Blair and McPherson, 1999), grain sorting (Pettijohn et al., 1973) and sedimentary structures (Cook and Mullins, 1983; Prior et al., 1984). A genetic interpretation of the deposits was based on earlier studies focusing on similar carbonate depositional environments (Krause and Oldershaw, 1979; Mullins and Cook, 1986; Spence and Tucker, 1997; Hughes, 2000; Reijmer et al., 2015b; Le Goff et al., 2015, 2019) and transport processes for MTDs and calciturbidites (Mulder and

Alexander, 2001; Moscardelli and Wood, 2008). A total of 150 thin sections were selected from 200 representative samples collected in the field. Petrographic analysis following the classifications of Dunham (1962) and Embry and Klovan (1971) enabled the definition of microfacies types. The correlation of the Cretaceous deposits was based on the benthic foraminiferal assemblages following the biozonal schemes for platform margin and external slope environments as defined by Velić (2007) and Chiocchini et al. (2008). Additionally, calpionellids and planktonic foraminifera were identified using the biozonal schemes proposed by Andreini et al. (2007) and Premoli Silva and Verga (2004). The chronostratigraphic distribution of rudists was based on Cestari and Sartorio (1995), Chiocchini et al. (2008) and Troya Garcia (2015).

The main biozones and biomarkers identified are summarized in Table 3.

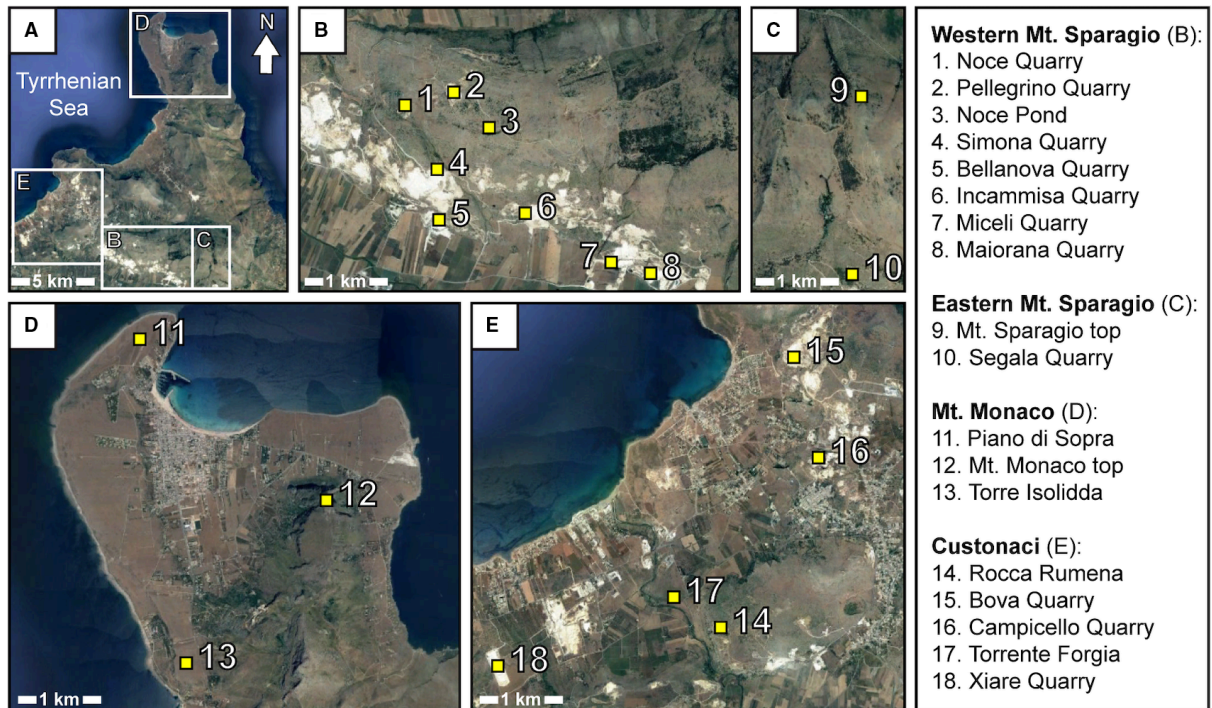


Fig. 3. Google Earth images showing the location of the studied sections. (A) General view of the study area (geological map is shown in Fig. 1C). White rectangles indicate the four areas investigated: (B) Western Mt. Sparagio; (C) Eastern Mt. Sparagio; (D) Mt. Monaco; (E) Custonaci.

Table 2. Terminologies adopted for bed thickness (left) and grain-sizes (right).

<i>Stratification</i>	<i>Thickness</i>	<i>Class</i>	<i>Particle length</i>
Very thick-bedded	> 1.20 m	Block (fine to medium)	4.1 - 16.4 m
Thick-bedded	0.6 - 1.20 m	Boulder	0.25 - 4.1 m
Thin-bedded	50 - 600 mm	Cobble	64 - 256 mm
Very thin-bedded	10 - 50 mm	Pebble	4 - 64 mm

Table 3. Main biomarkers and biozones identified along the Western Sicily Cretaceous Escarpment (WSCE). See Fig. 8 for their distribution in the studied sections.

<i>Sections</i>	<i>Fig. 8</i>	<i>Main biomarkers or biozones</i>	<i>Age</i>	<i>References</i>
Noce Quarry; Piano di Sopra; Rocca Rumena	1a	<i>Calpinella/Calpionellopsis</i> Zones	middle-late Berriasian	Andreini <i>et al.</i> (2007)
Piano di Sopra	1b	<i>Favusella hauerivica</i> Zone	late Berriasian- Hauterivian	Premoli Silva and Virga (2004)
Noce Quarry; Piano di Sopra; Rocca Rumena	2	<i>Protopenneroplis ultragranulata</i>	Berriasian- Valanginian	Chiocchini <i>et al.</i> 2008
Noce Quarry	3	<i>Moesiloculina</i> sp. and Radiolitids	Aptian	Chiocchini <i>et al.</i> (2008)
Noce Pond	4	<i>Mesorbitolina subconcava</i> Zone	early Albian	Velić (2007)
Top Sparagio; Torre Isolidda; Bova Quarry; Campicello Quarry	5a	<i>Pseudomarssonella turris</i> , <i>Cuneolina</i> sp., cfr. <i>Pseudorhapydionina dubia</i> ,	Albian- Cenomanian	Velić (2007), Chiocchini <i>et al.</i> (2008)
Simona Quarry; Incammisa Quarry; Top Monaco	5b	<i>Conocorbitolina</i> sp., <i>Cuneolina</i> <i>pavonia</i> , <i>Dicyclina</i> sp., <i>Caprina</i> cfr. <i>schiosensis</i>	Cenomanian	Velić (2007); Cestari and Sartorio (1995); Chiocchini <i>et al.</i> (2008)
Torrente Forgia	5c	<i>Dicarinella</i> and Radiolitidae Subzone	late Cenomanian	Chiocchini <i>et al.</i> (2008)
Maiorana Quarry; Segala Quarry	6	<i>Hippurites incisus</i>	Coniacian	Troya Garcia (2015)
Maiorana Quarry; Segala Quarry	7	<i>Dicarinella asymerica</i> Zone	Santonian	Premoli Silva and Virga (2004)
Xiare Quarry	8	<i>Globotruncanita elevata</i> Zone	early Campanian	Premoli Silva and Virga (2004)
Xiare Quarry	9	<i>Globotruncana</i> , <i>Globotruncanita</i> and <i>Orbitoides</i> Zone	late Campanian - Maastrichtian	Chiocchini <i>et al.</i> (2008)

4. Facies Analysis

The sedimentary rocks in the study area are intensely exploited as ornamental stones, particularly the Cretaceous limestones known as *Perlato di Sicilia*. The so-called *Bacino marmifero di Custonaci* expose the sedimentological features of the slope series in detail along the wire-cut walls in many quarries. Stratigraphic occurrences and depositional processes along the WSCE are described in this section. In addition, sedimentary and structural structures such as clinoforms, slump scars, synsedimentary faults, pinch-out geometries and imbricated clasts are analysed. Following the description of these features, sedimentary facies

are grouped into four facies associations, each of them reflecting a specific depositional setting, for example ramp, margin, slope, and “slope-to-basin”. The description and interpretation of the facies types are summarized in Table 4.

Table 4. Facies scheme of the Cretaceous limestones of the Capo San Vito Peninsula. Gst, Grainstone; Pst, Packstone; Wst, Wackestone.

<i>Facies</i>	<i>Texture</i>	<i>Grain sorting</i>	<i>Lithoclast size range</i>	<i>Main constituents</i>	<i>Sedimentary features</i>	<i>Depositional processes</i>	<i>Depositional environment(s)</i>
FA1: Fine-grained limestones with calpionellids and <i>Tubiphytes</i>	Wst	Good	-	Calpionellids, benthic foraminifera, <i>T. morronensis</i>	Thin bedded, bioturbation, nodular structure	Background sedimentation	Outer ramp
FB1: Rudist rudstone/floatstone	Wst/Pst	Poor	-	Rudist fragments, Orbitolinidae	Thin to thick bedded, chaotic distribution of the elements	Wave motion, tidal currents	Fore-bank / Shoal
FB2: Rudstone with rounded rudist fragments	Gst	Poor	-	Rounded rudist fragments, Orbitolinidae	Thin to thick bedded, chaotic distribution of the elements	Wave motion, tidal currents	Shoal
FB3: Rudist bedded floatstone	Gst	Good	-	Rudist fragments, Orbitolinidae	Thin to thick bedded	Wave motion, tidal currents	Fore-bank / Shoal
FC1: Bedded breccia with <i>Ellipsactinia</i>	Pst	Poor	Pebbles to boulders	<i>Ellipsactinia</i> , <i>B. irregularis</i> /L. <i>aggregatum</i>	Thin to very thick bedded, syndimentary faults	Debris flow	Upper slope to toe of slope
FC2: Bedded megabreccia with rudists	Pst	Poor	Pebbles to blocks	Rudist fragments, Orbitolinidae	Thin to very thick bedded, syndimentary faults	Debris flow	Upper slope to toe of slope
FC3: Chaotic megabreccia	Pst	Poor	Pebbles to blocks	Rudist fragments, rudist patch reef, Orbitolinidae	No bedding, chaotic distribution of the elements, slump scars	Rock fall, avalanche	Base of tectonic escarpments in the upper slope to lower slope
FC4: Chaotic megabreccia with poorly-cemented lithoclasts	Pst	Poor	Pebbles to boulders	Rudist fragments, Orbitolinidae	No bedding, chaotic distribution of the elements	Rock fall, avalanche	Base of tectonic escarpments in the upper slope to lower slope
FC5: Lenticular fine-grained skeletal limestones	Gst/Wst	Good	-	Rudist fragments	Thin bedded, lobate geometries, pinch-out terminations	Turbidity current	Lower slope to toe of slope
FD1: Fine-grained skeletal limestones	Gst/Wst	Good	-	Rudist fragments	Thin to very thin bedded, syndimentary faults, soft-sediment deformations	Turbidity current	Toe-of-slope
FD2: Lime mudstone with planktonic foraminifera	Wst	Good	-	Planktonic foraminifera, skeletal grains	Thin to very thin bedded	Background sedimentation	Toe-of-slope to basin

4.1. FA - Facies Association A (FA)

This facies association consist of structureless wackestone to packstone made up of pelagic and platform-derived grains. This facies type crops out at several different localities in the study area (locations 1, 2, 11 and 14 in Fig. 3).

FA1 - Fine-grained limestones with calpionellids and Tubiphytes

Description. This facies occurs in the lowermost part of the studied succession succeeding the Rosso Ammonitico (Middle-Upper Jurassic). Limestone layers reach a few metres in thickness and have a grey colour (Fig. 4A). In places, nodular structures are observed within thin beds. The facies shows a wackestone to packstone texture with both pelagic (for example aptychi, sponge spicules, calpionellids, calcified radiolarians and abundant calcispheres) and platform-derived skeletal constituents (echinoderm debris, benthic foraminifera and *Tubiphytes* “*Crescentiella*” *morroneis*) (Fig. 4B). Other identified constituents are; *Remaniella cadischiana*, *Calpionella alpina*, *Calpionellopsis* sp. and *Tintinnopsella* sp. (calpionellids).

Interpretation. Based on the calpionellid biozonation (Andreini et al., 2007) these deposits can be assigned to the Berriasian. The absence of bedload transport indices (for example, sorting, grading or lamination) suggests that FA1 was not emplaced through turbidity currents. The facies is exposed at the same stratigraphic position in several outcrops (locations 1, 2, 11 and 14 in Fig. 3). The co-occurrence of pelagic and platform-derived organisms is interpreted as the result of hemipelagic sedimentation along a gentle ramp situated below the storm wave base.

4.2. Facies Association B (FB)

Abundant orbitolinids and rudists characterize this facies association. Loose specimens and related fragments are scattered in the matrix while lithoclasts are totally absent which

clearly distinguishes facies association B from the other facies associations observed in the study area.

FB1 - Rudist rudstone/floatstone

Description. FB1 occurs as thin to thick beds at two locations within the study area (locations 10 and 13 in Fig. 3C and D). Abundant rudist fragments and well-preserved specimens of *Eoradiolites* sp. (Fig. 4C) and caprinids occur in association with orbitolinids (Fig. 4D). The texture mainly consists of packstone though a variable content of matrix is present between the clasts and, in places, it becomes dominant (matrix-supported). Smaller benthic foraminifera such as *Pseudomarssonella turris*, *Cuneolina* sp., cfr. *Pseudorhapydionina dubia*, and micro-encruster associations also occur, such as *Lithocodium aggregatum*/*Bacinella irregularis* and *Girvanella* sp./*Cayeuxia* sp.

Interpretation. Based on of the biozonations proposed by Velić (2007) and Chiocchini et al. (2008), the biotic assemblage of FB1 deposits can be assigned to the Albian-Cenomanian. Microboring is common in the rudist fragments suggesting long-lasting exposure of the skeletal grains to the activity of microbes, algae and fungi (Perry, 1998; Flügel, 2004; Chacón et al., 2006). Microboring is characteristic of shallow-water environments and very common in the Cenomanian shelf-to-margin limestones that crop out at Mt Pellegrino (north-western Sicily) (Di Stefano and Ruberti, 2000; Flügel, 2004). The packstone texture, the presence of shallow-water biota affected by microborings and the absence of lithoclasts suggest a depositional setting close to the platform margin with a moderate to high energy level, as described for forebank or platform shoal environments (Hughes, 2000).

FB2 - Rudstone with rounded rudist fragments

Description. The thickness of this facies is limited to a few metres and occurs in a single, thin to thick bedded carbonate series close to the top of Mt Monaco (location 12 in Fig. 3D).

FB2 is dominated by centimetre-scale whitish and well-rounded rudist fragments. Skeletal grains reveal a high variability in size and shapes and a random/chaotic distribution (Fig. 4E). The cements observed in thin section mainly consist of microcrystalline, fibrous and drusy calcite. *Radiolitidae* fragments with a typical cellular prismatic structure (millimetre- to centimetre-scale) frequently occur (Fig. 4F). The texture consists of grainstone to rudstone with rare benthic foraminifera such as orbitolinids, *Cuneolina* sp., *Cuneolina pavonia*, and *Dycyclina* sp.

Interpretation. The biotic assemblage identified in FB2 suggests a Cenomanian age (Velić, 2007; Chiocchini et al., 2008). The whitish colour of the rounded rudist fragments is due to pervasive re-crystallization. This facies is comparable to the coeval *well-rounded, coarse rudstone-to-grainstone* described in the Panormide Platform series by Di Stefano and Ruberti, (2000). In agreement with earlier interpretation by these authors, the rounding of the rudist fragments is likely the result of settling in a wave-agitated shelf or within a forebank environment. Consequently, FB2 is interpreted as the product of a prolonged action by wave/tidal currents reworking shoal environments on the platform margin.

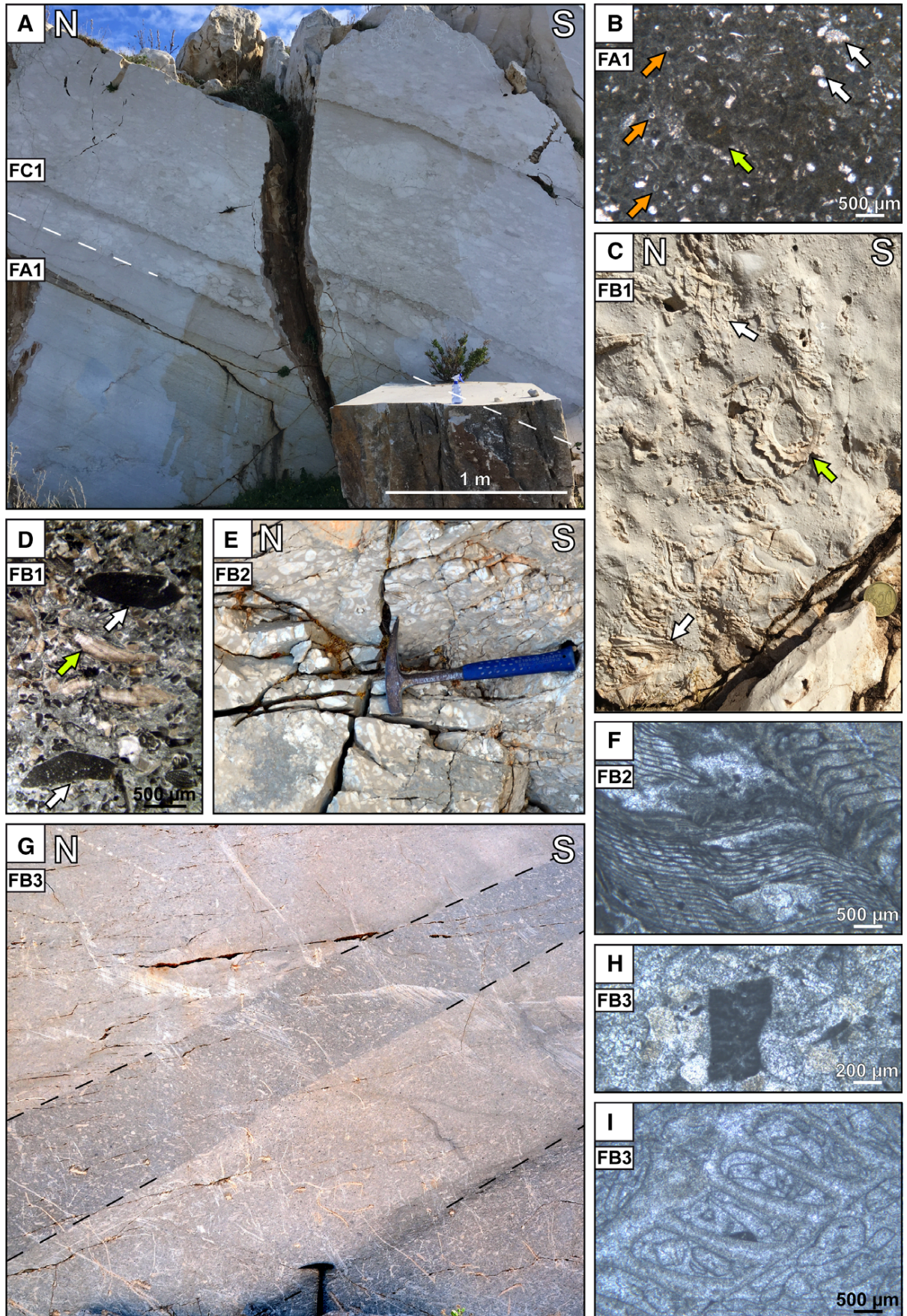
FB3 - Rudist bedded floatstone

Description. This facies occurs in thin to thick beds on the top of Mt Monaco above the aforementioned FB2 (location 12 in Fig. 3D). The components almost exclusively consist of well-sorted centimetre-sized rudist fragments, mostly derived from caprinid specimens (Fig. 4G). The grainstone texture shows skeletal grains and *T. morronensis* and rare fragments of benthic foraminifera (Fig. 4H).

Interpretation. These deposits accumulated in a high-energy platform margin setting (shoal, forebank) (Hughes, 2000; Al-Ghamdi, 2013). Based on thin section analysis most of the rudist fragments could be assigned to the Caprinidae family. The association of caprinids

(*Caprina* cfr. *schiosensis*; Fig. 4I) and orbitolinids suggest a Cenomanian age on the base of the biozonations proposed by Cestari and Sartorio (1995) and Chiocchini et al. (2008).

Fig. 4. Field and thin section photomicrographs of the facies associations A and B. (A) Noce Quarry - sharp contact between FA1 and FC1. (B) Photomicrograph of FA1 displaying a wackestone with calpionellids (orange arrows), echinoid fragments (white arrows) and *T. morronensis* (green arrow). (C) Mt. Sparagio top - rudist fragments (white arrows) and loose specimens (*Eoradiolites* sp., green arrow) in FB1. Coin for scale (2.1 cm diameter). (D) Photomicrograph of FB1 displaying a packstone-grainstone texture dominated by rudist fragments (green arrows) and Orbitolinidae (white arrows). (E) Mt. Monaco top - whitish rudist fragments rounded by wave abrasion (FB2). Hammer for scale (32.5 cm long). (F) Photomicrograph of FB2 showing a Radiolitidae fragment. (G) Mt. Monaco top - well-sorted rudist fragments in FB3. Hammer for scale (32.5 cm long). (H) Photomicrograph of FB2 showing a broken benthic foraminifer (*Cuneolina* sp.). (I) Photomicrograph of FB3 showing a grainstone texture with rudist fragments (cfr. *Caprina schiosensis*). All photomicrographs are taken in plane polarized light.



4.3. Facies Association C (FC)

This facies association combines calciclastic series - either bedded or massive - produced by gravitational collapse of well-cemented and/or poorly-cemented sediments (MTDs), mostly derived from platform margin environments. The dominant grain size of these slope deposits ranges from pebble to boulder size, and consist of clast-supported to matrix-supported breccias or, in places, of isolated blocks. The matrix of breccia bodies generally consists of finer (millimetre-scale) skeletal wackestone/grainstone or rudstone/floatstone. In this study the term “megabreccia” relates to massive or bedded sequences showing an abundance of metre-scale or larger sized boulders (*sensu* Bates and Jackson, 1984) that were either well-lithified (FC3), or poorly- lithified (FC4) at time of deposition.

FC1 - Bedded breccia with Ellipsactinia

Description. This facies consists of parallel bedded, clast- supported to matrix-supported and poorly-sorted, thin to very thick bedded breccias (Figs. 4A and 5A). Lithoclasts are very angular with dimensions ranging from pebble size to boulder dimensions. An upward inverse to normal grading is observed in some breccia beds. On the top of the beds, decimeter thick layers made up of finer-grained skeletal wackestone/packstone commonly occur (Fig. 5A). The sediment composition shows lithoclasts with *Ellipsactinia* sponges, corals and lithoclasts derived from the basement rocks (for example Rosso Ammonitico and peritidal limestones clasts; Fig. 5B). Other bioclasts identified are *Bacinella/Lithocodium* and *Tubiphytes morronensis* (Fig. 5C) and millimetre to decimetre-size corals and bryozoan fragments. Calcispheres and recrystallized planktonic foraminifera (very rare) are also found in the matrix. The nature of the grains in the breccia beds and in the overlying fine-grained cap is very similar. Centimetre-scale synsedimentary faults affecting FC1 are observed at Noce

Quarry (Fig. 5D). In the Custonaci area (Fig. 3E), the FC1 sediments that crop out along a Plio-Quaternary fault escarpment show northward dipping sigmoidal clinofolds (Fig. 5E).

Interpretation. FC1 is positioned above the Berriasian deposits (Fig. 4A). The presence of *Protopeneroplis ultragranulata* validates a Berriasian-Valanginian age for the lowermost beds. A Barremian/Lower Aptian age is inferred for the uppermost occurrences. The *Ellipsactinia* breccias are interpreted as calcidebrite deposits. The topmost, finer-grained deposits are derived from the turbidity cloud generated from grain sorting of sediments occurring at the snout of debris flows (Hampton, 1972). In the study area the fine-grained cap on top of the calcidebrites usually reaches a few decimetres in thickness. The presence of the FC1 coarse-grained litho-bioclastic deposits capping the FA1 *Tubiphytes*/calpionellid limestones (Fig. 4A) indicates a modification of the sedimentary regime. The occurrence of reef-derived bioclasts indicates the presence of an active coral/*Ellipsactinia* barrier reef rimming the steep slope. The presence of older clasts reflects the involvement of the underlying sedimentary substrate. The coarse-grained composition of the calcidebrite beds favoured a parallel-bedded slope geometry of the clinofolds with a down-dip inclination up to 35°. The scale of the studied outcrops (i.e. maximum 160 m) does not often allow for the determination the downslope thinning of the calcidebrite beds and/or downlap to planar surfaces. The outcrops strongly suggest that the thick successions of calcidebrite beds exposed in several quarries in the Mt Sparagio area are arranged in prograding, basinward dipping, clinofolds. Examples from slope settings show that clinofold-like geometries in outcrop can alternatively result from a progradation basinward (e.g. Rich, 1951; Bosellini, 1984; Maurer, 2000), or the up-dip onlapping of sedimentary bodies against the margin escarpment (e.g. Playton and Kerans, 2015a, b, 2018).

FC2 - Bedded megabreccia with rudists

Description. FC2 is the most widespread facies in the Mt. Sparagio area. This facies is organized in thick to very thick beds while the calcidebrite grains range from cobble to boulder sizes. It shows similarities with FC1 as it consists of bedded breccias with a finer grained cap (Fig. 5F). Differences with FC1 include: (i) the lithoclast composition, which is almost exclusively made up of rudist limestones; (ii) the size of the lithoclasts, as in FC2 metre-size boulders frequently occur, while small blocks are less; and (iii) the skeletal matrix between the lithoclasts, mainly revealing a rudist or rudist/orbitolinid packstone-rudstone (Fig. 5G). Well-preserved rudist specimens frequently occur in the matrix (Fig. 5H). In a similar fashion as for FC1, the same grain-types occur in both the breccia (at the base) and the topmost fine-grained cap (at the top). The well-bedded breccias are clast-supported, and often show inverse to normal grading (Fig. 5I). In places, the fine-grained cap is truncated upward by the overlying breccia bed. An irregular surface parallel to the bedding occurs on the top of a thick FC2 bed at Maiorana Quarry (Fig. 6A). In the Campicello Quarry, an uneven bowl-shaped surface about 12 m wide and 5 m deep filled with FC5 deposits affects the facies sequence consisting of FC2 and FC5 (Fig. 6B). Other sedimentary structures affect FC2, such as syndimentary faults with up to a couple of decimetre displacement occurring at Maiorana Quarry (Fig. 6C). Moreover, pinch-out geometries and imbricated clasts were observed in FC2 (Maiorana Quarry; Fig. 6C and D).

Interpretation. This facies occurs within the Aptian-Cenomanian interval as suggested by the rudist assemblage with predominant radiolitids and caprinids, and the occurrence of abundant orbitolinids (see Rudist Events D to H *sensu* Cestari and Sartorio, 1995) (localities 1, 3, 4, 5, 6, 17 in Fig. 3). FC2 is also present in the Coniacian (rudist assemblage with *Hippurites incisus*) to the lower Maastrichtian (*Orbitoides media*) (localities 7, 8, 10 and 18 in Fig. 3). Submarine carbonate breccia beds capped by a turbidite are interpreted as two-layer deposits in which the coarse calciclastic lower part is a calcidebrite while the fine-grained cap

is the result of a turbidity current that develops on top of the moving debris flow (Krause and Oldershaw, 1979; see also *FC1 - Bedded breccia with Ellipsactinia*). According to Krause and Oldershaw (1979) and Mullins and Cook (1986) a thickening of the bed cap can be observed in the downslope direction, which was accordingly observed in the study area (Fig. 5F). The bowl-shaped structure observed at Campicello quarry is interpreted as a decametre-size slump scar. The rough surfaces observed in FC2 have been interpreted as erosional structures created by the subsequent debris flows on the slope surface. The pinch-out geometries result from erosional truncations covered by downslope thickening wedges of sediments (white arrows in Fig. 6C). Such structures are interpreted as “intraformational truncation surfaces” or “cut and fill structures” (Wilson, 1969; McIlreath and James, 1978). Another explanation might be the sudden freezing of debris flows producing sharp pinch-out geometries (e.g. Talling et al., 2012, 2013). However, the deposits are clearly truncated upward by the subsequent debris flow. In all these examples, the erosive character of gravity flows is a common feature shown by the deposits. In various sedimentary environments where debris flows act as the main transport mechanism, imbrication of discoidal or flat pebbles/cobbles is frequently observed (Sohn et al., 2002). The orientation of the imbricated lithoclasts indicates the up-dip direction of the slope (Cook and Mullins, 1983), which in several FC2 calcidebrite beds (for example, Incammisa, Miceli and Maiorana quarries) suggests a northward down-dip orientation (Fig. 6D).

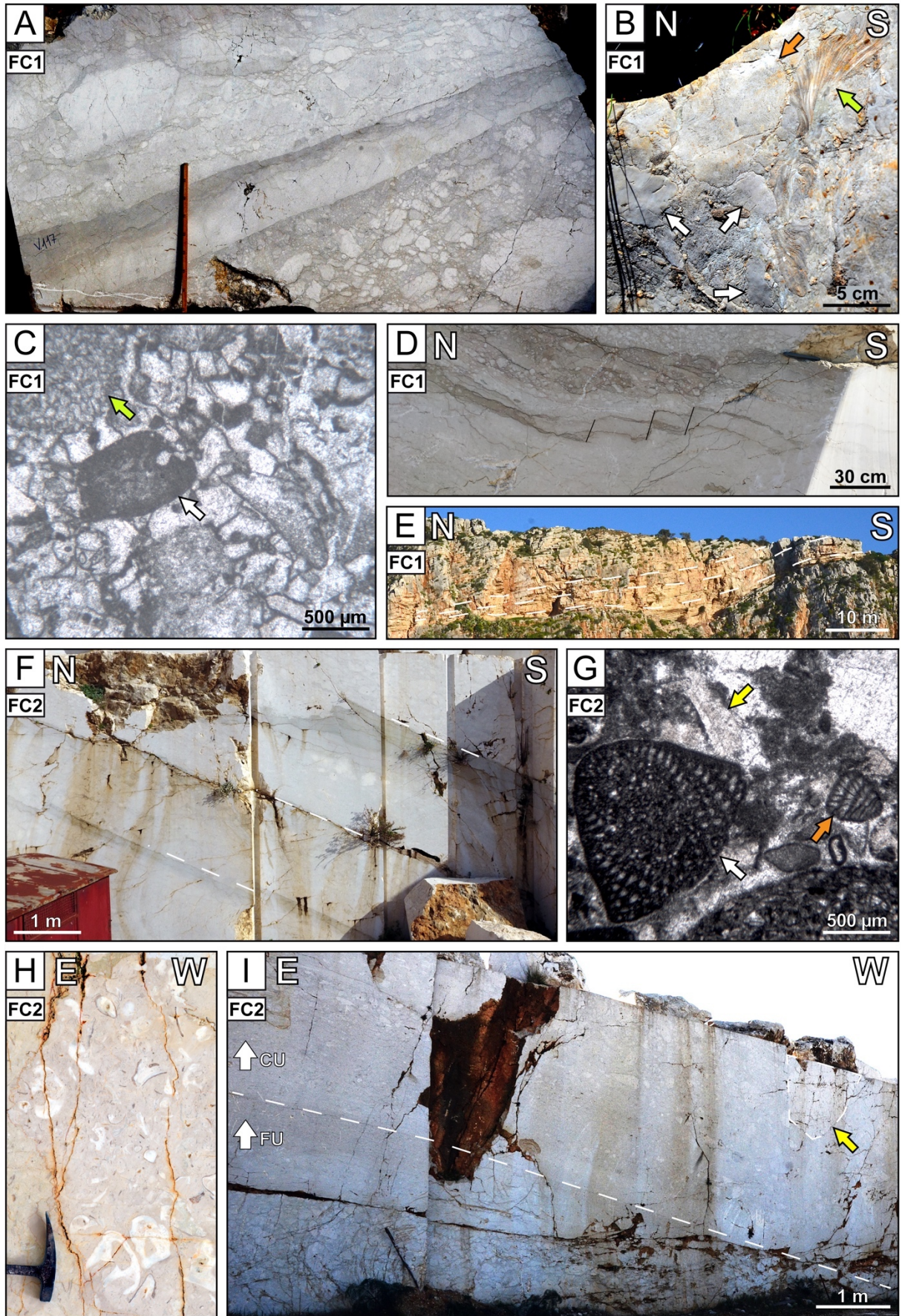


Fig. 5. Field and thin section photomicrographs of the Facies Association C. (A) Noce Quarry - breccia bed and finer grained level (above) reflecting a general fining-upward trend observed in a polished block (FC1). Scale bar=1 m. (B) Piano di Sopra - large skeletal fragments of *Ellipsactinia* (orange arrow), bryozoans (green arrow) and lithoclasts from the underlying substrate (white arrows) in FC1. (C) Photomicrograph of FC1 showing a grainstone texture with pervasive *Bacinella irregularis*, *Lithocodium aggregatum*, *Tubiphytes* (white arrow) and bryozoan (green arrow). (D) Noce Quarry - north dipping syndimentary faults in FC1. (E) Rocca Rumena - northward-dipping sigmoidal clinofolds (FC1). (F) Noce Quarry - breccia bed with fine grained cap (FC2). (G) Photomicrograph of FC3 of a packstone dominated by large Orbitolinidae (white arrows) and rudist fragments (green arrow). (H) Campicello Quarry - large rudist fragments embedded in skeletal rudstone/packstone (FC2). Hammerhead for scale (18.5 cm long). (I) Campicello Quarry - fining upward (FU) and coarsening upward (CU) trend and metre-size boulder (white arrow) in FC2. All photomicrographs are taken in plane polarized light.

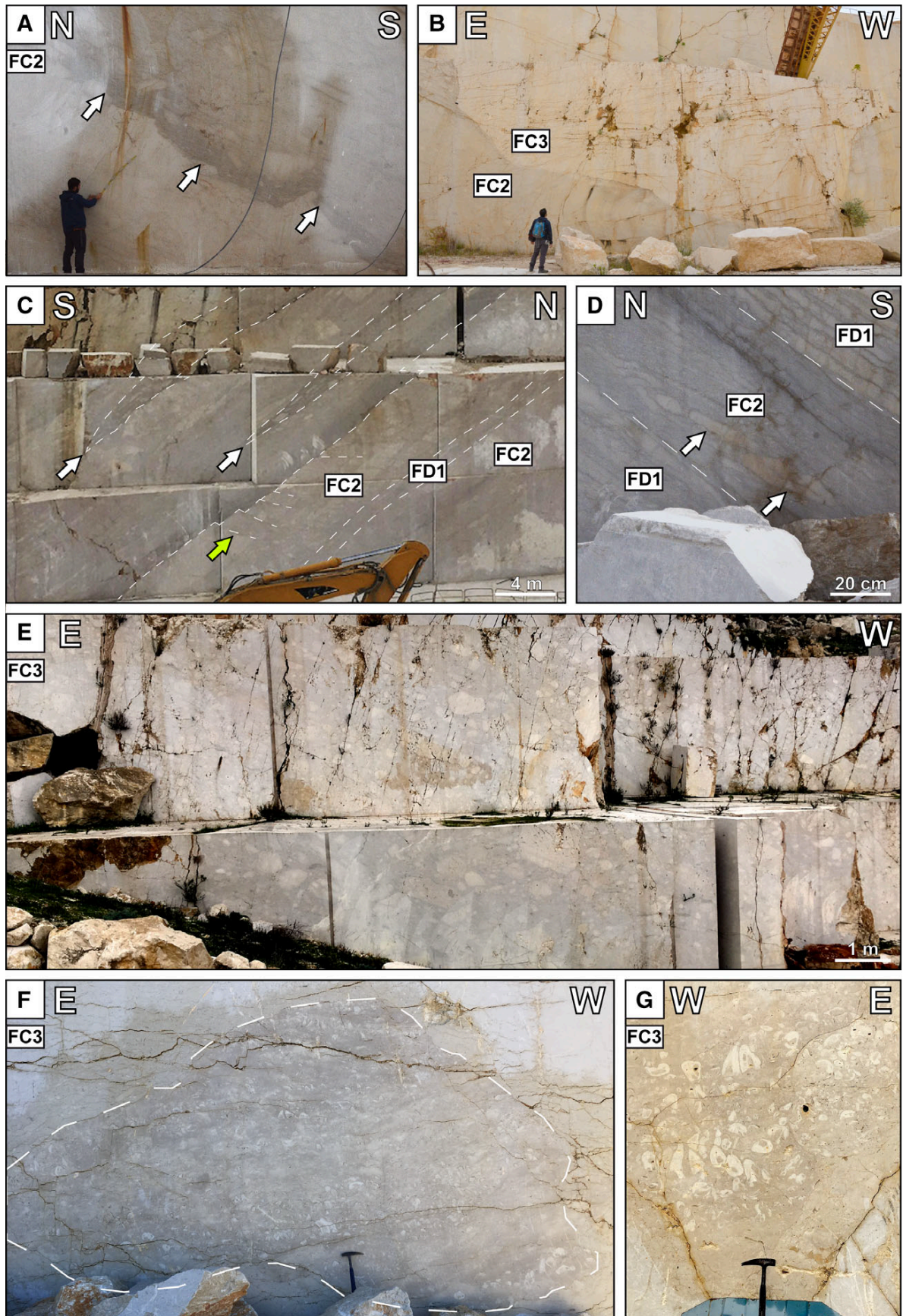
FC3 - Chaotic megabreccia

Description. FC3 consists of thick carbonate bodies (up to 40 m) made up of matrix-supported megabreccias (Fig. 6E). They mainly occur in the south-western sector of the study area (locations 1, 2, 3, 15 and 16 in Fig. 3). The lithoclasts are highly variable in shape and size and chaotically distributed in the individual carbonate bodies. Very angular metre-size boulders prevail, but moderately rounded lithoclasts are also present. Most of the constituents are derived from a Cretaceous reef margin as shown by the occurrence of rudist colonies (boundstone; Fig. 6F and G). The lower part of the Bova Quarry (Fig. 3E) exposes boulders and blocks consisting of rudist boundstone and coral, sponge and chaetetid rudstone (known under the tradename of *Crema di Roccia*, Rocky Cream; Fig. 7A and B). In addition, lithoclasts containing *Ellipsactinia* breccias and ammonitic limestones (Jurassic) can be found. *Aptychi* and/or planktonic foraminifera-bearing clay chips are also present. The rudstone/packstone matrix mainly consists of rudist fragments and orbitolinids. Stylolites are frequent in the matrix, but do not cross the lithoclasts. In the study area, this facies is always located close to submarine basalt intercalations (Noce Pond, Forgia Outcrop; Fig. 3B and E) or slump scars (Bova Quarry, Campicello Quarry; Fig. 3E). Several sharp concave-up

erosional truncations (5-10 m) affect the WSCE. They are well exposed in several quarry walls in the Custonaci area (Fig. 3E) with the most outstanding example affecting FC3 (Fig. 7C and D). In the Bova Quarry (Fig. 3E), FC2 is obliquely truncated (Fig. 7C) and overlapped by a bedded sedimentary infill (FC3).

Interpretation. The fossil content in the matrix of FC3 allows the stratigraphic distribution of this facies to be constrained to the Barremian–Aptian (locality 1 in Fig. 3B) as suggested by the presence of *Moesiloculina danubiana* and to the Albian–Cenomanian (locality 3, 15 and 16 in Fig. 3B and E) as supported by abundant specimens of *Mesorbitolina* sp. and *Conicorbitolina* sp. The presence of lithoclasts derived from the underlying Jurassic substrate and the frequent occurrence of chaotic masses with boulders suggest that the settling of FC3 is related to rock falls or avalanches generated along steep scarps. The coarse and very coarse boulders in FC3 show a down-dip toppling (Varnes, 1978) consistent with the underlying pinch-out geometry of FC5 (Fig. 7D). Many truncation structures involving FC3 are interpreted as slump scars produced by the collapse of pre-lithified material in a talus environment.

Fig. 6. Field and thin section photomicrographs of the Facies Associations C. (A) Maiorana Quarry - sharp erosional surface (arrows) affecting the top of a FC2 calcidebrite. Geologist for scale, *ca.* 1,8 m tall. (B) Campicello Quarry - metre-scale, bowl-shaped slump scar truncating FC2. Geologist for scale, *ca.* 1.8 m tall. (C) Maiorana Quarry - panoramic view of wire-cut walls displaying northward dipping synsedimentary faults (green arrow) and cut-and-fill structures (white arrows) in FC2 - FD1 facies stacking. (D) Maiorana Quarry - large tabular lithoclasts in FC2 showing a southward (up-slope) imbrication. Lithoclasts are calciturbidite fragments indicating the “cannibalization” of the slope sediments. (E) Noce Quarry - massive and chaotic megabreccia body (FC3). (F) Campicello Quarry - metre-scale boulder in FC3. Consistent upside-down life position of the rudists suggests a provenance from a rudist shoals. Hammer for scale (32.5 cm long). (G) Bova Quarry - overturned boulder consisting in a boundstone with radiolitids arranged in life position (FC3). Hammer for scale (32.5 cm long).



FC4 - Chaotic megabreccia with poorly-cemented lithoclasts

Description. This facies comprises up to 20 m thick sediment bodies of matrix-supported megabreccias. It is widespread in the Western Mt Sparagio area and was observed in detail in the wire-cut walls of Simona Quarry (i.e. location 4 in Fig. 3B). The lithoclasts are highly variable in shape and size (from pebbles to boulders) and are relatively well-rounded. FC4 differs from FC3 while it contains lithoclasts with a blurry outlined outer shape (Fig. 7E and F) commonly highlighted by stylolites. In places well-lithified lithoclasts occur. Both matrix and lithoclasts exhibit similar types of grains which consist of rudstone-packstone dominated almost exclusively by rudist fragments and orbitolinids. Lithoclasts are frequently densely-packed limiting the amount of matrix. They can display plastic deformation (Fig. 7G). One specific characteristic of FC4 is the occurrence of lithoclasts dominated by orbitolinids. Rudist fragments are commonly well-sorted, but poor sorting also occurs.

Interpretation. FC4 was deposited during the Cenomanian as supported by the occurrence of abundant large orbitolinids (e.g. *Conicorbitolina* sp.). The blurry outline of the lithoclasts is most likely due to poor lithification and partial dissolution of the outer part of the clasts. The lithoclasts are packed and show plastic deformation that probably results from downdip movement of a high-density gravity flow. These carbonate bodies result from downslope-migrating sediment masses involving surficial unlithified sediments and the underlying semi-lithified strata.

FC5 - Lenticular fine-grained skeletal limestones

Description. This facies is organized in thin beds consisting of very fine-grained (micron to millimetre-size) skeletal grainstone grading upward into packstone and/or wackestone (Fig. 7H). Sometimes beds show metre-scale lobate geometries (Fig. 7I). Clear downdip pinch-outs can also be observed (Fig. 7D). The skeletal grains of FC5 are well-sorted and associated with minor pelagic elements such as calcispheres.

Interpretation. FC5 revealed no valuable biomarkers that could be used to determine the age of this deposit. Notwithstanding, its stratigraphic position allowed assigning FC5 to the Albian-Cenomanian (location 16 in Fig. 3E) and lower Senonian (location 7 in Fig. 3B). Well-sorted skeletal grains have been interpreted as very fine rudist debris. FC5 results from turbidites that originated from the flow transformation between cohesive debris flows and low-density turbidity currents. Pinch-out geometries observed in FC5 are related to the down-dip thinning of calciturbidite beds (Fig. 7D, dashed lines).

4.4. Facies Association D (FD)

The facies association comprises two facies characterized by thin to very thin beds composed of well-sorted fine to very fine-grained sediments (micron to millimetre-size). Such features are comparable with those observed in facies association A, but strongly differ from those of facies association B and C. Rudist fragments are still one of the main constituents in facies association D.

FD1 - Fine-grained skeletal limestones

Description. FD1 occurs as thin to very thin parallel beds of whitish, fine-grained skeletal grainstones. Closely-packed and well-sorted rudist fragments up to 1 mm in size dominate the deposits. Sedimentary structures such as upper plane bedding (Fig. 7J), soft-sediment deformation and synsedimentary faults (Fig. 7K) have also been observed. Centimetre-scale synsedimentary faults affecting FD1 were observed in the Maiorana Quarry (Fig. 3B).

Interpretation. The stratigraphic position and the facies analysis suggest that FD1 was deposited during the Coniacian to Maastrichtian (locations 8, 10 and 18 in Fig. 3). Unlike what was observed in FC5, no lobate geometries and/or pinch-out terminations occur in FD1.

These deposits are interpreted as the distal parts of turbidites in continuation with FC5 deposits. This observation is supported by the gradual transition to pelagites of FD2.

FD2 - Lime mudstone with planktonic foraminifera

Description. Thin to very thin bedded wackestone to mudstone characterize the sediments of this facies. FD2 crops out in the south-western and in the south-eastern sectors of the study area (locations 8, 10 and 18 in Fig. 3). Planktonic foraminifera, rudist fragments, calcispheres, and sponge spicules were identified as the most abundant constituents (Fig. 7L). Chert nodules also occur at certain levels. In this facies, centimetre-scale syndimentary faults were observed in the Maiorana Quarry.

Interpretation. On the basis of the biozonation proposed by Premoli Silva and Verga (2004), the identified planktonic foraminifer assemblages allow ascribing FD2 to the late Berriasian–Hauterivian (*Favusella hauterivica* Zone) (location 11 in Fig. 3D), to the Santonian (*Dicarinella asymetrica* Zone) (locations 8 and 10 in Fig. 3B and C) and to the Campanian–Maastrichtian (*Globotruncanita elevata*) (location 18 in Fig. 3E). The facies is interpreted as a pelagic sediment (background sedimentation) deposited in the slope to basin and basin area.

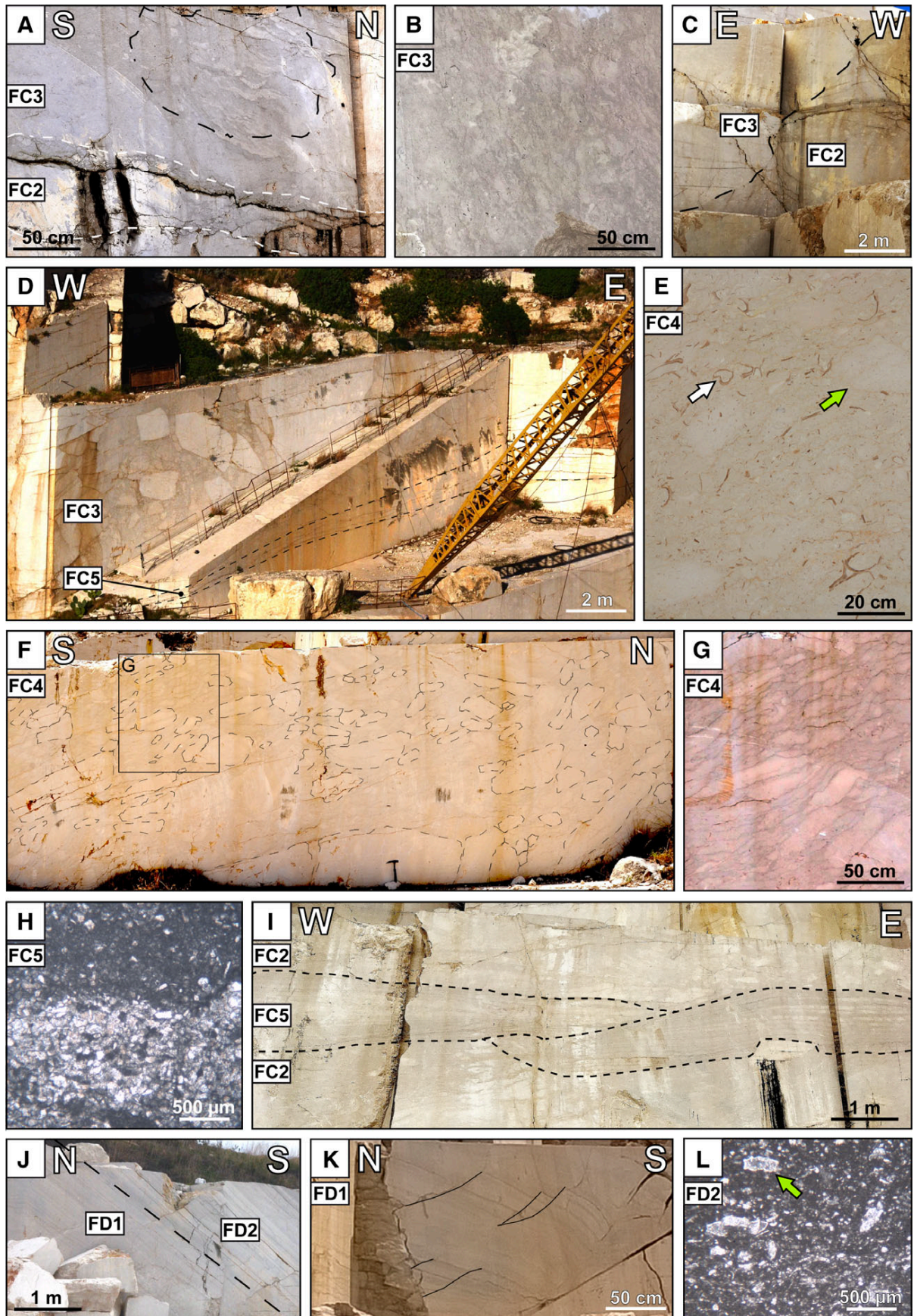


Fig. 7. Field and thin section photomicrographs of the Facies Associations C and D. (A) Bova Quarry - facies stacking showing the upward transition between bedded calcidebrites (FC2) and coarse megabreccia (FC3). The latter reveals a large boulder showing the same features described in Fig. 7B (dashed lines). (B) Bova Quarry - polished block that consist of rudstone with massive corals, calcareous sponges/chaetetids and rudists fragments embedded in a skeletal matrix (FC3). Hammer for scale (32.5 cm long). (C) Bova Quarry - metre-scale slump scar showing abrupt contact between FC2 and FC3. (D) Campicello Quarry - thick megabreccia body (FC3) made-up with metre-scale angular lithoclasts. The boulders are interpreted as part of the same block, fragmented during a massive rock fall. The toppling of the boulders suggests a westward-oriented movement. The downslope movement direction is consistent with the pinch-out geometry suggested by the underlying turbidite beds (FC5, dashed lines). (E) FC4 polished block exhibiting large rudist fragments (white arrow) and poorly-cemented lithoclasts (green arrow). (F) Simona Quarry - early lithified lithoclasts revealed on a wire-cut wall (FC4). Hammer for scale (32.5 cm long). (G) Simona Quarry - poorly-cemented lithoclasts displaying a significant packing and consistent orientation (FC4). (H) Photomicrograph of FC5 that consists of an alternation of skeletal grainstone and wackestone. (I) Miceli Quarry - wire-cut wall exhibiting an alternation of rudist calcidebrite (FC2) and calciturbidites (FC5) with a suggested channel-levee geometry. (J) Maiorana Quarry - transition between fine-grained skeletal limestone (FD1) and the overlying lime mudstone with planktonic foraminifera (FD2). (K) Maiorana Quarry - northward-dipping syndepositional faults in FD1. (L) Photomicrograph of FD2 showing a wackestone rich in planktonic foraminifera. *Globotruncana linneiana* is shown (green arrow). All photomicrographs are taken in plane polarized light.

5. Facies stacking

The vertical facies succession along the WSCE is exposed in several sectors, namely, Western Mt Sparagio, Eastern Mt Sparagio, Mt Monaco and Custonaci (Figs. 8 and 9). Each sector comprises several sections described in stratigraphic order and followed by interpretations related to the inferred sedimentary evolution. The correlation between the different sections is based on biostratigraphic data and their stratigraphic position (Table 3; Fig. 8).

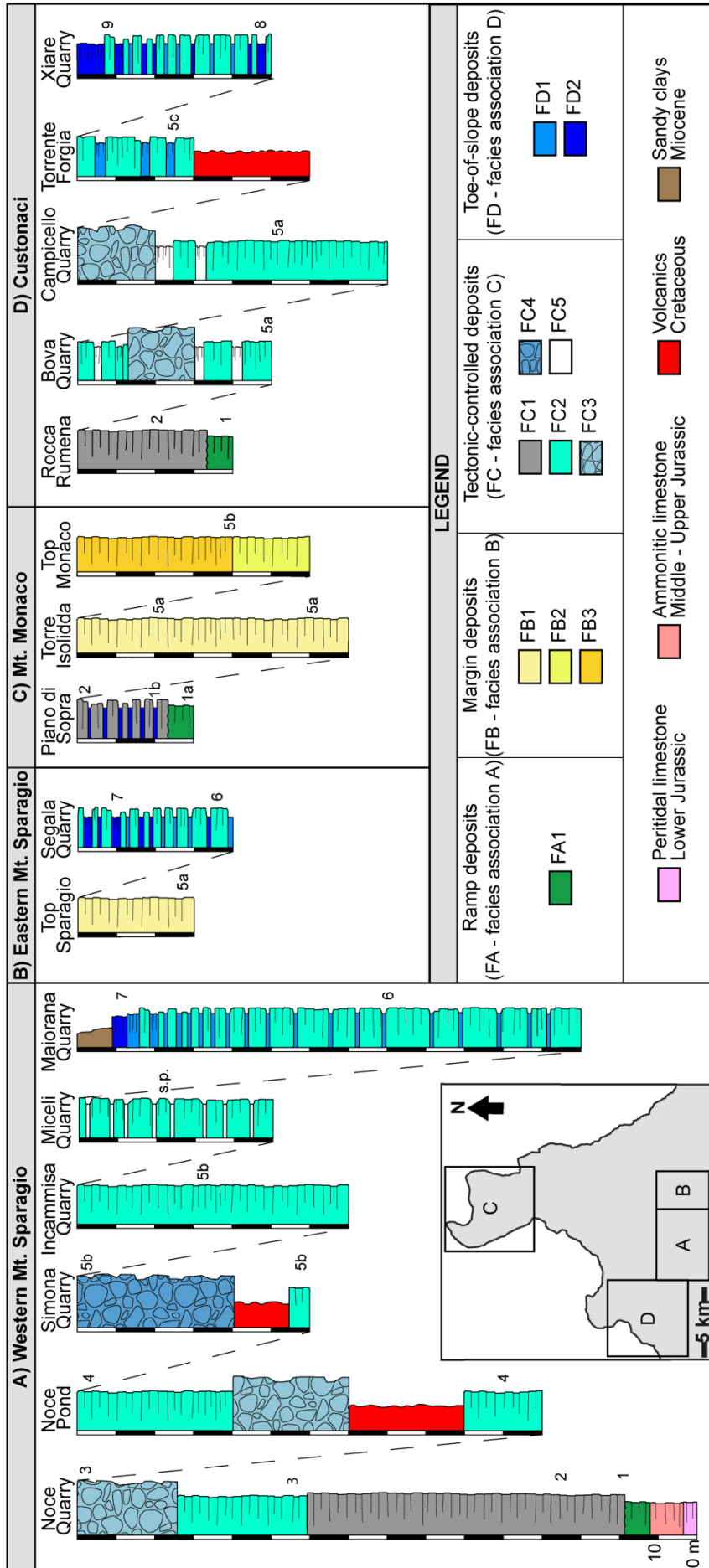


Fig. 8. Stratigraphic sections in the Western Mt. Sparagio, Eastern Mt. Sparagio, Mt. Monaco and Custonaci areas. Simplified map of the study area is shown in the lower left. For further details related to the quarry locations, see Fig. 3. Numbers refers to biomarkers and biozones identified in the different sections as reported in Table 3; s.p. stands for correlation based on stratigraphic position.

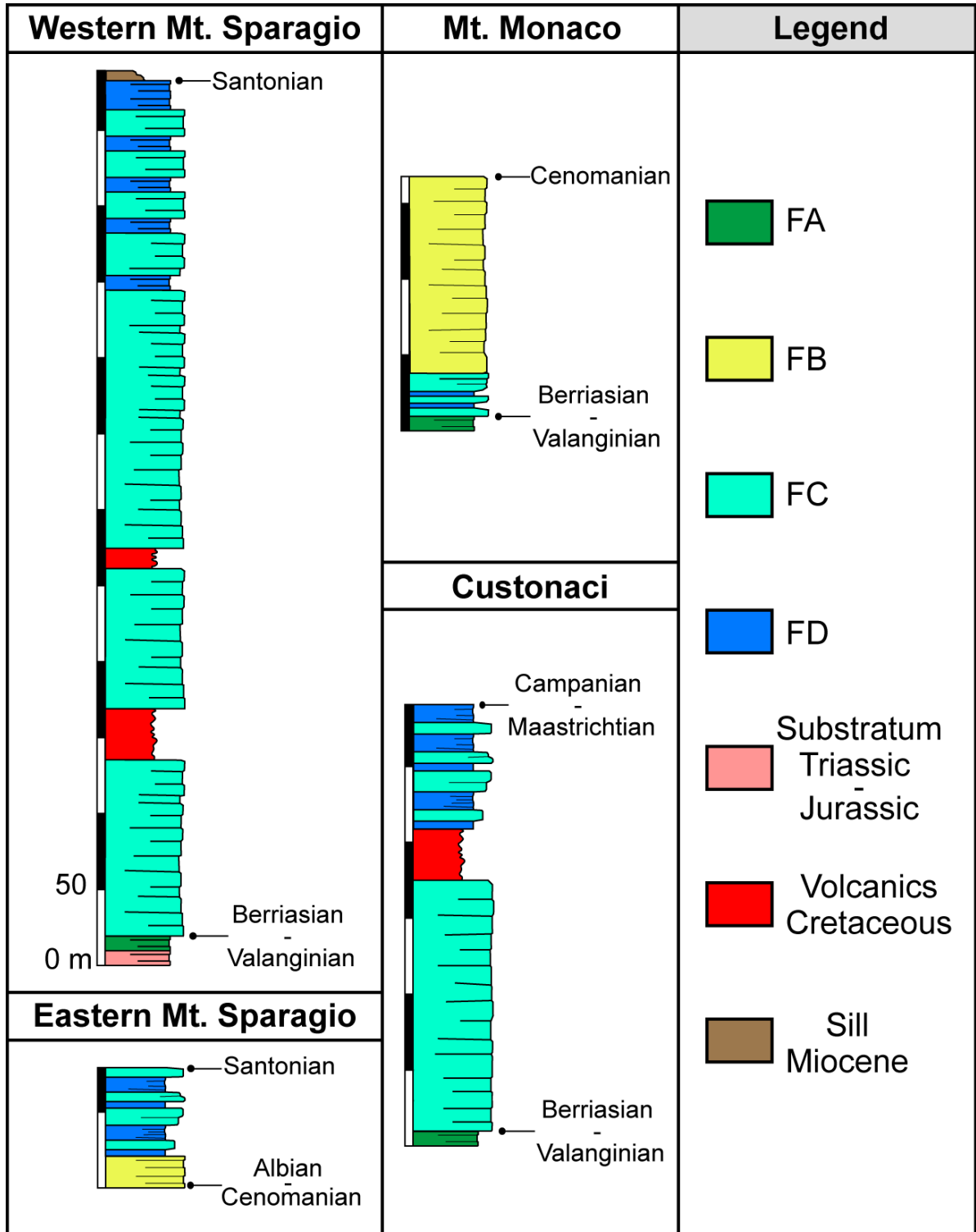


Fig. 9. Composite lithostratigraphy based on sections presented in Fig. 8 and showing the vertical distribution of the facies associations in the four sectors of the Western Sicily Cretaceous Escarpment (WSCE).

5.1. Western Mount Sparagio

The facies succession in this area was reconstructed using six exposures distributed along a WNW-ESE direction (Fig. 3B). Most of the sections are exposed in the frontal part of a ramp anticline dipping southward with a 30 to 40° angles.

The oldest Cretaceous facies (Berriasian) are exposed in the Noce Quarry and consist of calpionellid/*Tubiphytes* limestones (FA1). They are truncated upward by *Ellipsactinia* breccias (FC1), which in turn pass over to thick (*ca* 35 m at Noce Quarry) and regularly bedded rudists calcidebrites (FC2). An erosional surface marks the upward transition to a matrix-supported megabreccia with lithoclasts of rudist limestones (FC3) containing minor lithoclasts of the underlying Jurassic substratum. The abrupt contact between fine-grained limestones with calpionellids and *Tubiphytes* (FA1) and bedded breccias with *Ellipsactinia* (FC1) is interpreted as a tectonically-driven change in depositional profile from a gentle ramp to a steep, escarpment-type of slope. Instabilities during this period are recorded with the emplacement of chaotic megabreccias (FC3).

In the nearby Noce Pond locality, in stratigraphic continuity with Noce Quarry (Fig. 8), early Albian bedded calcidebrites of FC2 are exposed in the lower part of the section and are interrupted by heavily altered volcanics (tuffites). Chaotic megabreccias (FC3) and bedded calcidebrites (FC2) lacking fine-grained caps are found above the volcanites.

In the Simona Quarry the next segment of the Cretaceous facies succession in Western Mt. Sparagio area crops out. This late Albian-Cenomanian section, consists of a few metres of bedded calcidebrites (FC2) covered by 15 m of altered pillow lavas and tuffites (Fig. 10). The section continues with a chaotic megabreccia body containing poorly-cemented lithoclasts (FC4) with orbitolinid and rudist rudstone to floatstone.

In the Incammisa Quarry, a thick series of calcidebrites with rudists (*ca* 70 m) are exposed, identified as FC2. In the Miceli quarry they are succeeded by an alternation of bedded megabreccia with rudists (FC2), and fine-grained skeletal limestones (FC5) with

lenticular to convex-up bodies (Fig. 7I). The presence of breccia boulders in FC2 account for re-deposition, cannibalization of the slope deposits along the WSCE (Chiocci et al., 2003; Pickering and Corregidor, 2005).

The Maiorana Quarry section forms the upper part of the Cretaceous succession in the western Mt Sparagio area (Figs. 3B and 8). Together with the Incammisa and Miceli Quarry sections, it covers a Cenomanian to Coniacian time interval. This section shows an alternation of well-bedded calcidebrites (FC2) and fine-grained skeletal limestones (FD1). FC2 is characterized by metre-sized, sub-rounded to rectangular boulders (Fig. 11) and *Hippurites incisus* as a main skeletal element. In places, angular, tabular-like lithoclasts reaching up to 2 m across with an upslope imbrication supports a northward transport direction (Fig. 6D). The facies succession describes a fining-upward sequence with increasing occurrence of fine-grained turbidites (FD1) (Figs. 8 and 9). A gradual transition to planktonic foraminifera -rich mudstones (FD2) is observed (Fig. 7J). The latter trend points to the onset of a pelagic sedimentation during Santonian in this area. An erosional truncation marks the contact upward with Miocene deposits.

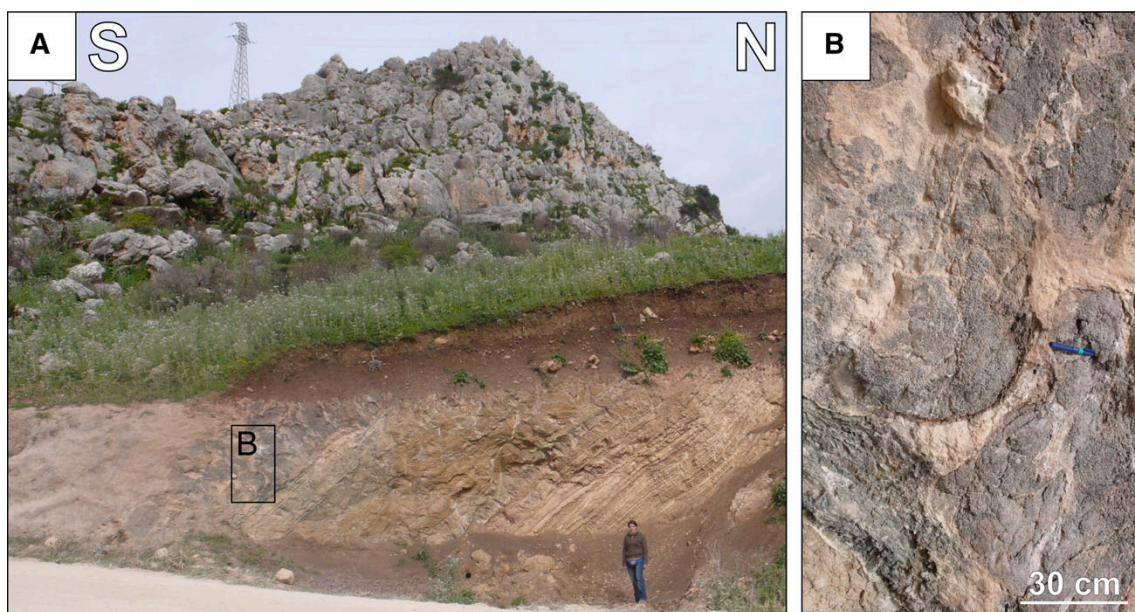


Fig. 10. (A) Altered tuffs and pillow basalts cropping out in the Western Mt. Sparagio area. Geologist for scale, *ca* 1.8 m tall. (B) Close-up of altered pillow basalts.

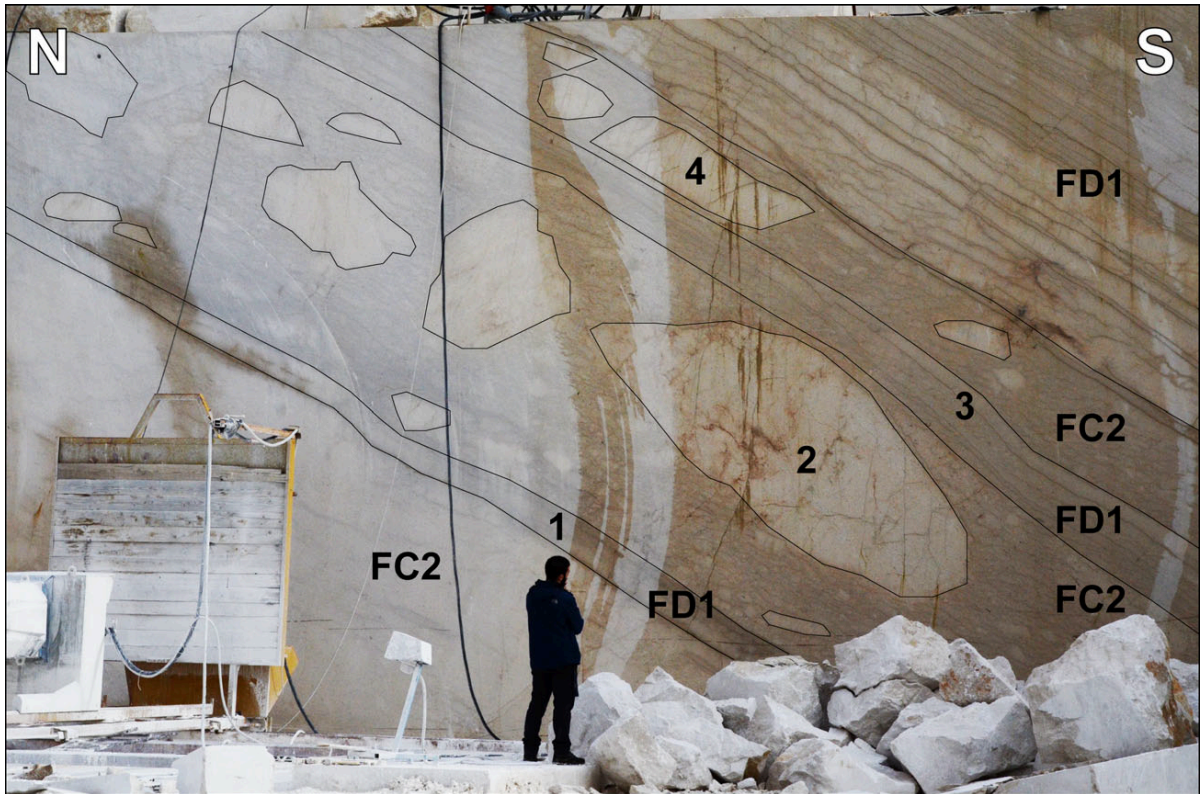


Fig. 11. Facies stacking in the Maiorana Quarry section. From the base to the top: 1 = FD1 consisting in thin beds of skeletal grainstones; 2 = FC2 characterized by large boulders floating in a rudstone matrix; 3 = FD1 accommodating the hummocky topography created by the boulders; 4 = FC2 showing large rectangular lithoclasts overlain by thin beds of FD1. Geologist for scale, *ca* 1.8 m tall.

5.2. Eastern Mount Sparagio

The Mt Sparagio top and Segala Quarries expose parts of the Cretaceous succession forming a north-south transect in the eastern part of Mt Sparagio (Fig. 3C). The Mt Sparagio top section shows rudist rudstone to floatstone (FB1) containing loose radiolitid specimens and benthic foraminifera that suggest a platform margin depositional setting. The Segala Quarry section contains calciturbidites (FD1) and lime mudstones rich in planktonic foraminifera (FD2) interbedded with coarse calcidebrites (FC2). The biostratigraphic content in FD2 establishes the correlation with the Maiorana Quarry section (Western Mt Sparagio; Figs 8 and 9). However, unlike the Maiorana Quarry section where pelagic conditions prevail, coarse calcidebrites (FC2) characterize the Segala Quarry.

The Eastern Mt Sparagio succession shows the evolution from a Cenomanian platform margin to a Coniacian-Santonian “toe of slope” domain. Both the downfaulting of a segment of the platform edge and the backstepping of the WSCE in this area support this observation.

5.3. Mount Monaco

The sections at Piano di Sopra, Mt Monaco top, and Torre Isolidda expose the facies succession in the northern zone of the study area (Fig. 3D). However, the quality of exposures is not optimal due to Cenozoic tectonic processes and Quaternary detrital cover.

At Piano di Sopra (Fig. 3D), the lowermost part of the WSCE shows a sharp contact between the FA1 and FC1 as also observed in the Western Mt Sparagio area. Similarities between the two sections, for example, facies arrangement and biostratigraphic content, suggest a synchronous (Berriasian-Valanginian) evolution from a gentle ramp to a steep, tectonically-controlled escarpment between the two localities, presently situated 14 km apart.

The Torre Isolidda section exclusively exposes rudist floatstone-rudstone (FB1). The biota composition of this facies agrees with a platform margin setting. The foramol assemblage suggests that the FB1 at this locality spans from the Albian to the Cenomanian. The section at Mt Monaco top also shows typical platform margin facies (FB) with rudstone containing rounded rudist fragments (FB2) overlain by rudist bedded floatstone (FB3).

Facies association FB at Mt Monaco and Eastern Mt Sparagio areas are nearly coeval based on the biostratigraphic content. The sediments in both outcrops can be considered as the most proximal deposits in the whole study area. Moreover, the upward facies evolution from FC to FB suggests a progradation of the carbonate platform margin on the slope deposits that is constrained by the biostratigraphic data to the Albian-Cenomanian interval.

5.4. *Custonaci*

The Cretaceous facies succession in the westernmost sector of the Capo San Vito Peninsula (Fig. 3), following an ENE-WSW transect, comprises the Rocca Rumena outcrop, the Bova and Campicello Quarries, the Torrente Forgia outcrop and the Xiare Quarry (Fig. 3E). The lowermost part of the succession at Rocca Rumena exposes the same sharp facies contact between calpionellid/*Tubiphytes* limestones (FA1) and well-bedded calcidebrites (FC1) as previously described for the Western Mt Sparagio and Mt Monaco areas.

In the Bova Quarry section, a thick (18 m) chaotic megabreccia body (FC3) occurs embedded within an alternation of rudist calcidebrites (FC2) and fine-grained limestones (FC5). The former reveals large rudist boundstone blocks and boulders with corals, sponges and chaetetids. Alternations of well-bedded calcidebrites (FC2) and lenticular skeletal fine-grained limestones (FC5) form the top of the section. The presence of a large number of boundstone blocks suggests the proximity of the productive platform margin. The foramol assemblage in the FC2 matrix indicates an Albian-Cenomanian age.

The Campicello Quarry section consists of rudist calcidebrites (FC2) in the lower part, followed by a series of interbedded skeletal turbidites (FC5) in turn overlain by a chaotic megabreccia (FC3). The last facies supports a major episode of instability that can be biostratigraphically-constrained to the Albian-Cenomanian (similarly as for Miceli Quarry).

The Torrente Forgia outcrop exposes the upward development of the facies succession that consists of altered volcanics overlain by rudist calcidebrites (FC2) and calciturbidites (FD1) alternations. The matrix of FC2 is rich in planktonic foraminifera, rudists and benthic foraminifera that allow to constrain the volcanic intercalation to the upper Cenomanian.

The uppermost part of the Cretaceous succession in the Custonaci area is exposed at Xiare Quarry (Fig. 3E). This section consists of an alternation of calcidebrites (FC2), skeletal

turbidites (FD1) and lime mudstone with planktonic foraminifera (FD2). The latter predominates in the uppermost part of the section. Biostratigraphic analyses indicate a late Campanian-early Maastrichtian age for these deposits. The interfingering of distal low-density flow beds (FC2 and FD1) and pelagites (FD2) suggests a toe of slope to basin depositional environment for these deposits.

6. Discussion

The physiography and the evolution of the Western Sicily Cretaceous Escarpment (WSCE) during the Cretaceous was reconstructed using: (i) the facies links with the source area, (ii) the stratigraphic architecture and correlation of sediment bodies; and (iii) the presence of volcanic intercalations. Furthermore, the sedimentary features of the WSCE were compared with other tectonically-controlled examples and its evolution was linked to the geodynamic scenario of the western Tethys.

6.1 Volcanic intercalations

The volcanic rocks along the WSCE consist of fine-grained tuffs with a glassy structure, in places associated with pillow lavas that are characterized by a porphyritic texture with plagioclase, augitic pyroxene as well as rare olivine, iron and titanium oxides (Fig. 10) (Bellia et al., 1981). No absolute age constraints are available as a result of weathering processes affecting these volcanics, hence, their age is based on biostratigraphic data of the surrounding slope carbonates. According to Bellia et al. (1981), they are respectively related to “middle” and Upper Cretaceous-Eocene intervals in the Western Mt Sparagio and Custonaci areas (Fig. 3B and E). Biostratigraphic data acquired in this study for the Western Mt. Sparagio area suggest lower Albian and upper Albian-lower Cenomanian ages (Noce Pond and Simona Quarry sections), while a Cenomanian-lowermost Turonian age is proposed for the Custonaci area (Torrente Forgia outcrop).

Geochemical analyses of the magmatic rocks using Nb/Y, Zr/P₂O₅ and Zr/TiO₂ ratios indicate that the volcanic intercalations result from a continental alkaline magmatism. Higher TiO₂ contents were detected in comparison with the Jurassic tholeiitic rocks of western Sicily (Bellia et al., 1981), which directly relates to enhanced pressure (MacGregor, 1969) but is unrelated to the alkalinity level (Chayes, 1965). The volcanic effusions of the WSCE thus originated from a magma generated at great depth likely linked to extensional crustal faults within an extensional/transensional tectonic regime (Bellia et al., 1981).

6.2. *Physiography of the Western Sicily Cretaceous Escarpment*

Slope carbonates of the WSCE presently form a 600 m thick accumulation extending over a distance of about 15 km and exposed over 225 km². The effective extension of the slope most likely is largely underestimated considering the shortening related to the Maghrebian orogeny. The uncertainties for an accurate restoration of the WSCE-physiography are: (i) the intensive Maghrebian contraction of the original crustal sector (Nigro and Renda, 1999), (ii) the clockwise rotations (up to 90°) of the thrust sheets (Oldow et al., 1990; Speranza et al., 2000); and (iii) the extensional/transensional post-orogenic displacements (Abate et al., 1993). Analyzing the sediment composition, the WSCE can be classified as a debris-dominated slope apron (*sensu* Playton et al., 2010) as megabreccias (FC2, FC3 and FC4) are the most abundant deposits. The original slope angle of the WSCE can be estimated based on the grain-supported fabrics, that with or without mud can reach angles of repose between 20° and 35° (Kenter, 1990). Slump scars occurring in the slope deposits (Figs. 6B and 7C and D) as well as reworked slope lithoclasts (Fig. 6D) suggest that the sediment source was not exclusively located on the platform (Fig. 12). Specific paleoslope indicators were retrieved:

(1) In the Western Mt Sparagio, where soft-sediment deformations and syndimentary extensional faults are all consistent with a northward orientation of the slope (Figs. 5D, 6C and 7K). A similar downslope direction is supported by the imbricated clasts in

some calcidebrites from this area (Fig. 6D). Moreover, the orientation of the lobate geometries at Miceli Quarry are a possible further indication of a south-north outlined slope (Fig. 7I).

(2) In the Custonaci area, the toppling orientation of large megabreccia boulders and pinch-out geometries suggest a west-orientated downslope direction (for example, Rocca Rumena, Fig. 5E; Campicello Quarry, Fig. 7D). Hence, the acquired data suggest at least two main downslope directions of the WSCE, i.e. northward for the Western Mt Sparagio area, and westward for the Custonaci area. Taking into consideration the clockwise rotations of about 90° experienced by the tectonic units of the area, the possible corrected palaeoslope directions would be towards the west and the south.

The divergent slope orientation of the WSCE is not surprising, because several studies on modern carbonate slopes (for example Bahamas) discussed the morphological heterogeneity over relatively short distances (Tournadour et al., 2015; 2017). Scalloped margins can form pluri-kilometre bankward-convex embayments (Mullins and Hine, 1989), which have been described both in modern and ancient studies and relate to catastrophic margin collapses causing failures of massive sediment bodies (Mullins and Hine, 1989; Jo et al., 2015). An embayment configuration was recently proposed for the Apulian Platform margin in Italy to explain the co-occurrence of eastward and southward oriented slope aprons in the Gargano area (Hairabian et al., 2015). Similarly, the various slope orientation and dip directions observed for the WSCE suggest a physiography that most likely was characterized by km-scale embayments.

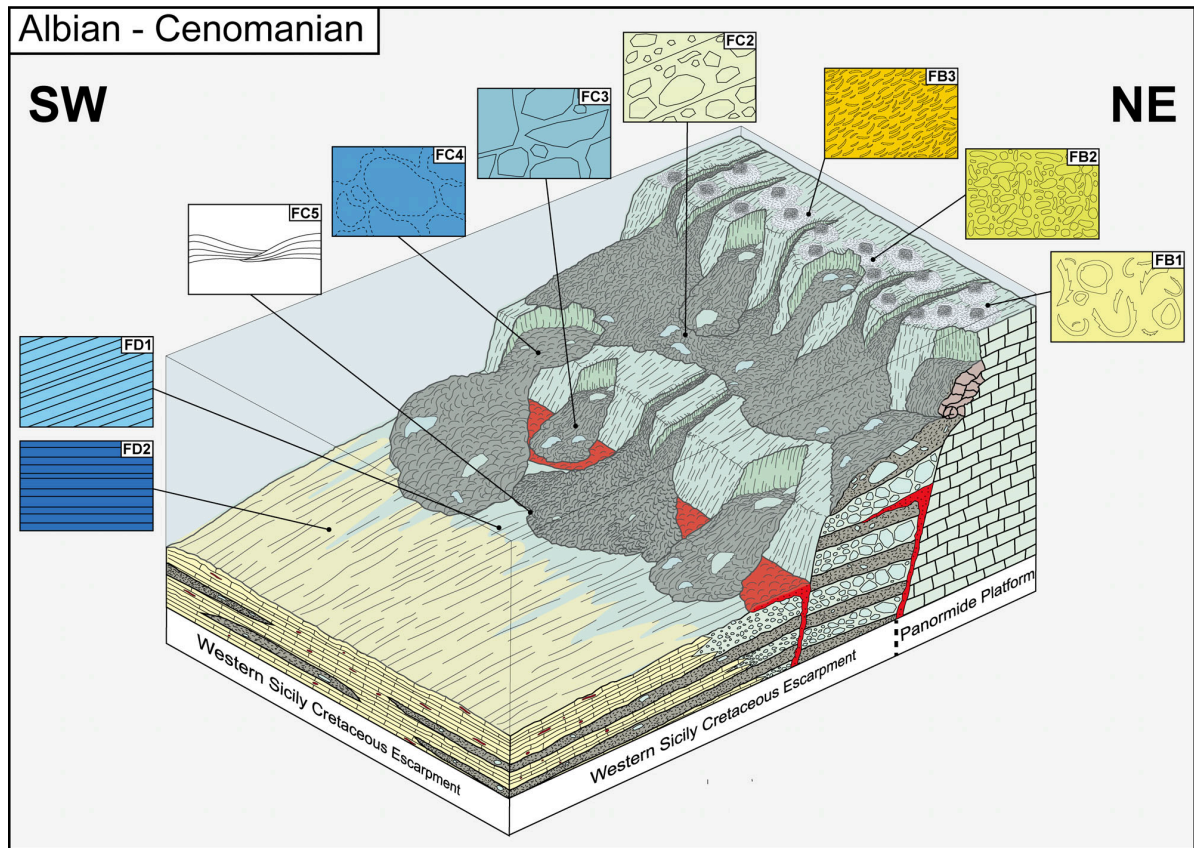


Fig. 12. Proposed three-dimensional model showing the depositional environment and associated facies distribution along the Western Sicily Cretaceous Escarpment (WSCE) during the Albian-Cenomanian. The model shows the restored orientation of the escarpment as discussed in the text. Not to scale.

6.3. Source area and evolution of the Western Sicily Cretaceous Escarpment

The Panormide carbonate platform almost certainly was the source area of the WSCE (Fig. 1B; Di Stefano and Ruberti, 2000) since most of the other Mesozoic shallow-water paleogeographic sectors of Sicily drowned during the Cretaceous (Catalano and D'Argenio, 1982). Therefore, the evolution of the WSCE has been correlated to that of the Panormide Platform whose Cretaceous evolution had been described by many authors (Montanari, 1964; Camoin, 1982; Catalano and D'Argenio, 1982; Zarcone et al., 2010) (Fig. 13). Distance reconstructions between the WSCE (sink) and the Panormide Platform (source) through time remains open because of outcrop limitations. However, a minimum distance of 15 km can be inferred based on the present-day setting.

The Berriasian-Valanginian marks the onset of slope re-sedimentation as indicated by the abrupt facies contact between *Tubiphytes*/calpionellid limestones (FA1) and bedded breccia with *Ellipsactinia*, forming FC1. This change in sediment composition suggests that part of the platform margin collapsed, which resulted in the downslope transport of lithoclasts derived from the sedimentary substrate combined with loose skeletal grains produced on the platform (Fig. 14). This process possibly relates to the development of an upslope fault escarpment dissecting the carbonate ramp as documented in several sections of the study area (locations 1, 2, 11 and 14 in Fig. 3). It also demonstrates the significant lateral extension (> 15 km) of this destabilization zone affecting the ramp. The *ca* 200 m thick almost continuous succession with abundant bedded breccia with *Ellipsactinia* (Fig. 8; Noce Quarry) accounts for a long-lasting period of instability along the escarpment. Approximately 80% of sediments exposed in aforementioned quarries are calcidebrites, which for the entire WCSE make up nearly 50% of all sediments. Similar slope facies series were also identified in the Imerese Basin in Sicily (Catalano and D'Argenio, 1982). Their emplacement is interpreted as a response to the tectonic dismantling of the bioconstruction at the margin of the Panormide Platform.

During the Aptian, the bedded breccia with *Ellipsactinia* (FC1 – calcidebrites) were replaced by rudist calcidebrites (FC2). This evolution indicates that extended rudist shoals edged the platform and were in turn affected by collapses leading to the progressive retreat of the margin (Figs. 13 and 14). An alternative interpretation for the emplacement of a vast series of re-sedimented foreslope deposits was discussed for the Canning Basin (Playton and Kerans, 2015a, b) where debris-dominated foreslopes are linked to large-scale backstepping of the platform margin followed by aggradation, and subsequent repeated failure of platform margin deposits during progradation of the platform. However, the upper slope of the Canning Basin is dominated by calcimicrobial boundstones, unlike the Panormide Platform margin. In addition, lithoclasts derived from the underlying substrate frequently occur in the WSCE, suggesting the exposure of older sequences probably because of tectonic displacement along

normal faults. Finally, slump scars affect the re-sedimented slope facies and document the instability of the upper slope deposits likely due to steep scarps of normal faults. Hence, the aforementioned data together present a strong case for the link between tectonic processes and the emplacement of the re-sedimented slope deposits.

The Aptian-early Albian time interval marks a second period of major tectonically-induced dismantling of the carbonate platform margin marked by the emplacement of thick chaotic megabreccia bodies (FC3) (Table 2). This sedimentary development is supported by the occurrence of submarine volcanic extrusions in the Western Mt Sparagio area (Noce Pond, Fig. 8). These extrusion events are coeval with an episode of crustal shear affecting the western Tethys. During the same time interval, the Panormide Platform experienced an uplift and a subsequent drowning as rudist limestones were truncated by a karstified surface and draped by pelagic lime mudstone (Madonie Mountains; Camoin, 1982).

The Albian-Cenomanian interval is dominated by alternations of rudist megabreccias and skeletal calciturbidites with abundant orbitolinids. Carannante et al. (2007) identified a drastic turnover of rudist assemblages from recumbent forms (for example, caprinids) to elevator morphotypes (for example, radiolitid and ichtiosarcolitids) in response to eustatic sea-level oscillations and associated climatic changes during the Cenomanian in the peri-Tethyan realm. During the same time interval, the Panormide Platform experienced a period with high carbonate productivity with the development of extended shoals populated by large caprinids (*Neocaprina gigantea*) and radiolitids, which were surrounded by large amounts of rudist debris. The hyper-production of carbonate sediments resulted in the vast export of skeletal debris shed toward the basin as shown by the large amount of rudist rudstones forming the matrix of the thick megabreccia bodies (for example, FC3, FC4) (Di Stefano and Ruberti, 2000). In particular, the Cenomanian stage records the presence of platform margin deposits consisting of rudist floatstone/rudstone (FB1 and FB3) associated with rounded rudist rudstone (FB2). In the Eastern Mt Sparagio and Mt Monaco areas these deposits occur above

the slope breccias and relate to facies association C. This facies trend supports either the onset of a restricted shelf environment on uplifted blocks of the WSCE or alternatively fast progradation of the margin due to an increased sediment production on the shelf (Figs. 13, 14).

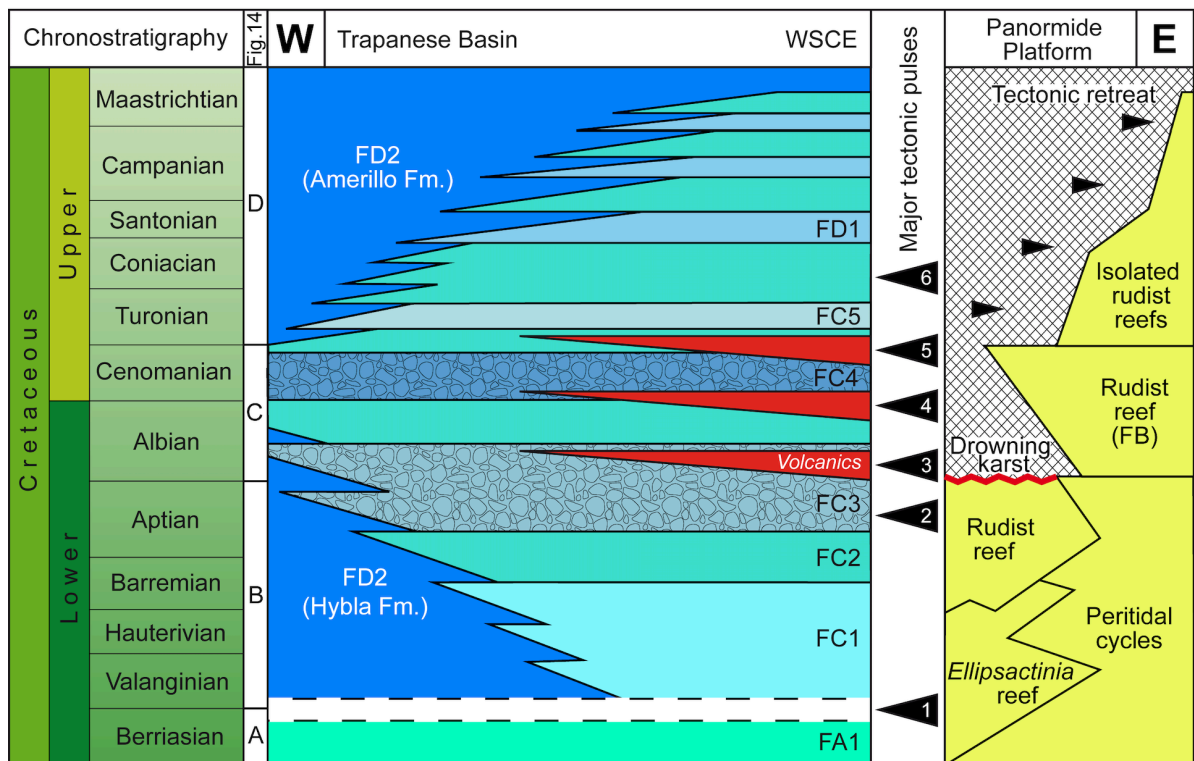
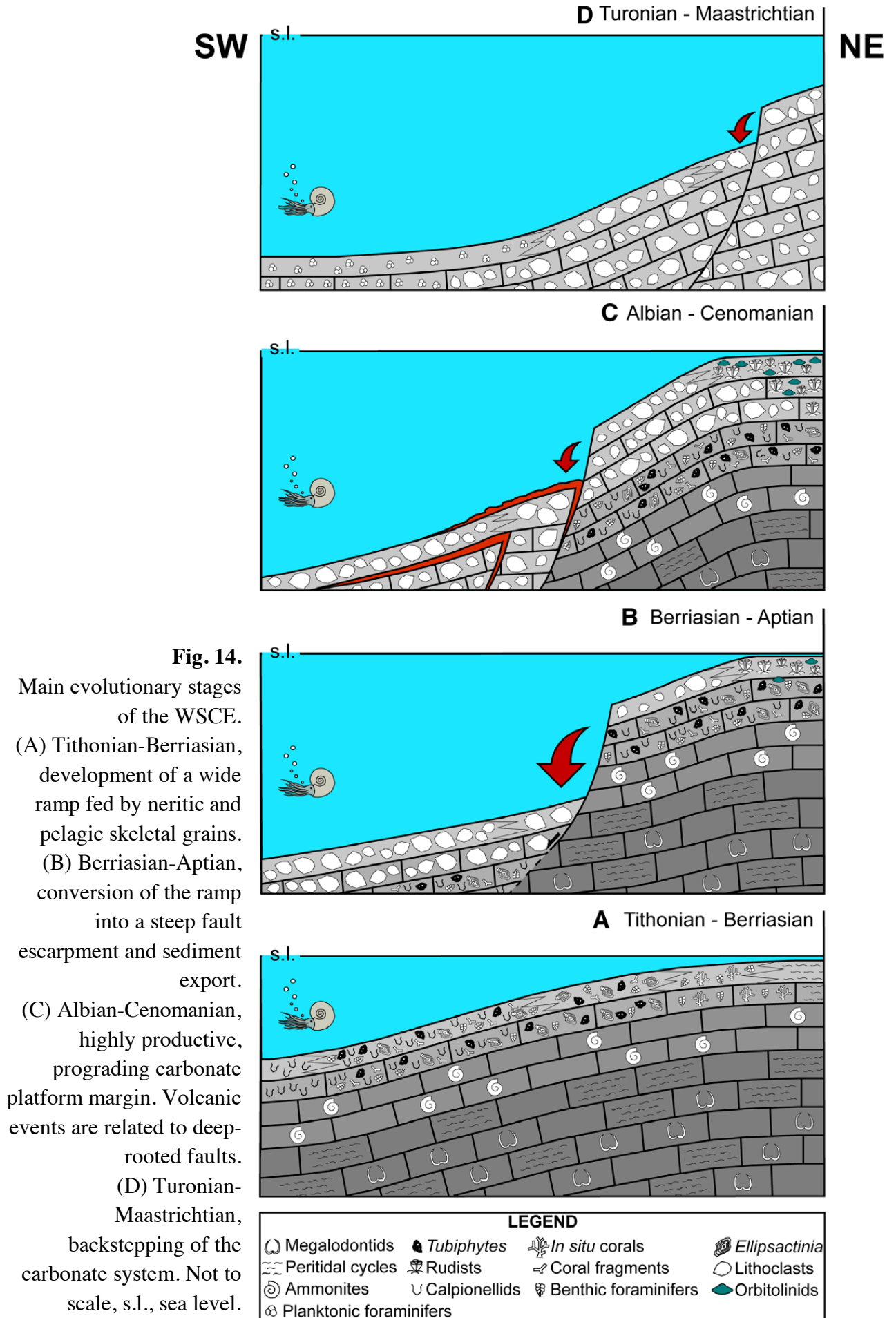


Fig. 13. Proposed evolution of Western Sicily Cretaceous Escarpment (WSCE) and its source area (Panormide Platform) during the Cretaceous.

A further episode with basaltic extrusions occurred at the end of the Cenomanian and corresponds to a new period with uplift and erosion of the Panormide Platform. This third episode predates a maximum peak of tectonic instability during Turonian-Coniacian times along the WSCE that led to the emplacement of thick megabreccia beds with numerous large boulders (FC2). Upsection, the gradual transition from coarse calcidebrites (FC2) to finer grained turbidites (FD1) and lime mudstone (FD2) points to the end of the calciclastic input

in the Western Mt Sparagio area (Maiorana Quarry) or alternatively to the rerouting of the gravity flow delivery system. The sequence is interpreted to document the drowning of large portions of the adjacent carbonate platform that caused a decrease in sediment production and export (Figs 13 and 14). Conversely, calciclastic sedimentation persists in a coeval section in the Eastern Mt Sparagio area (Segala Quarry) and during the Campanian-Maastrichtian in the Custonaci area (for example, Xiare Quarry). This suggests a dismembering of the Panormide Platform in smaller isolated platforms that each experienced an autonomous evolution, at least since the Coniacian, as also shown for the Gargano-Apulia region (Borgomano, 2000). Isolated rudist patches, Turonian-Maastrichtian in age, are known from the Panormide succession near Palermo (Montanari, 1964), and suggest a progressive tectonic reduction of the shelf areas and subsequent decrease of carbonate production (Fig. 14).



6.4. Comparison with other tectonically-controlled carbonate margins

Sea-level variations were proposed as a process causing carbonate slope instability (Spence and Tucker, 1997) and sediment export (Schlager et al., 1994; Adams and Kenter, 2013; Reijmer et al., 2015a; Mulder et al., 2017). However, the deposition of large-scale re-sedimented carbonates is often associated with tectonic and seismic processes (Drzewiecki and Simo, 2002; Payros and Pujalte, 2008). Latter processes are also invoked as the main trigger producing the re-sedimented limestones of the Southern Provence Basin (middle Turonian-lower Coniacian; Hennuy and Floquet, 2002; Hennuy, 2003). Similarly, most of the MTDs along the WSCE can be interpreted as "seismobreccias" (*sensu* Mutti et al., 1984 and Shiki et al., 2000). In the Gargano–Murge region (Borgomano, 2000) the uplift of the platform margin and tectonic processes are documented by synsedimentary faults and re-sedimented blocks (with karstic evidence) derived from a platform setting that revealed much older ages than the embedding slope facies. The re-sedimented blocks encountered along the WSCE showed clear evidence of substrate reworking into younger sediments but did not reveal karstification features pointing to subaerial exposure. Examples of progradational deposition patterns in grain-dominated slopes reported in Playton and Kerans (2015a, b, 2018; Canning Basin, Devonian, Australia; Delaware Basin, Permian, Texas, USA) revealed that autogenic control of carbonate (microbial) production can shape the architecture of carbonate slopes, hence being independent of allocyclic controls such as tectonic activity or eustatic processes. However, the nature of deposits along the WCSE is different, i.e. thick bodies of coarse and chaotic megabreccias, and the WSCE lacks a deep microbial production system. The tight stratigraphic link between the slope deposits and volcanic extrusions strongly suggests that tectonic events reorganized the escarpment and subsequently triggered re-sedimentation events. In addition, the high TiO₂ content of the WSCE volcanics accounts for the presence of deep-rooted extensional faults (Bellia et al., 1981). Earthquakes related to tectonic activity

are also invoked as the most likely triggering mechanism for margin collapse observed in the Miocene Mut Basin in South-Central Turkey and its modern analogue in the South China Sea (Janson et al., 2010). In both regions, large regional faults were found close to the margin collapse locations. Along the WSCE, besides small metre-scale palaeofaults (Figs 5D, 6C and 7K), no evidence of large Cretaceous faults was found. The absence of large faults most likely resulted from the tectonic inversion and/or reactivation of most of the normal Mesozoic faults during the Tertiary, thus generating thrusts and/or transtensional structures. As shown in Fig. 2, some of the deep-rooted faults could have been related to the reactivation of older faults (Lower Jurassic) occurring in Sicily that were related to the drowning of the carbonate platforms (Di Stefano et al., 2002). Among several regional examples, reactivation of pre-existing extensional faults that account for slope instability and reworked sediments resulting in large MTDs are described from the Eocene Thebes Formation, exposed along the eastern coastline of the Gulf of Suez (Corlett et al., 2018). Similarly, along the WSCE, faulting occurring during the Cretaceous created a series of escarpments that became prone to instability and lead to megabreccias and olistoliths deposition. In this respect, the WSCE shows an evolution comparable to large Cretaceous escarpments known from the Ligurian Alps where paleofault planes have been remodelled by fault-related gravity-driven rock fall processes (Bertok et al., 2012).

6.5 Palaeogeographic and geodynamic scenario

The paleogeographic evolution of western Sicily during the Mesozoic is part of the development of the Tethyan domain and was intimately tied to the interaction between two oceanic realms: the Ionian and the Alpine Tethys (Fig. 15A). The Ionian Tethys (Finetti, 2005) is also known as the East Mediterranean Basin (Stampfli et al., 2001; Garfunkel, 2004). The origin of this oceanic domain at the western termination of the Neotethys, dates back to

Permian (Catalano et al. 1991). The Alpine Tethys separated Europe from Africa during Jurassic and Cretaceous periods (Rosenbaum et al., 2004; Handy et al., 2010).

Several lines of evidence such as paleomagnetic (Channell et al., 1979; Muttoni et al. 2001), stratigraphic and paleontological data (Zarcone and Di Stefano 2010; Zarcone et al., 2010) suggest the presence of a crustal connection between Africa and Adria after the opening of the Alpine Tethys. This connection could have enabled the migration of African dinosaurs to Apulia via the Panormide and the Apennine platforms during the Lower Cretaceous (Zarcone et al., 2010) (Fig. 15B and C). From the Albian-Cenomanian onward the extensional deformations led to the progressive dismantling of the connection between Africa and Adria and, in particular, of the Panormide Carbonate Platform (Fig. 15C). This process is recorded by the volcanic eruptions related to deep-rooted extensional faults occurring at the WSCE. Extension episodes, anorogenic magmatic manifestations and associated deformation processes also affected the Apulian and Apennine domains during the Albian up to the Late Cretaceous (D'Argenio and Mindszenty, 1995; Graziano, 2000; Carannante et al., 2009; Tavani et al., 2013; Vitale et al., 2018 and references therein). An intensive phase of deformation in the latest Cretaceous is also well documented in the deep-water basins of Sicily, in which massive megabreccia bodies accumulated in Scaglia-type lime mudstones owing to the creation of tectonically-controlled submarine escarpments (Di Stefano et al., 1996).

The extensional deformations along the African margin are related to the opening of the Sirte Basin, that has been affected by north-west/south-east normal faults from the Cenomanian onward (Frizon de Lamotte et al., 2011; Fig. 15A). Furthermore, the Sellaoué Basin and Tellian Trough along the Pelagian Block were also controlled by dextral shears and volcanism associated to the Sirte rift during the Cretaceous (Jongsma et al., 1985). During the Santonian, the convergence between Africa and Eurasia plates led to the progressive closure of the Alpine Tethys and the onset of its subduction below the Iberian Plate (Dercourt et al.,

1986; Rosenbaum et al., 2002). Furthermore, another subduction zone was active between the Ionian Tethys and the Eurasian Plate (Fig. 15A). The subduction dynamics related to this particular 3D geometry most likely played a major role in the development of the Sirte rift and during its continuous subsidence (Capitanio et al., 2009; Frizon de Lamotte et al., 2011). In agreement with Vitale et al. (2018), from the “middle” Cretaceous onward, the extensional phases recorded by the Panormide Platform, the WSCE and the larger region of the western Tethys can be considered to result from processes occurring along the northern prolongation of the Sirte Basin Province Rift (Fig. 15A and C).

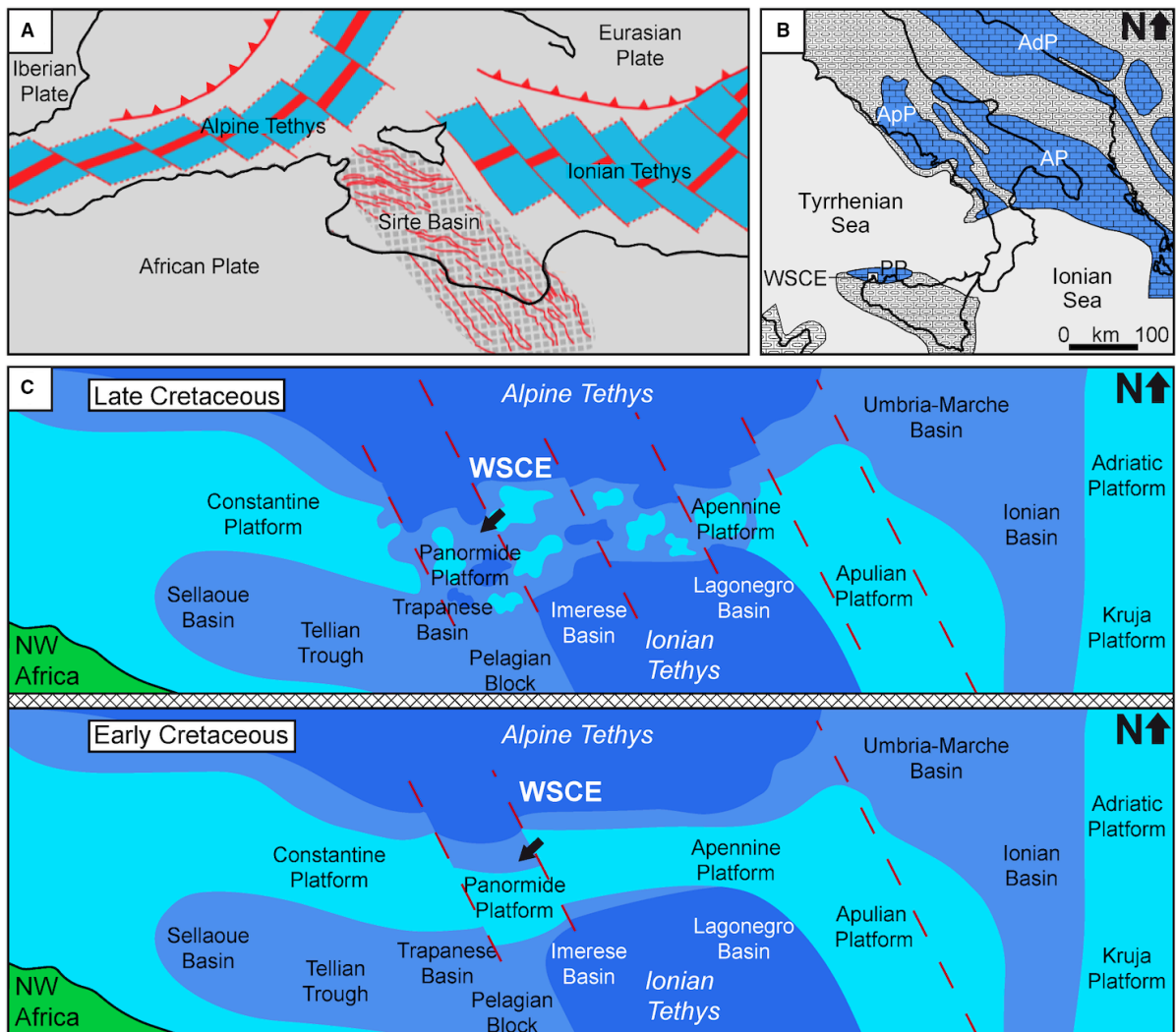


Fig. 15. Proposed paleogeographic and geodynamic scenario for the Southern Tethyan margin during the Cretaceous. (A) Paleogeographic map of the Central Mediterranean area during the latest Cretaceous showing the subduction zones in the Ionian and Alpine Tethys and the extensional stress field in the Sirte Basin (in red) as well as the location of the palaeogeographic sectors of Sicily (modified after Frizon de Lamotte et al., 2011). Not to scale. (B) Present-day location of the study area and the main carbonate platforms (blue) and pelagic basins (white) (modified after Zappaterra, 1994). AP, Apulian Platform; AdP, Adriatic Platform; ApP, Apennine Platform; PP, Panormide Platform. (C) Evolution of the continental connection between Africa and Apulia during Early (below) and Late (above) Cretaceous (not to scale; modified after Zarcone et al., 2010). Red dashed lines are deeprooted extensional faults. Not to scale. WSCE, Western Sicily Cretaceous Escarpment.

7. Conclusions

This study proposes a model to explain the facies heterogeneity along a Cretaceous tectonically-controlled carbonate slope, the Western Sicily Cretaceous Escarpment (WSCE). The evolutionary history of the WSCE during the Cretaceous is reconstructed from the re-sedimented slope series and stratigraphic relationships with the source area (Panormide Platform). The onset of the escarpment dates back to the lowermost Cretaceous when an abrupt changeover occurs from a gentle carbonate ramp to a steep slope. A clear increase in sediment shedding and a shallowing-upward trend in the facies stacking has been documented during the Albian-Cenomanian. The gradual transition to pelagites observed along the WSCE suggests a progressive drowning and subsequent shutdown of the carbonate factory as the end of the Santonian. The final signs of sediment export from a likely isolated and reduced carbonate platform occur in the early Maastrichtian. Several volcanic intercalations (for example, tuffites and pillow lavas) of crustal origin as shown by their TiO_2 content alternate with the carbonate gravity flow deposits. These features, along with slump scars, thick megabreccia bodies and extensional synsedimentary faults, strongly suggest repeated seismic shocks as the most likely trigger mechanism for the emplacement of the gravity flows. This study provides further validation of the severe phase of crustal shear affecting the connection between Adria and Africa and leading to its dismantling during the Late Cretaceous.

Acknowledgements

The PhD grant to VR was supported by the FSE SICILIA 2020 via University of Palermo. Research granted by PD project R4D14-P5F5RISS_MARGINE (University of Palermo). The College of Petroleum Engineering and Geosciences (CPG) of the King Fahd University of Petroleum and Minerals (KFUPM) is thanked for the research stage and funding offered to VR (Start-up fund to JJGR). Dr. Arnoud Sloopman, Dr. Scott Whattam, Dr. Alex Hairabian, Dr. Jalel Jaballah, from KFUPM-CPG are thanked for suggestions and constructive criticism. This is Carbonate Sedimentology Group at CPG (CSG@CPG) contribution no. 43. Francesco La Monica provided the high-resolution drone pictures collected during his MSc thesis project. The owners of the quarries and marble sawmill and in particular Pellegrino, Bova, Maiorana, Santoro, Bellanova and Miceli industries of the Custonaci area are warmly acknowledged for their permission to access the properties and facilities. Angel Puga-Bernabeu, Ted Playton and two anonymous reviewers, Associate Editor Jody Webster and Editor Peir Pufahl are thanked for their comments and critical reviews that helped to improve the manuscript.

References

- Abate, B., Di Maggio, C., Incandela, A., Renda, P.** (1991) Nuovi dati sulla geologia della Penisola di Capo San Vito (Sicilia Nord-Occidentale). *Soc. Geol. Ital. Mem.*, 47, 15-25.
- Abate, B., Di Maggio, C., Incandela, A., Renda, P.** (1993) Carta geologica dei Monti di Capo San Vito, scala 1 : 25.000. Dipartimento di Geologia e Geodesia dell'Università di Palermo.
- Adams, E.W., Kenter, J.A.M.** (2013) So different, yet so similar: comparing and contrasting siliciclastic and carbonate slopes. In: *Deposits, Architecture and Controls of Carbonate Margin, Slope and Basinal Settings*. (Eds. Verwer, K., Playton, T.E., Harris, P.M.), *SEPM Spec. Publ.*, 14-25.
- Agate, M., Mancuso, M., Lo Cicero, G.** (2005) Late Quaternary sedimentary evolution of the Castellammare Gulf (North-Western Sicily offshore). *Boll. Soc. Geol. Ital.*, 124(1), 21-40.
- Al-Ghamdi, N.M.** (2013) Integrated core-based sequence stratigraphy, chemostratigraphy and diagenesis of the Lower Cretaceous (Barremian-Aptian), Biyadh and Shu'aiba formations, a giant oil field, Saudi Arabia. PhD Thesis, AandM Univ., Texas, 239 pp.
- Andreini, G., Caracuel, J. E., Parisi, G.** (2007) Calpionellid biostratigraphy of the upper Tithonian - upper Valanginian interval in Western Sicily (Italy). *Swiss J. Geosci.*, 100, 179-198.
- Artoni, A., Bernini, M., Papani, G., Rizzini, F., Barbacini, G., Rossi, M., Rogledi, S., Ghielmi, M.** (2010) Mass-transport deposits in confined wedge-top basins: surficial processes shaping the Messinian orogenic wedge of Northern Apennine of Italy. *Ital. J. Geosci.*, 129, 101-118.
- Bates, R.L., Jackson, J.A.** (1984) *Dictionary of Geological Terms*. Anchor Press, Garden City, New York, 571 pp.
- Beaubouef, R., Abreu, V.** (2010) MTCs of the Brazos-Trinity slope system; thoughts on the sequence stratigraphy of MTCs and their possible roles in shaping hydrocarbon traps. In: *Submarine mass movements and their consequences* (Eds. D. C. Mosher, R. C. Shipp, L. Moscardelli, J. D. Chaytor, C. D. P. Baxter, H. J. Lee, and R. Urgeles), 475-490. Springer, Dordrecht.

- Bellia, S., Lucido, G., Nuccio, P.M., Valenza, M.** (1981) Magmatismo in area trapanese in relazione all'evoluzione geodinamica della Tetide. *Rend. SIMP*, 38, 163-174.
- Bertok, C., Martire, L., Perotti, E., D'Atri, A., Piana, F.** (2012) Kilometre-scale paleoescarpments as evidence for Cretaceous synsedimentary tectonics in the External Briançonnais Domain (Ligurian Alps, Italy). *Sed. Geol.* 251-252, 58-75.
- Betzler, C., Hubscher, C., Lindhorst, S., Ludmann, T., Reijmer, J.J.G., Braga, J.-C.** (2016) Lowstand wedges in carbonate platform slopes (Quaternary, Maldives, Indian Ocean). *Deposit. Rec.*, 2, 196–207.
- Blair, T.C. and McPherson, J.G.** (1999) Grain-size and textural classification of coarse sedimentary particles. *J. Sed. Res.*, 69(1), 6-19.
- Borgomano, J.R.F.** (2000) The Upper Cretaceous carbonates of the Gargano-Murge region, Southern Italy: a model of platform-to-basin transition. *A.A.P.G. Bull.*, 84, 1561-1588.
- Bosellini, A.** (1984) Progradation geometries of carbonate platforms: examples from the Triassic of the Dolomites, northern Italy. *Sedimentology*, 31, 1–24.
- Broquet, P., Mascle, G.** (1972) Les grands traits stratigraphiques et structuraux des Monts de Trapani (Sicile occidentale), *Ann. Soc. Geol. Nord.*, 92, 139-146.
- Bull, S., Cartwright, J., Huuse, M.** (2009) A review of kinematic indicators from mass-transport complexes using 3D seismic data. *Mar. Petrol. Geol.*, 26, 1132-1151.
- Camoin, G.** (1982) *Plates-formes carbonates et recifs a rudistes du Cretace de Sicile*. Phd Thesis, Univ. Provence, Marseille, 244 pp.
- Capitanio, F. A., Faccenna, C., Funiciello, R.** (2009) The opening of Sirte Basin: Result of slab avalanching? *Earth Planet. Sci. Lett.*, 285, 210-216.

- Carannante, G., Ruberti, D., Simone, L., Vigliotti, M.** (2007) Cenomanian carbonate depositional settings: case histories from the central-southern Apennines (Italy). In: *Cretaceous Rudists and Carbonate Platforms: Environmental Feedback* (Ed. Scott, R.W.), SEPMSpec. Publ., 87, 11–25.
- Carannante, G., Pugliese, A., Ruberti, D., Simone, L., Vigliotti, M., Vigorito, M.** (2009) Evoluzione cretacea di un settore della Piattaforma Apula da dati di sottosuolo e di affioramento (Appennino Campano-Molisano). *Boll. Soc. Geol. Ital.*, 128, 3–31.
- Catalano, R., D'Argenio, B.** (1982) Schema Geologico della Sicilia. In: *Guida alla Geologia della Sicilia Occidentale* (Eds R. Catalano and B. D'Argenio), Soc. Geol. Ital., guide geologiche regionali, 9-41.
- Catalano, R., D'Argenio, B., Gregor, C.B., Nairn, A.E.M., Nardi, G.** (1984) The Mesozoic volcanism of Western Sicily. *Geol. Rdsch.*, 73, 577-598.
- Catalano, R., Di Stefano, P., Kozur, H.** (1991) Permian circumpacific deep-water faunas from the western Tethys (Sicily, Italy) - new evidences for the position of the Permian Tethys. *Palaeogeogr., Palaeoclimatol., Palaeoecol.*, 87, 75-108.
- Catalano, R., Agate, M., Basilone, L., Di Maggio, C., Mancuso, M., Sulli, A.** (2011) Note illustrative della Carta Geologica d'Italia alla scala 1: 50.000, Foglio n. 593 “Castellammare del Golfo” e carta geologica allegata. Regione Siciliana - Ispra.
- Cestari, R., Sartorio, D.** (1995) Rudists and facies of the Periadriatic Domain. Milano, AGIP, 207 pp.
- Chacón, E., Berrendero, E., Garcia Pichel, F.** (2006) Biogeological signatures of microboring cyanobacterial communities in marine carbonates from Cabo Rojo, Puerto Rico. *Sed. Geol.*, 185(3-4), 215-228.
- Channell, J.E.T., D'Argenio, B., Horvath, F.** (1979) Adria, the African promontory, in Mesozoic Mediterranean palaeogeography. *Earth-Sci. Rev.*, 15.3, 213-292.
- Chayes, F.** (1965) Statistical petrography. Year Book, *Cameg. Inst. Washington*, 64, 153-165.
- Chiocchini, M., Chiocchini, R.A., Didaskalau, P., Potetti, M.** (2008) Micropalaeontological and biostratigraphical researches on the Mesozoic of the Latium-Abruzzi carbonate platform (Central Italy).

Memorie descrittive della Carta Geologica d'Italia. ISPRA, Servizio Geologico d'Italia, Dipartimento Difesa del Suolo 17.

Chiocci, F.L., Martorelli, E., Bosman, A. (2003) Cannibalization of a continental margin by regional scale mass wasting: an example from the central Tyrrhenian Sea. In: *Submarine Mass Movements and their consequences* (Eds. J. Locat and J. Mienert), 409-416.

Cook, H.E., Mullins, H.T. (1983) Basin margin. In: *Carbonate Depositional Environments* (Eds D.G. Bebout and C.H. Moore), *AAPG Spec. Publ.*, 539–618.

Corlett, H.J., Bastesen, E., Gawthorpe, R.L., Hirani, J., Hodgetts, D., Hollis, C., Rotevatn, A. (2018) Origin, dimensions, and distribution of remobilized carbonate deposits in a tectonically active zone, Eocene Thebes Formation, Sinai, Egypt. *Sed. Geol.*, 372, 44-63.

Crevello, P.D., Schlager, W. (1980) Carbonate debris sheets and turbidites, Exuma Sound, Bahamas. *J. Sed. Petrol.*, 50, 1121–1148.

D'Argenio, B., Mindszenty, A. (1995) Bauxites and related paleokarst: tectonic and climatic event markers at regional unconformities. *Eclogae Geol. Helv.*, 88(3), 453–499.

Dercourt, J., Zonenshain, L.P., Ricou, L.E., Kuzmin, V.G., Le Pichon, X., Knipper, A.L., Grandjacquet, C., Sbortshikov, I.M., Geysant, J., Lepvrier, C., Pechersky, D.H., Boulin, J., Sibuet, J.C., Savostin, L.A., Sorokhtin, O., Westphal, M., Bazhenov, M.L., Lauer, J.P., Biju-Duval, B. (1986) Geological evolution of the Tethys belt from the Atlantic to the Pamir since the Lias. *Tectonophysics*, 123, 241-315.

Di Stefano, P., Ruberti, D. (2000) Cenomanian rudist-dominated shelf- margin limestones from the Panormide Carbonate Platform (Sicily, Italy): facies analysis and sequence stratigraphy. *Facies*, 42, 133-160.

Di Stefano, P., Alessi, A., Gullo M. (1996) Mesozoic and Paleogene magabreccias in Southern Sicily: new data on the Triassic paleomargin of the Siculo-Tunisian platform. *Facies*, 34, 101-122.

Di Stefano, P., Galácz, A., Mallarino, G., Mindszenty A., Vörös, A. (2002) Birth and early evolution of a Jurassic escarpment: Monte Kumeta, Western Sicily. *Facies*, 46: 273-298.

- Drzewiecki, P.A., Simo, J.A.** (2002) Depositional processes, triggering mechanisms and sediment composition of carbonate gravity flow deposits: examples from the Late Cretaceous of the south-central Pyrenees, Spain. *Sed. Geol.*, 146 (1-2), 155-189.
- Dunham, R.J.** (1962) Classification of carbonate rocks according to depositional texture. In: *Classification of Carbonate Rocks* (Eds W.E. Ham), 1, AAPG Mem., 108-121.
- Eberli, G.P., Ginsburg, R.N.** (1989) Cenozoic progradation of northwestern Great Bahama Bank, a record of lateral platform growth and sea-level fluctuations. In: *Controls on Carbonate Platforms and Basin Development* (Eds J.L. Crevello, J.L. Wilson, J.F. Sarg, J.F. Read), *SEPM Spec. Publ.*, 44, 339-351.
- Eberli, G.P., Bernoulli, D., Sanders, D., Vecsei, A.** (1993) From aggradation to progradation: the Maiella Platform, Abruzzi, Italy. In: *Cretaceous Carbonate Platforms* (Eds T. Simo, R.W. Scott and J.P. Masse), AAPG Mem., 56, 213-232.
- Eberli, G.P., Anselmetti, F.S., Betzler, C., Van Konijnenburg, J.-H., Bernoulli, D.** (2004) Carbonate platform to basin transitions on seismic data and in outcrops: Great Bahama Bank and the Maiella platform margin, Italy. In: *Seismic Imaging of Carbonate Reservoirs and Systems* (Eds Eberli, G.P., Masferro, J.L. and Sarg, J.F.), AAPG Memoir, 81, 207–250.
- Embry, A.F. III, Klovan, J.S.** (1971) A Late Devonian reef tract on north-eastern Banks Island, NWT. *Bull. Can. Petrol. Geol.*, 4, 730–781.
- Enos, P.** (1977) Tamabra limestone of the Poza Rica trend, Cretaceous, Mexico. In: *Deep-water Carbonate Environments* (Eds Cook, H.E. and Enos, P.), *SEPM Spec. Publ.*, 25, 273–314.
- Finetti, I.** (2005) CROP Project: Deep seismic exploration of the Central Mediterranean and Italy. *Atlases in Geoscience*, 1, Elsevier, Amsterdam, 794 pp.
- Floquet, M., Hennuy, J.** (2003) Evolutionary gravity flow in the middle Turonian - early Coniacian Southern Provence basin (SE France): origins and depositional processes. In: *Submarine Mass Movements and their Consequences* (Eds: J. Lcat and J. Minert), Springer, Dordrecht, pp. 417 - 424.

- Floquet, M., Gari, J., Hennuy, J., Léonide, P., Philip, J.** (2005) Sédimentations gravitaires carbonatées et silicoclastiques dans un bassin en transtension, séries d'âge Cénomaniens à Coniaciens moyens du Bassin Sud-Provençal. 10ème Congrès Français de Sédimentologie 52. Publ ASF, Paris, Giens, 80 pp.
- Flügel, E.** (2004) Microfacies of carbonate rocks. Analysis, interpretation and application. Springer. 984 pp.
- Frizon de Lamotte, D., Raulin, C., Mouchot, N., Wrobel-Daveau, J.-C., Blanpied, C., Ringenbach, J.C.,** (2011) The southernmost margin of the Tethys realm during the Mesozoic and Cenozoic: initial geometry and timing of the inversion processes. *Tectonics*, 30, 94-104.
- Garfunkel, Z.** (2004) Origin of the Eastern Mediterranean basin: a reevaluation. *Tectonophysics*, 391, 11-34.
- Giunta, G. and Liguori, V.** (1972) Geologia della estremità Nord-Occidentale della Sicilia. *Riv. Min. Sicil.*, 136-138, 165-226.
- Giunta, G. and Liguori, V.** (1973) Evoluzione paleotettonica della Sicilia nord-occidentale. *Boll. Soc. Geol. Ital.*, 92, 903-924.
- Giunta, G., Nigro, F., Renda, P.** (2002) Inverted structures in Western Sicily. *Boll. Soc. Geol. Ital.*, 121, 11-17.
- Graziano, R.** (2000) The Aptian-Albian of the Apulia Carbonate Platform (Gargano Promontory, Southern Italy): evidence of palaeoceanographic and tectonic controls on the stratigraphic architecture of the platform margin. *Cretaceous Res.*, 21, 106-127.
- Hairabian, A., Borgomano, J., Masse, J.P., Nardon, S.** (2015) 3-D stratigraphic architecture, sedimentary processes and controlling factors of Cretaceous deep-water resedimented carbonates (Gargano Peninsula, SE Italy). *Sed. Geol.*, 317, 116-136.
- Hampton, M.A.** (1972) The role of subaqueous debris flow in generating turbidity currents. *J. Sed. Petrol.*, 42, 775-793.
- Handy, M. R., Schmid, S. M., Bousquet, R., Kissling, E., Bernoulli, D.** (2010) Reconciling plate-tectonic reconstructions of Alpine Tethys with the geological-geophysical record of spreading and subduction in the Alps. *Earth-Sci. Rev.*, 102, 121-158.

- Haughton, P., Davis, C., McCaffrey, W., Barker, S.** (2009) Hybrid sediment gravity flow deposits - classification, origin and significance. *Mar. Petrol. Geol.*, 26, 1900-1918.
- Hennuy, J.** (2003) Sedimentation carbonatée et silicoclastique sous contrôle tectonique, le bassin sud-provençal et sa plate-forme carbonatée du Turonien moyen au Coniacien moyen. Evolution séquentielle, diagenétique, paléogéographique. Unpubl. PhD Thesis, Univ. Provence, Marseille. 252 pp.
- Hennuy, J., Floquet, M.** (2002) Sedimentation dans un bassin en transtension: exemple du Bassin Sud-Provençal au Turonien moyen pro-parte - Coniacien inférieur. *Docum. Lab. Geol. Lyon*, 156, 125-126.
- Heubeck, C., Ergaliev, G., Evseev, S.** (2013) Large-scale seismogenic deformation of a carbonate platform straddling the Precambrian-Cambrian boundary, Karatau Range, Kazakhstan. *J. Sed. Res.*, 83(11), 1004-1024.
- Hine, A.C., Wilber, R.J., Neumann, A.C.** (1981) Carbonate sand bodies along contrasting shallow bank margins facing open seaways: Northern Bahamas. *AAPG Bull.*, 65, 261-290.
- Hine, A.C., Locker, S.D., Tedesco, L.P., Mullins, H.T., Hallock, P., Belknap, D.F., Gonzales, J.L., Neumann, A.C., Snyder, S.W.** (1992) Megabreccia shedding from modern, low-relief carbonate platforms, Nicaraguan Rise. *Geol. Soc. Am. Bull.*, 104, 928-943.
- Hughes, G.W.** (2000) Bioecostratigraphy of the Shu'aiba Formation, Shaybah field, Saudi Arabia. *GeoArabia*, 5(4), 545-578.
- Janson, X., Eberli, G.P., Lomando, A.J., Bonnaffé, F.**, (2010) Seismic characterization of large-scale platform-margin collapse along the Zhujiang carbonate platform (Miocene) of the South China Sea, based on Miocene outcrop analogs from Mut Basin, Turkey. In: *Cenozoic Carbonate Systems of Australasia* (Eds. W.A. Morgan, A.D. George, P.M. Harris, J.A. Kupecz, J.F. Sarg), *SEPM Spec. Publ.* 95, 73-92.
- Janson, X., Kerans, C., Loucks, R., Marhx, M.A., Reyes, C., Murguía, F.** (2011) Seismic architecture of a Lower Cretaceous platform-to-slope system, Santa Agueda and Poza Rica fields, Mexico. *AAPG Bull.*, 95, 105-146.
- Jo, A., Eberli, G.P., Grasmueck, M.** (2015) Margin collapse and slope failure along South-Western Great Bahama Bank. *Sed. Geol.*, 317, 43-52.

- Jongsma, D., van Hinte, J. E., Woodside, J. M.** (1985) Geologic structure and neotectonics of the North African Continental Margin south of Sicily. *Mar. Petrol. Geol.*, 2, 156-179.
- Kenter, J.A.M.** (1990) Carbonate platform flanks, slope angle and sediment fabric. *Sedimentology*, 37(5), 777-794.
- Kneller, B., Dykstra, M., Fairweather, L., Milana, J.P.** (2016) Mass-transport and slope accommodation: implications for turbidite sandstone reservoirs. *AAPG Bull.*, 100, 213–235.
- Krause, F.F., Oldershaw, A.E.** (1979) Submarine carbonate breccia beds - a depositional model for two-layer, sediment gravity flows from the Sekwi Formation (Lower Cambrian), McKenzie Mountains, Northwest Territories, Canada. *Can. J. Earth Sci.*, 16, 89-199.
- Lamarche, G., Mountjoy, J., Bull, S., Hubble, T., Krastel, S., Lane, E., Micallef, A., Moscardelli, L., Mueller, C., Pecher, I., Woelz, S.** (2016) Submarine Mass Movements and Their Consequences: Progress and Challenges. In: *Submarine Mass Movements and Their Consequences: 7th International Symposium*, 487-496.
- Le Goff, J., Cerepi, A., Swennen, R., Loisy, C., Caron, M., Muska, K., El Desouky, H.** (2015) Contribution to the understanding of the Ionian Basin sedimentary evolution along the eastern edge of Apulia during the Late Cretaceous in Albania. *Sed. Geol.*, 317, 87-101.
- Le Goff, J., Reijmer, J.J.G., Cerepi, A., Loisy, C., Swennen, R., Heba, G., Cavailhes, T., De Graaf, S.** (2019) The dismantling of the Apulian carbonate platform during the late Campanian-early Maastrichtian in Albania. *Cretaceous Res.*, 96, 83-106.
- Loucks, R.G., Kerans, C., Janson, X., Marhx Rajano, M.A.** (2011) Lithofacies analysis and stratigraphic architecture of a deep-water carbonate debris apron: Lower Cretaceous (latest Aptian to latest Albian) Tamabra Formation, Poza Rica Field area, Mexico. In: *Mass-transport Deposits in Deepwater Settings* (Eds Shipp, R.C., Weimer, P. and Posamentier, H.W.), *SEPM Spec. Publ.*, 96, 367–389.
- MacGregor, I.D.** (1969) The system MgO-SiO₂-TiO₂, and its bearing on the distribution of TiO₂ in basalts. *Am. J. Sci.*, 267A, 342-363.
- Maurer, F.** (2000) Growth mode of Middle Triassic carbonate platforms in the Western Dolomites (Southern Alps, Italy). *Sed. Geol.*, 134, 275–286.

- Mauz, B., Renda, P.** (1991) Evoluzione tettono-sedimentaria del bacino Plio-Pleistocenico di Castellammare del Golfo (Sicilia Nord-occidentale). *Soc. Geol. Ital. Mem.*, 47, 167-180.
- McIlreath, I.A., James, N.P.** (1978) Facies Models 13: Carbonate slopes. *Geosci. Can.*, 5, 189-199.
- McKee, E.D., Weir, G.W.** (1953) Terminology for stratification and cross-stratification in sedimentary rocks. *Bull. Geol. Soc. Am.*, 64, 381-390.
- Meckel III L.D.** (2011) Reservoir characteristics and classification of sand-prone submarine mass-transport deposits. *SEPM Spec. Publ.*, 96, 432-452.
- Montanari, L.** (1964) Geologia del Monte Pellegrino (Palermo). *Riv. Min. Sic.*, 15/88-90, 1-64.
- Morsilli, M., Bosellini, A., Rusciadelli, G.** (2004) The Apulia carbonate platform margin and slope, Late Jurassic to Eocene of the Maiella and Gargano Promontory: physical stratigraphy and architecture. In: 32nd International Geological Congress - Field Trip Guidebook (Eds APAT), Roma, 1–44.
- Moscardelli, L., Wood, L.** (2008) New classification system for mass transport complexes in offshore Trinidad. *Basin Res.*, 20, 73–98.
- Mulder, T., Cochonat, P.** (1996) Classification of offshore mass movements. *J. Sed. Res.*, 66, 43-57.
- Mulder, T., Alexander, J.** (2001) The physical character of subaqueous sedimentary density currents and their deposits. *Sedimentology*, 48, 269-299.
- Mulder, T., Ducassou, E., Gillet, H., Hanquiez V., Principaud, M., Chabaud, L., Eberli, G.P., Kindler, P., Billeaud, I., Gonthier, E., Fournier, F., Leonide, P., Borgomano, J.** (2014) First Discovery of Channel-Levee Complexes In A Modern Deep-Water Carbonate Slope Environment. *J. Sed. Res.*, 84, 1139–1146.
- Mulder, T., Joumes, M., Hanquiez, V., Gillet, H., Reijmer, J.J.G., Tournadour, E., Chabaud, L., Principaud, M., Schnyder, J.S.D., Borgomano, J., Fauquembergue, K., Ducassou, E., Busson, J.** (2017) Carbonate slope morphology revealing sediment transfer from bank-to-slope (Little Bahama Bank, Bahamas). *Mar. Petrol. Geol.* 83, 26-34.

Mulder, T., Gillet, H., Hanquiez, V., Ducassou, E., Fauquembergue, K., Principaud, M., Conesa, G., Le Goff, J., Ragusa, J., Bashah, S., Bujan, S., Reijmer, J.J.G., Cavailhes, T., Droxler, A.W., Blank, D.G., Guiastrrenec, L., Fabregas, N., Recouvreur, A., Seibert, C. (2018) Carbonate slope morphology revealing a giant submarine canyon (Little Bahama Bank, Bahamas). *Geology*, 46(1), 31-34.

Mullins, H.T., Hine, A.C. (1989) Scalloped bank margins: beginning of the end for carbonate platforms? *Geology*, 17(1), 30-33.

Mullins, H.T., Gardulski, A.F., Hine, A.C. (1986) Catastrophic collapse of the west Florida carbonate platform margin. *Geology*, 14, 167-170.

Mullins, H.T., Breen, N., Dolan, J., Wellner, R.W., Petruccione, J.L., Gaylord, M., Andersen, B., Melillo, A.J., Jurgens, A.D., Orange, D. (1991) Retreat of carbonate platforms: response to tectonic processes. *Geology*, 19(11), 1089-1092.

Mutti, E., Ricci Lucchi, F., Seguret, M. and Zanzucchi, G. (1984) Seismoturbidites: a new group of reseedimented deposits. *Mar. Geol.*, 55, 103-116.

Muttoni G., Garzanti E., Alfonsi L., Cirilli S., Germani D., Lowrie W. (2001) Motion of Africa and Adria since the Permian: paleomagnetic and paleoclimatic constraints from Northern Libya. *Earth Planet. Sci. Lett.*, 192, 159-174.

Neri, C. (1993) Stratigraphy and sedimentology of the Monte Acuto Formation (Upper Cretaceous-Lower Paleocene, Gargano Promontory, Southern Italy). *Ann. Univ. Ferrara, Sezione Scienze della Terra*, 4, 13-44.

Neri, C., Luciani, V. (1994) The Monte S. Angelo Sequence (Late Cretaceous-Paleocene, Gargano Promontory, Southern Italy): physical stratigraphy and biostratigraphy. *Giorn. Geol.*, 56, 149-165.

Nigro, F., Renda, P. (1999) Evoluzione geologica ed assetto strutturale della Sicilia Centro-Settentrionale. *Boll. Soc. Geol. Ital.*, 118, 375-388.

Oldow, J.S., Channel, J.E.T., Catalano, R., D'Argenio, B. (1990) Contemporaneous thrusting and large-scale rotations in the Western Sicilian fold and thrust belt. *Tectonics*, 9(4), 661-681.

- Payros, A., Pujalte, V.** (2008) Calciclastic submarine fans: an integrated overview. *Earth-Sci. Rev.*, 86, 203-246.
- Perry, C.T.** (1998) Grain susceptibility to the effects of microboring: implications for the preservation of skeletal carbonates. *Sedimentology*, 45, 39-51.
- Pettijohn, F.J., Potter, P.E., Siever, R.** (1973) *Sand and Sandstones*. Springer Verlag, New York.
- Pickering, K.T., Corregidor, J.** (2005) Mass Transport complexes and tectonic control on confined basin-floor submarine fans, Middle Eocene, South Spanish Pyrenees. In: *Submarine Slope Systems: Processes and Products* (Eds. D.M. Hodgson and S.S. Flint). *Geological Society London, Spec. Publ.*, 244, 51-74.
- Pireno, G.E., Cook, C., Yuliong, D., Lestari, S.** (2009) Berau carbonate debris flow as reservoir in the Ruby Field, Sebuku Block, Makassar straits: a new exploration play in Indonesia. In: *Proceedings Indonesian Petroleum Association 33rd Annual Convention and Exhibition 2009*, Indonesian Petroleum Association, p. 19.
- Playton, T.E., Kerans, C.** (2015a) Late Devonian carbonate margins and foreslopes of the Lennard Shelf, Canning Basin, Western Australia, Part A: development during backstepping and the aggradation-to-progradation transition. *J. Sed. Res.*, 85, 1334–1361.
- Playton, T.E., Kerans, C.** (2015b) Late Devonian carbonate margins and foreslopes of the Lennard Shelf, Canning Basin, Western Australia, part B: development during progradation and across the Frasnian-Famennian biotic crisis. *J. Sed. Res.*, 85, 1362–1392.
- Playton, T.E., Kerans, C.** (2018) Architecture and genesis of prograding deep boundstone margins and debris-dominated carbonate slopes: examples from the Permian Capitan Formation, Southern Guadalupe Mountains, West Texas. *Sed. Geol.*, 370, 15–41.
- Playton, T.E., Janson, X., Kerans, C.** (2010) Carbonate slopes. In: *Facies Models 4* (Eds N.P. James and R.W. Dalrymple). *GEOtext 6: Geological Association of Canada, St John's, Newfoundland*. 449-476.
- Posamentier, H.W., Kolla, V.** (2003) Seismic geomorphology and stratigraphy of depositional elements in deep-water settings. *J. Sed. Res.*, 73, 367-388.

- Posamentier, H.W., Martinsen, O.J.** (2011) The character and genesis of submarine mass-transport deposits: insights from outcrop and 3D seismic data. In: *Mass-Transport Deposits in Deepwater Settings* (Eds Shipp, R.C., Weimer, P. and Posamentier, H.W.), SEPM Spec. Publ., 96, 7–38.
- Premoli Silva, I., Verga, D.** (2004) Practical manual of Cretaceous planktonic foraminifera. In: *International School on Planktonic Foraminifera: 3rd Course* (Eds D. Verga and R. Rettori), Perugia, Italy, Universities of Perugia and Milan, pp. 283.
- Principaud, M., Mulder, T., Gillet, H., Borgomano, J.** (2015) Large-scale carbonate submarine mass-wasting along the northwestern slope of the Great Bahama Bank (Bahamas): morphology, architecture, and mechanisms. *Sed. Geol.*, 317, 27-42.
- Prior, D.B., Bornhold, B.D., Johns, M.W.** (1984) Depositional characteristics of a submarine debris flow. *J. Geol.*, 92, 707-727.
- Puga-Bernabeu, A., Webster, J.M., Beaman, R.J., Guilbaud, V.** (2013) Variation in canyon morphology on the Great Barrier Reef margin, north-eastern Australia: the influence of slope and barrier reefs. *Geomorphology*, 191, 35–50.
- Puga-Bernabeu, A., Beaman, R.J., Webster, J.M., Thomas, A.L., Jacobsen, G.** (2017) Gloria Knolls Slide: a prominent submarine landslide complex on the Great Barrier Reef margin of north-eastern Australia. *Mar. Geol.*, 385, 68–83.
- Reijmer, J.J.G., Betzler, C., Kroon, D., Tiedemann, R., Eberli, G.** (2002) Bahamian carbonate platform development in response to sea-level changes and the closure of the Isthmus of Panama. *Int. J. Earth Sci.*, 91, 482-489.
- Reijmer, J.J.G., Palmieri, P., Groen, R.** (2012) Compositional variations in calciturbidites and calcidebrites in response to sea-level fluctuations (Exuma Sound, Bahamas). *Facies*, 58 (4), 493-507.
- Reijmer, J.J.G., Mulder, T., Borgomano, J.** (2015a) Carbonate slopes and gravity deposits. *Sed. Geol.*, 317, 1-8.

- Reijmer, J.J.G., Palmieri, P., Groen, R., Floquet, M.** (2015b) Calciturbidites and calcidebrites: sea-level variations or tectonic processes? *Sed. Geol.*, 317, 53-70.
- Rich, J. L.** (1951) Three critical environments of deposition, and criteria for recognition of rocks deposited in each of them. *Geol. Soc. Am. Bull.*, 62, 1-20.
- Rosenbaum, G., Lister, G.S., Duboz, C.** (2002) Relative motions of Africa, Iberia and Europe during Alpine orogeny, *Tectonophysics*, 359, 117-129.
- Rosenbaum, G., Lister, G.S., Duboz, C.** (2004) The Mesozoic and Cenozoic motion of Adria (central Mediterranean): a review of constraints and limitations. *Geodin. Acta*, 17(2), 125–139.
- Ross, W.C., Halliwell, B.A., May, J.A., Watts, D.E., Syvitski, J.P.M.** (1994) Slope readjustment: a new model for the development of submarine fans and aprons. *Geology*, 22(6), 511-514.
- Rusciadelli, G.** (2005) The Maiella escarpment (Apulia platform, Italy): geology and modeling of an Upper Cretaceous scalloped erosional platform margin. *Boll. Soc. Geol. Ital.*, 124, 661–673.
- Rusciadelli, G., Sciarra, N., Mangifesta, M.** (2003) 2D modelling of large-scale platform margin collapses along an ancient carbonate platform edge (Maiella Mt., Central Apennines, Italy): geological model and conceptual framework. *Palaeogeogr., Palaeoclimatol., Palaeoecol.*, 200, 189-203.
- Rustichelli, A., Iannace, A., Tondi, E., Di Celma, C., Cilona, A., Giorgioni, M., Parente, M., Girundo, M., Invernizzi, C.** (2017) Fault-controlled dolomite bodies as palaeotectonic indicators and geofluid reservoirs: new insights from Gargano Promontory outcrops. *Sedimentology*, 64, 1871-1900.
- Schlager, W., Ginsburg, R.N.** (1981) Bahama carbonate platforms - the deep and the past. *Mar. Geol.*, 44, 1-24.
- Schlager, W., Reijmer, J.J.G., Droxler, A.** (1994) Highstand shedding of carbonate platforms. *J. Sediment. Res.*, B64, 270-281.
- Shiki, I., Cita, M.B., Gorsline, D.S.** (2000) Sedimentary features of seismites, seismo-turbidites and tsunamites - an introduction. *Sed. Geol.*, 135, vii-ix.

Sohn, Y.K., Choe, M.Y., Jo, H.R. (2002) Transition from debris flow to hyperconcentrated flow in a submarine channel (the Cretaceous Cerro Toro Formation, Southern Chile). *Terra Nova*, 14, 405-415.

Spence, G.H., Tucker, M.E. (1997) Genesis of limestone megabreccias and their significance in carbonate sequence stratigraphic models: a review. *Sed. Geol.*, 112(3-4), 163-193.

Speranza, F., Maniscalco, R., Mattei, M., Funiciello, R. (2000) Palaeomagnetism in the Sicilian Maghrebides: review of the data and implications for the tectonic styles and shortening estimates. *Mem. Soc. Geol. Ital.*, 55, 95-102.

Speziale, S. (1997) Il Magmatismo Mesozoico-Paleogenico della Sicilia Occidentale. PhD Thesis, Università degli Studi di Catania, 256 pp.

Stampfli, G.M., Mosar, J., Favre, P., Pillecuit, A., Vannay, J.C. (2001) Permo-Mesozoic evolution of the western Tethyan realm: the Neotethys/East-Mediterranean connection. In: *PeriTethys Memoir 6: Peritethyan Rift/wrench Basins and Passive Margins, IGCP 369* (Eds P.A. Ziegler, W. Cavazza, A.H.F Robertson and S. Crasquin-Soleau), *Mem. Mus. Natl Hist. Nat.*, 186, 51-108.

Talling, P.J., Masson, D.G., Sumner, E.J., Malgesini, G. (2012) Subaqueous sediment density flows: depositional processes and deposit types. *Sedimentology*, 59, 1937–2003.

Talling, P.J., Paull, C.K., Piper, D.J.W. (2013) How are subaqueous sediment density flows triggered, what is their internal structure and how does it evolve? Direct observations from monitoring of active flows. *Earth-Sci. Rev.*, 125, 244–287.

Tanos, C.A., Kupecz, J., Warren, J.K., Lestari, S., Baki, A. (2012) Depositional and diagenetic effects on reservoir properties in carbonate debris deposits: comparison of two debris flows within the Berai Fm., Makassar Strait, Indonesia. AAPG Search and Discovery Article #50768, AAPG International Conference and Exhibition, Singapore.

Tavani, S., Iannace, A., Mazzoli, S., Vitale, S., Parente, M. (2013) Late Cretaceous extensional tectonics in Adria: insights from soft-sediment deformation in the Sorrento Peninsula (Southern Apennines). *J. of Geodynamics*, 68, 49-59.

- Todaro, S., Di Stefano, P., Zarcone, G., Randazzo, V.** (2017) Facies stacking and extinctions across the Triassic-Jurassic boundary in a peritidal succession from Western Sicily. *Facies*, 63:20.
- Todaro, S., Rigo, M., Randazzo, V., Di Stefano, P.** (2018) The end-Triassic mass extinction: a new correlation between extinction events and $\delta^{13}C$ fluctuations from a Triassic-Jurassic peritidal succession in Western Sicily. *Sed. Geol.*, 368, 105-113.
- Tournadour, E., Mulder, T., Borgomano, J., Hanquiez, V., Ducassou, E., Gillet, H.** (2015) Origin and architecture of a Mass Transport Complex on the northwest slope of Little Bahama Bank (Bahamas): relations between off-bank transport, bottom current sedimentation and submarine landslides. *Sed. Geol.*, 317, 9-26.
- Tournadour, E., Mulder, T., Borgomano, J., Gillet, H., Chabaud, L., Ducassou, E., Hanquiez, V., Etienne, S.** (2017) Submarine canyon morphologies and evolution in modern carbonate settings: the northern slope of Little Bahama Bank, Bahamas. *Mar. Geol.*, 391,76-97.
- Troya Garcia, L.** (2015) Rudistas (Hippuritida, Bivalvia) del Cenomaniense-Coniaciense (Cretácico Superior) del Pirineo meridional-central. PhD Thesis, Universitat Autònoma de Barcelona, 519 pp.
- Varnes, D.J.** (1978) Slope movement types and processes. In: *Landslides, Analysis and Control* (Eds. R.L. Schuster, R.J. Krizek), *National Academy of Sciences, Washington, Spec. Rep.*, 176, 11-33 pp.
- Vecsei, A., Sanders, D.K., Bernoulli, D., Eberli, G.P., Pignatti, J.S.** (1998) Cretaceous to Miocene sequence stratigraphy and evolution of the Maiella carbonate platform margins, Italy. *SEPM Spec. Publ.*, 60, 53-73.
- Velić, I.** (2007) Stratigraphy and palaeobiogeography of Mesozoic benthic foraminifera of the Karst Dinarides (SE Europe). *Geol. Croat.*, 60, 1-60.
- Vitale, S., Amore, O.F., Ciarcia, S., Fedele, L., Grifa, C., Prinzi, E.P., Tavani, S., D'Assisi Tramparulo, F.** (2018) Structural, stratigraphic, and petrological clues for a Cretaceous-Paleogene abortive rift in the southern Adria domain (Southern Apennines, Italy). *Geol. J.*, 53, 660-681.
- Webster, J.M., Beaman, R.J., Puga-Bernabeu, A., Ludman, D., Renema, W., Wust, R.A.J., George, N.P.J., Reimer, P.J., Jacobsen, G.E., Moss, P.** (2012) Late Pleistocene history of turbidite sedimentation in a

submarine canyon off the northern Great Barrier Reef, Australia. *Palaeogeogr. Palaeoclimatol. Palaeoecol.*, 331–332, 75–89.

Webster, J.M., George, N.P.J., Beaman, R.J., Hill, J., Puga-Bernabeu, A., Hinestrosa, G., Abbey, E.A., Daniell, J.J. (2016) Submarine landslides on the Great Barrier Reef shelf edge and upper slope: a mechanism for generating tsunamis on the north-east Australian coast? *Mar. Geol.*, 371, 120–129.

Wilson, J.L. (1969) Microfacies and sedimentary structures in “deeper water” lime mudstones. In: *Depositional environment in carbonate rocks*, (Eds G.M. Friedman), *Soc. Econ. Paleontol. Mineral. Spec. Publ.*, 14, 4-19.

Wunsch, M., Betzler, C., Lindhorst, S., Lüdmann, T., Eberli, G.P. (2016) Sedimentary dynamics along carbonate slopes (Bahamas archipelago). *Sedimentology*, 64, 631-657.

Zappaterra, E. (1994) Source-Rock Distribution of the Periadriatic Region. 3 (78), 333-354.

Zarcone, G., Di Stefano, P. (2010) La Piattaforma Carbonatica Panormide: un caso anomalo nell'evoluzione dei bacini della Tetide giurassica. *Boll. Soc. Geol. It.*, 129, 188-194.

Zarcone, G., Petti, F.M., Cillari, A., Di Stefano, P., Guzzetta, D., Nicosia, U. (2010) A possible bridge between Adria and Africa: new palaeobiogeographic and stratigraphic constraints on the Mesozoic palaeogeography of the Central Mediterranean area. *Earth-Sci. Rev.*, 103(3-4), 154-162.

3. A Cretaceous Carbonate Escarpment from Western Sicily (Italy): biostratigraphy and tectono-sedimentary evolution

Randazzo, Vincenzo (1); Di Stefano, Pietro (1); Todaro, Simona (1); Cacciatore, Maria Simona (2)

(1) University of Palermo - Department of Earth and Marine Sciences, Palermo, Italy.

Corresponding author: vincenzo.randazzo04@unipa.it

(2) Eni S.p.A. Upstream and Technical Services, San Donato Milanese, Italy.

Abstract

The presence of a huge carbonate slope of Cretaceous age is recorded in some imbricated thrust sheets from the Maghrebian fold-and-thrust belt cropping out in northwesternmost Sicily (southern Italy). The sedimentological features of this escarpment, named as the Western Sicily Cretaceous Escarpment (WSCE), have been recently described. The present paper aims to provide a detailed bio-chronostratigraphic characterization of the different facies types that occur in the four lithostratigraphic units spanning the whole slope depositional system. The detailed biostratigraphic analysis and correlation of a number of well-exposed sections allowed to differentiate eight informal biozones and to place the different studied sections, either from a single tectonic unit or from different ones, in a reliable chronostratigraphic frame. The integration of sedimentological and biostratigraphic data allowed in turn to time-constrain the main tectono-sedimentary events along the WSCE. In particular: i) the abrupt transformation from a carbonate ramp to a tectonically-controlled escarpment during the Berriasian-Valanginian; ii) the peak of tectonic instability leading to the emplacement of thick megabreccia bodies and repeated submarine volcanic emissions during the Aptian- Cenomanian; iii) the almost coeval increase in the skeletal supply in

response to highstand shedding occurred during the Albian-Cenomanian; iv) the tectonic backstepping of the carbonate depositional system during the Senonian ending with the definitive shutdown of the carbonate factory in the late Maastrichtian. The acquired biostratigraphic dataset is in large part new for the Cretaceous of Sicily and provides information on the associations that populated a southwestern Tethyan carbonate platform during the Cretaceous.

Keywords: Cretaceous, Slope, Biostratigraphy, Rudists, Tectonics, Carbonates

1. Introduction

In Sicily, shallow water carbonates of Cretaceous age were formed in a paleogeographic sector of the western Tethys known as the Panormide Carbonate Platform (Catalano and D'Argenio, 1982; Zappaterra, 1990). This platform was flanked toward east by the Imerese Basin, a slope to deep-water basin since Permian and Triassic times (Di Stefano and Gullo, 1997) that, during Cretaceous, hosted siliceous sediments with thick clastic carbonate intercalations (Crisanti Formation, Scandone et al., 1972; Schmidt di Friedberg, 1965). Since early Miocene, owing to the Maghrebic orogeny, both the Panormide and Imerese paleogeographic sectors were fragmented into several tectonic units that nowadays crop out from the Palermo Mountains to the Madonie Mountains (Catalano et al., 1996) (Fig. 1).

Panormide-derived Cretaceous slope sediments were accumulated also in a different paleogeographic sector that was located west and southwest of the platform (Western Sicily Cretaceous Escarpment, WSCE in Randazzo et al., *in press*). The tectonic units formerly belonging to this sector are now cropping out in northwestern Sicily (i.e. the Capo San Vito Peninsula). Allochthonous gravity-flow deposits formed carbonate aprons on drowned blocks of Upper Triassic-Lower Jurassic platform carbonates, thus in a different palaeotectonic context as compared to the Imerese Basin (Fig. 1). These limestones are intensely exploited as ornamental stone commercially known as *Perlato di Sicilia* (Bellanca, 1969).

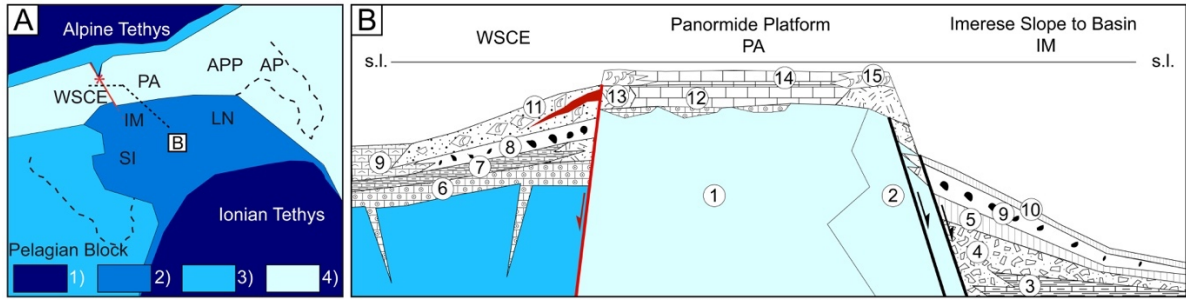


Fig. 1. (A) Paleogeographic sketch of the Central Mediterranean area during Albian showing the inferred location of the WSCE (mod. after Zarcone and Di Stefano, 2010): 1) oceanic basins; 2) deep-water basins on thinned continental crust; 3) carbonate platforms drowned during the Early Jurassic; 4) carbonate platforms; PA = Panormide Platform, IM = Imerese Basin; SI = Sicanian Basin; LN = Lagonegro Basin; APP = Apennine Platform, AP = Apulia Platform. (B) Schematic palinspastic section (not to scale) across the Panormide Platform and the adjacent escarpments (see black dotted line in A for the location of the section): 1) Peritidal carbonates (U. Triassic-L. Jurassic); 2) Sponge limestones (U. Triassic); 3) *Halobia* limestones (U. Triassic); 4) Dolo-debrites and dolo-turbidites (U. Triassic-L. Jurassic); 5) Radiolarites (Jurassic); 6) Rosso Ammonitico (M.-U. Jurassic); 7) Calpionellid limestones (Tithonian-Berriasian); 8) *Ellipsactinia* breccias (L. Cretaceous); 9) *Aptychus* marls (L. Cretaceous); 10) Spongolites (L. Cretaceous); 11) Rudist calcidebrites and megabreccias (L. Cretaceous); 12) Peritidal limestones (U. Jurassic-L. Cretaceous); 13) *Ellipsactinia* limestones (U. Jurassic-L. Cretaceous); 14) Peritidal limestones (L. Cretaceous); 15) Rudist limestones (L. Cretaceous).

The biostratigraphic characterization of the Cretaceous carbonates of the Panormide Platform has been based both on rudists and microfossils (Bucur et al., 1996; Camoin, 1982; Di Stefano, 1898; Di Stefano and Ruberti, 2000; Gemmellaro G.G., 1865; Montanari, 1964; Senowbari-Daryan et al., 1994; Sirna, 1982). Less detailed is the biostratigraphy of the slope sediments both from the Imerese and Capo San Vito slopes. The latter were object of several studies dealing with geological mapping and stratigraphy (Abate et al., 1993, 1991; Catalano et al., 2011; Giunta and Liguori, 1972, 1973). Pillow basalts and tuffites related to extensional crustal faults characterize such Cretaceous slope succession (Bellia et al., 1981). These previous contributions generically assign to the Cretaceous these slope limestones and to the Albian-Cenomanian and to the Upper Cretaceous-Eocene intervals the volcanic intercalations (Bellia et al., 1981). This study aims at presenting the results of biostratigraphic and carbonate

microfacies investigations performed on the Cretaceous slope limestones from the Capo San Vito Peninsula. Besides the original description of the different fossil and microfossil assemblages, these data allow to reconstruct the sedimentary evolution of the slope throughout the Cretaceous by means of the definition of tight chronostratigraphic constraints and provide an indirect characterization of the facies associations at the margins of the Panormide Platform. Moreover, the bio-chronostratigraphic data allow a better calibration of the main extensional events recorded in the Sicilian sector of the southwestern Tethys during the Cretaceous.

2. Geological setting

The Capo San Vito Peninsula is located in northwestern Sicily, southern Italy (Fig. 2). As most of Sicily, this area is part of the Maghrebian fold-and-thrust belt and consists of a south-verging nappe stack that was emplaced during late Oligocene and Miocene times (Abate et al., 1991; Catalano and D'Argenio, 1982; Giunta and Liguori, 1972). Paleomagnetic data indicate that during their emplacement the individual nappes experienced up to 90° clockwise rotations (Oldow et al., 1990; Speranza et al., 2000). Later, NW-SE and NE-SW oriented extensional and strike-slip faults crosscut the fold and thrust belt from late Pliocene onwards (Nigro and Renda, 2002) as consequence of the formation of the Tyrrhenian margin (Pepe et al., 2000). The stratigraphic setting of the nappe stack in the Capo San Vito Peninsula allows to reconstruct the evolutionary history of a Mesozoic carbonate succession (Abate et al., 1991; Giunta and Liguori, 1972; Todaro et al., 2017; Fig. 2 D). The lower part of nappes consists of some 1000 m thick peritidal limestone and dolostone Upper Triassic-Lowermost Jurassic in age (Todaro et al., 2018). Discontinuous lenses of condensed Middle-Upper Jurassic ammonitic limestones followed by some metre thick calpionellid limestones Tithonian-lowermost Cretaceous in age overlie the peritidal carbonates through a drowning unconformity. They are in turn covered by some 700 m of Cretaceous gravity-flow deposits

containing *Ellipsactinia* in the lower part and rudists in the upper part (Randazzo et al., *in press*). The rudist gravity-flow deposits contain several intercalations of basaltic volcanics in form of tuffites and more rare pillow lavas (Bellia et al., 1981). Upward the carbonate succession consists of pelagic lime mudstone (“scaglia”-type) Late Cretaceous-Eocene in age and of nummulitic calcarenites of late Eocene-Oligocene age (Abate et al., 1991). The succession is truncated by a deep erosional surface with a karstic overprint and covered through an angular unconformity by lower Miocene glauconitic calcarenites and marls. As already stated in Randazzo et al. (*in press*), the source area of the Cretaceous slope carbonates object of the present paper can be envisaged in the Panormide Platform as Cretaceous *Ellipsactinia* and rudist shallow-water carbonates were present exclusively in this palaeodomain.

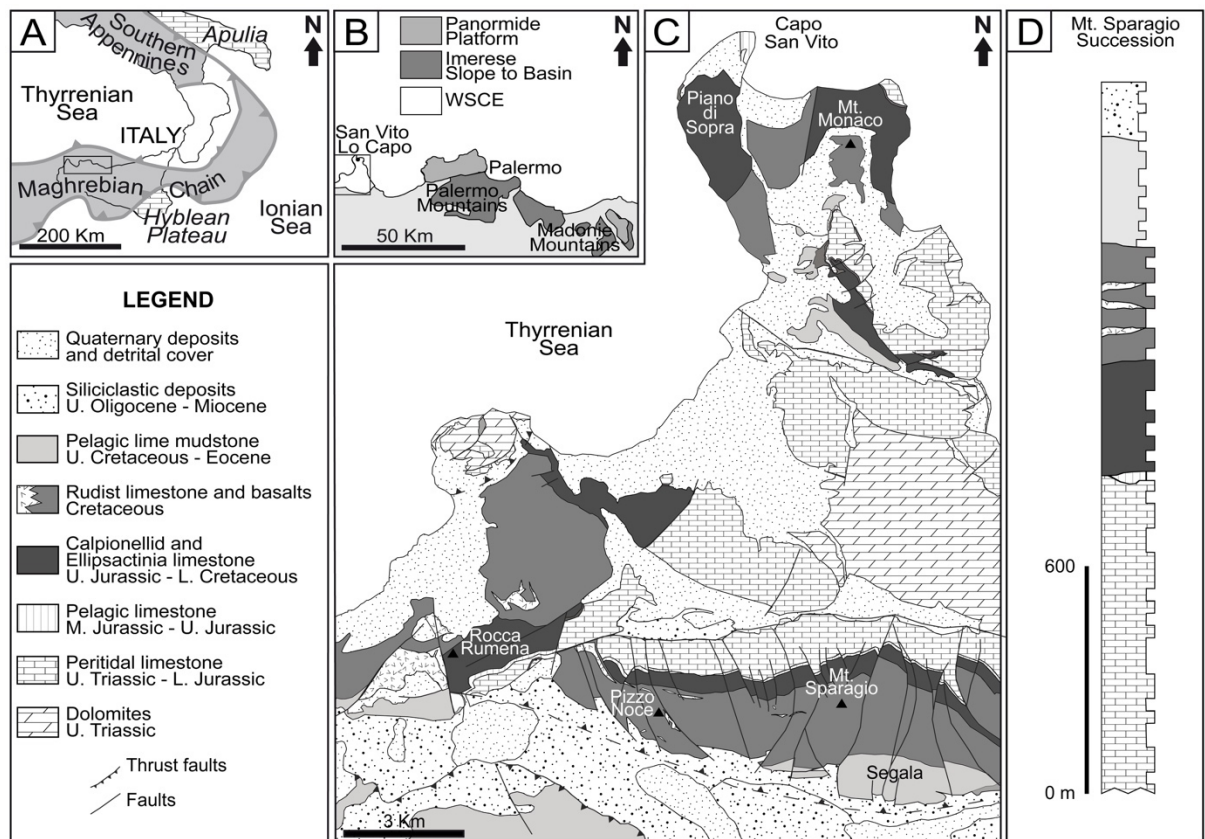


Fig. 2. A) Tectonic sketch of the central Mediterranean area. B) Simplified map of the north-western Sicily showing the present-day location of the Panormide Platform and WSCE-derived thrust sheets. C) Geological map of the Capo San Vito Peninsula (based on (Abate et al., 1993) and location of the studied sections. D) Composite stratigraphic column of the tectonic units from the Capo San Vito area.

3. Material and methods

The presence of several well-exposed outcrops and quarries allows to perform a detailed field work aimed at reconstructing a composite section across the whole slope depositional system (see localities in Fig. 2). Four informal lithological units have been differentiated on the base of the observed sedimentological features. So-called “windows”, rectangles of about 1 square metre, were selected as representative parts of the lithological units for macroscopic description. Textural analysis has been performed both in the field and on about 100 thin sections from collected samples following the classifications proposed by Dunham (1962) and Embry and Klovan (1971). The biostratigraphic characterization of the Cretaceous limestones was performed in order to define specific chronostratigraphic intervals. In this respect, this study is based on the distribution ranges for the Western Tethys realm proposed by previous studies (Andreini et al., 2007; Cestari and Sartorio, 1995; Chiocchini, 2008; Chiocchini et al., 2008; Premoli Silva and Verga, 2004; Petrizzo et al., 2017; Troya Garcia L., 2015; Velić, 2007). As result, nine informal biozones were defined on the base of several biomarker occurrences. The age of the WSCE gravity-flows deposits has been defined on the base of the biomarkers observed in the matrix. Calpionellids, rudists, calcareous algae, benthic and planktonic foraminifers are the main biota constituting the biostratigraphic associations. The age of the lithoclasts has been considered as well in order to define the involvement of the sedimentary rocks exposed on the foot wall block successions.

The studied material (including the comprehensive photographic documentation, rock samples and thin sections) is stored in the Laboratory of Stratigraphic Geology at the Department of Earth and Marine Sciences, University of Palermo, Italy (collection V. Randazzo).

Table 1. Biozonal schemes of the Cretaceous shallow water carbonates according to Chiocchini et al., (2008) and Velić (2007).

Chronostratigraphic units		Chiocchini et al., 2008		Velic, 2007	
		Platform margin	Outer slope	AdCP benthic forams	
CRETACEOUS	Upper	Maastrichtian	Orbitoides	<i>Globotruncana, Globotruncanita and Orbitoides</i>	<i>Kalveziconus lecalvezae, Murciella cuvillieri</i>
		Campanian			<i>Kalveziconus lecalvezae</i>
		Santonian	Hippuritidae and Radiolitidae	<i>Globotruncanita and Hippuritidae</i>	<i>Keramosphaerina tergestina</i>
		Coniacian			<i>Murgella lata</i>
		Turonian			<i>Dicyclina schlumbergeri, Murgella lata</i>
		Cenomanian			<i>Scandonea samnitica, Dicyclina schlumbergeri</i>
					<i>Pseudocyclammina sphaeroidea, Scandonea samnitica</i>
	Lower	Albian	Orbitolina	<i>Rotalipora and Orbitolina</i>	<i>Chrisalidina gradata, Pseudocyclammina sphaeroidea</i>
					<i>Chrisalidina gradata</i>
		Aptian	Lithocodium aggregatum	<i>Colomisphaera, Radiolaria and Lithocodium aggregatum</i>	<i>Conicaorbitolina conica / Conicorbitolina cuvillieri</i>
					<i>Neoiraquia convexa</i>
					<i>'Valdanchella' dercourtii</i>
		Barremian	Lithocodium aggregatum	<i>Calpionellopsis, Calpionelites and Lithocodium aggregatum</i>	<i>Mesorbitolina subconcava</i>
		Hauterivian			<i>Mesorbitolina texana</i>
Valanginian	<i>Mesorbitolina parva</i>				
	<i>Palorbitolina lenticularis</i>				
Berriasian	Lithocodium aggregatum and Tubiphytes moronensis	<i>Crassicollaria, Calpionella, Lithocodium aggregatum and Tubiphytes moronensis</i>	<i>Campanellula capuensis, Palorbitolina lenticularis</i>		
			<i>Campanellula capuensis</i>		
				<i>Vercorsella camposauri, Campanellula capuensis</i>	
				<i>Vercorsella camposaurii</i>	
				<i>Protopenereplis ultragranulata, Vercorsella camposauri</i>	
				<i>Protopenereplis ultragranulata</i>	

4. Lithostratigraphy

Four informal lithostratigraphic units of Cretaceous age are differentiated in this study in the area of San Vito Lo Capo. They partly coincide with the lithostratigraphic units already recognized by Abate et al. (1991). As reported in the geological setting the studied successions covers a thick series of shallow water limestones and dolostones of Triassic and lowermost Jurassic age.

4.1 Unit A [*Calpionellid/Crescentiella* limestones (Tithonian-lowermost Cretaceous p.p.)]

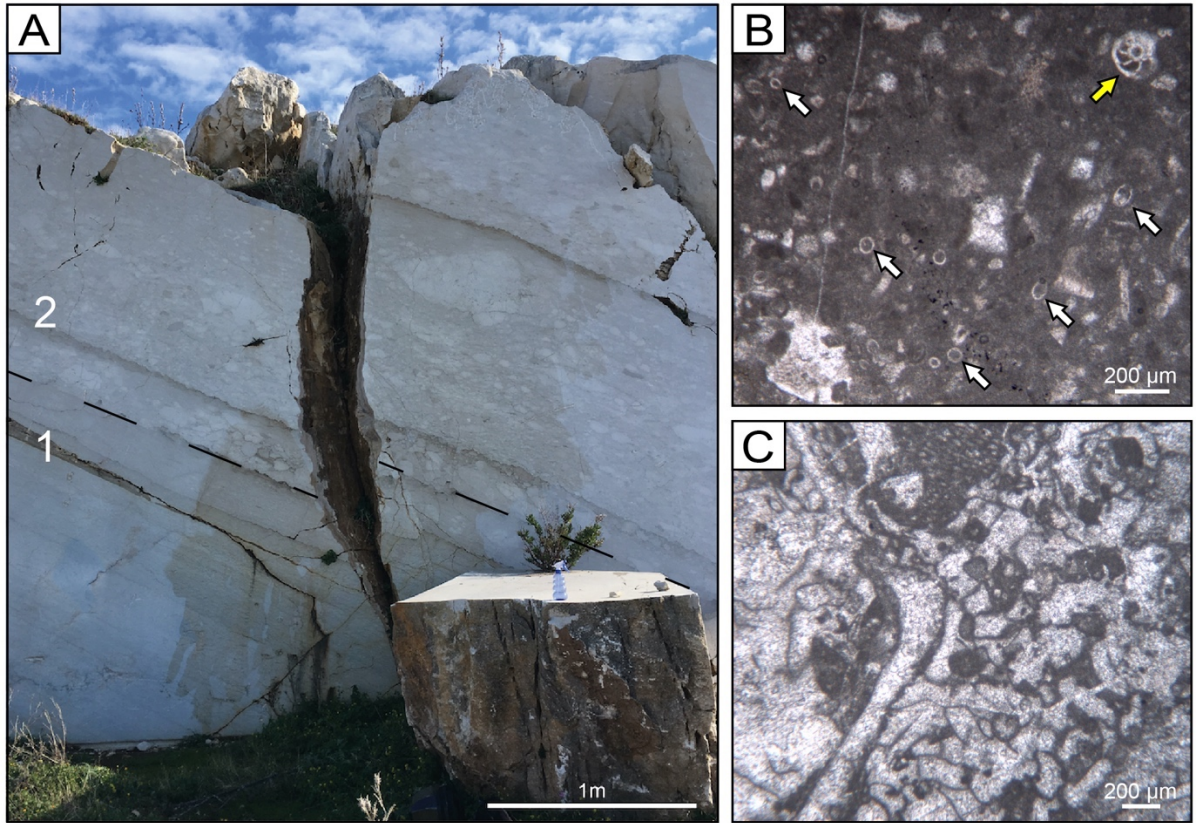
This unit covers the lowermost part of WSCE succession and consists of fine-grained (silt to sand) reddish-greyish limestones often featured by a nodular structure (Fig. 3A). Texture consists of wackestone and thin layer of isopachous calcite cements often rims grains. A brownish micrite matrix fill up the intergranular spaces (Fig. 3B). Unit A comprises the

ammonitic limestones and the lower part of the *calpionellid and Ellipsactinia limestones* (*sensu* Abate et al., 1991; 1993), since no significant lithologic changes are observed if we exclude the microfossil content (i.e. the calpionellids in the upper part), while a sharp lithological contact occurs between the calpionellid wackestone and the coarse *Ellipsactinia* breccias (Unit B) (Fig. 3A).

4.2 Unit B [*Ellipsactinia breccias* (Lower Cretaceous p.p.)]

The top of Unit A is abruptly truncated by clast- to matrix-supported bedded breccias constituting Unit B. These breccias are whitish in colour and display parallel beds up to a couple metre thick. They consist of angular extraclasts up to some decimetres, associated to cm-sized skeletal fragments such as corals, bryozoans, sponges and stromatoporoids (i.e. *Ellipsactinia*). Greyish levels of finer grained skeletal wackestone-packstone cap the calcirudite beds. The matrix of the calcirudite is a wackestone to fine rudstone, while extraclasts often derived from the footwall block succession (Fig. 3). In the northern sector of the study area (Piano di Sopra, see Fig. 2C) the calcirudite beds of this unit alternate to altered marly lime mudstones.

Fig. 3. A) Field photograph showing the abrupt contact between the calpionellid limestones of the Unit A (1) and the overlying *Ellipsactinia* breccias of Unit B (2). Locality Pizzo Noce. B) Microfacies of Unit A consisting of wackestone with pelagic (white arrows) and platform-derived skeletal grains (yellow arrow), sample FM8, locality Pizzo Noce. C) Microfacies of Unit B showing a pervasive *Bacinella/Lithocodium* incrustation, sample N113, locality Pizzo Noce.



4.3 Unit C [*Rudist breccias (Lower Cretaceous p.p.-Upper Cretaceous p.p.)*]

This is the main and thicker unit of the studied Cretaceous succession. The first occurrence of rudists marks the passage from Unit B to Unit C. The latter is the result of the alternation of MTDs (Mass Transport Deposits), such as bedded megabreccias and massive (chaotic) megabreccia bodies, and finer-grained skeletal calciturbidites. Several volcanic intercalations lie in different stratigraphic levels of this unit (Fig. 4 and 5). These volcanics are altered basalts and tuffites and account for an intense submarine volcanic activity (Bellia et al., 1981; Speziale, 1997). The massive megabreccia bodies are closely associated to these volcanic intercalations. The matrix of the megabreccias consists of a bioclastic packstone to rudstone mainly made of rudist fragments. Calcareous sponges, chaetetids, planktonic and benthic foraminifers occur as well (Fig. 4). In places, very thin peloids constitute the matrix. Lithoclasts consist of large (up to several metres) rudist/coral boundstone or pebbles and

cobbles from the lower units (A, B) and the underlying sedimentary substrate (Rosso Ammonitico). Calciturbidites consist of finer grained grainstone-packstone mainly made of comminuted rudist fragments.

In the Mt. Monaco area (see location in Fig. 2C) this unit records significant facies variations to rudist rudstone and grainstone lacking extraclasts. This facies is well comparable with the *Well-rounded, coarse rudstone-to-grainstone* previously described in the Panormide Platform (Mt. Pellegrino, Di Stefano and Ruberti, 2000). In the eastern sector of the Mt. Sparagio ridge, similar platform margin limestones are overlapped by slope deposits. Upward, Unit C shows a well-exposed transition to Unit D. In the western sector of the Mt. Sparagio ridge, an erosional and karstified surface covered by Miocene calcarenites truncate Unit C.

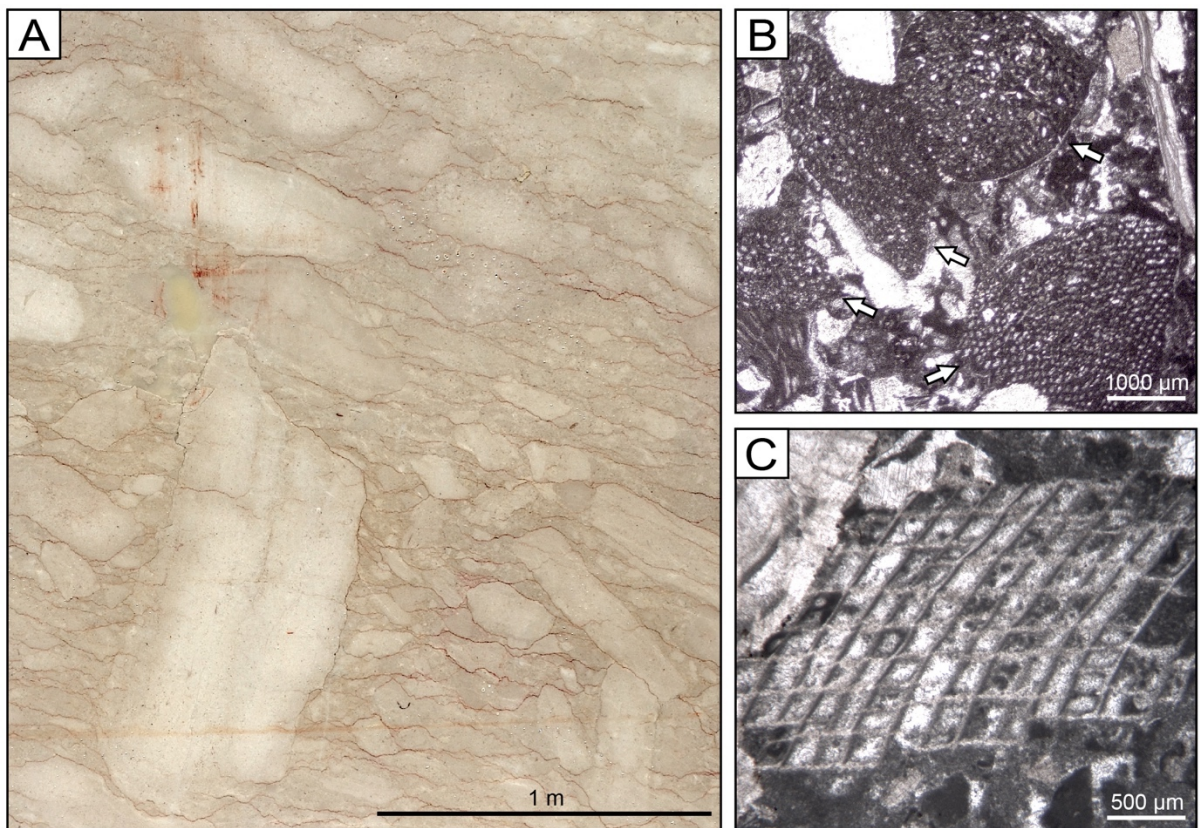


Fig. 4. A) Field photograph of the Rudist breccias occurring in Unit C. Locality Pizzo Noce. B) Matrix of the same breccias that consists of a rudstone with orbitolinids (white arrows), sample Cms3, locality Pizzo Noce. C) Rudist fragments occurring in the rudstone matrix, sample Nq2, locality Pizzo Noce.

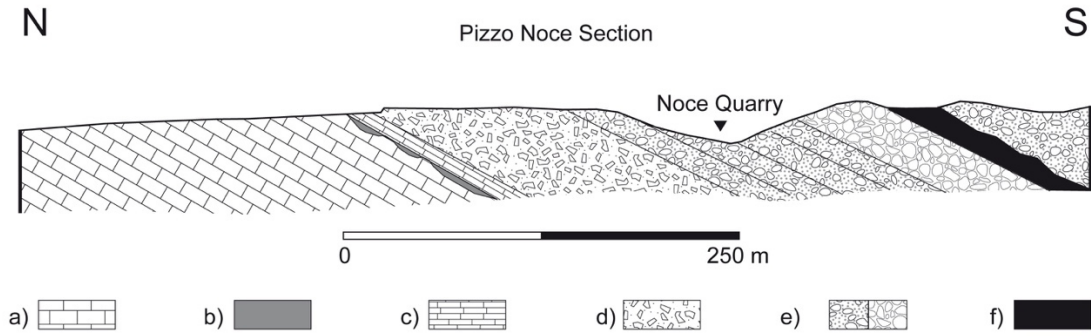


Fig. 5. Geological cross-section of the Pizzo Noce area showing the facies evolution from the Late Triassic to the Early Cretaceous (see Fig. 2 for cross-section location): a) Peritidal Limestone (Upper Triassic-lowermost Jurassic); b) Condensed Rosso Ammonitico (Middle-Upper Jurassic); c) *Saccocoma* and calpionellid limestones (uppermost Jurassic-Berriasian); d) *Ellipsactinia* limestone (Valanginian-Barremian); e) Bedded calcidebrite and chaotic megabreccia (Aptian); f) Basaltic tuffites and pillow lavas.

4.4 Unit D [*Scaglia*-type calcilutites interbedded with calcidebrites (Senonian)]

This unit occurs at the top of the studied succession and consists of alternations of deep-water lime mudstones (Amerillo Fm.) and breccia beds (Fig. 6). The main constituents in the lime mudstones are planktonic foraminifers and comminuted rudist fragments. On the other hand, a rudstone matrix and pebble to cobble size lithoclasts characterize the breccia beds. Both lithoclasts and matrix usually show a comparable skeletal content as they consist of rudist fragments and benthic foraminifers (Fig. 6). Biostratigraphic evaluations support a lateral and upward transition of the alternations of pelagic lime mudstones with breccia beds and fine-grained calciturbidites to pure pelagic lime mudstone. This transition is exposed along two transects crossing the Capo San Vito Peninsula and located in the Rocca Rumena and Mt. Sparagio areas (Fig. 2C).

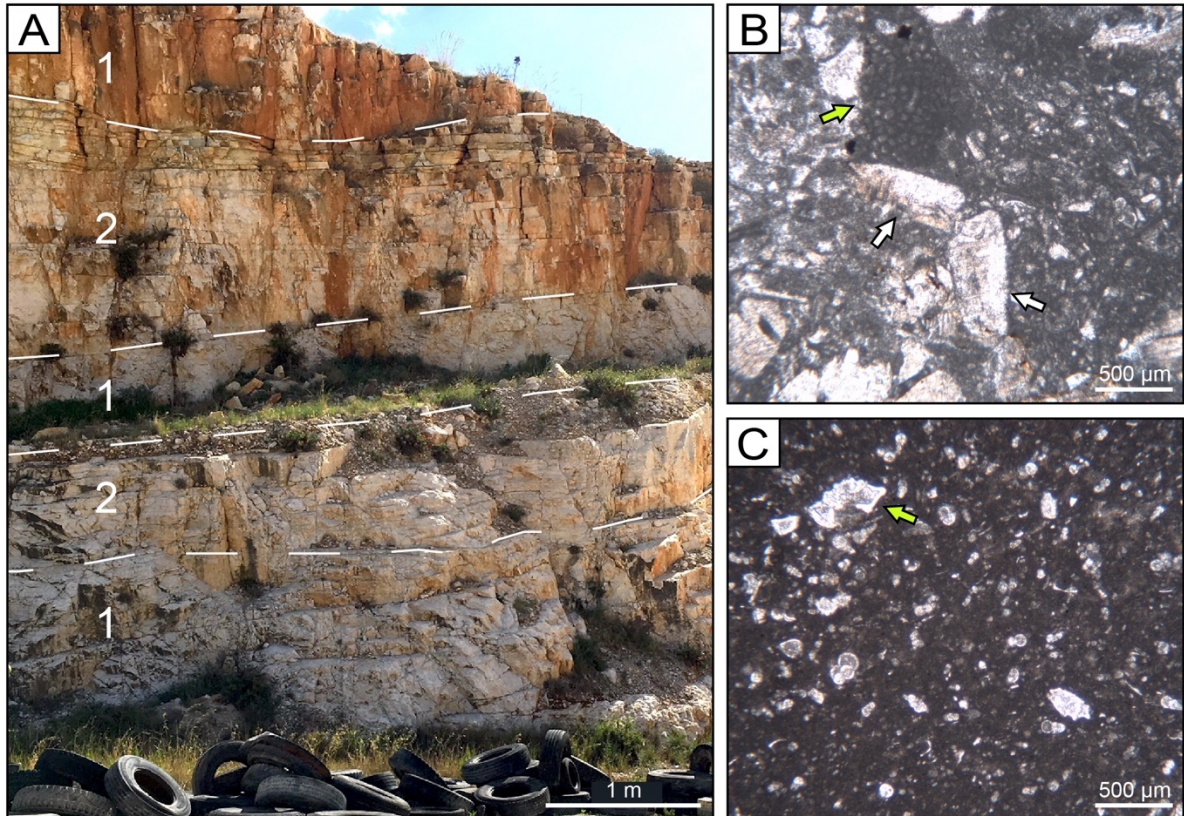
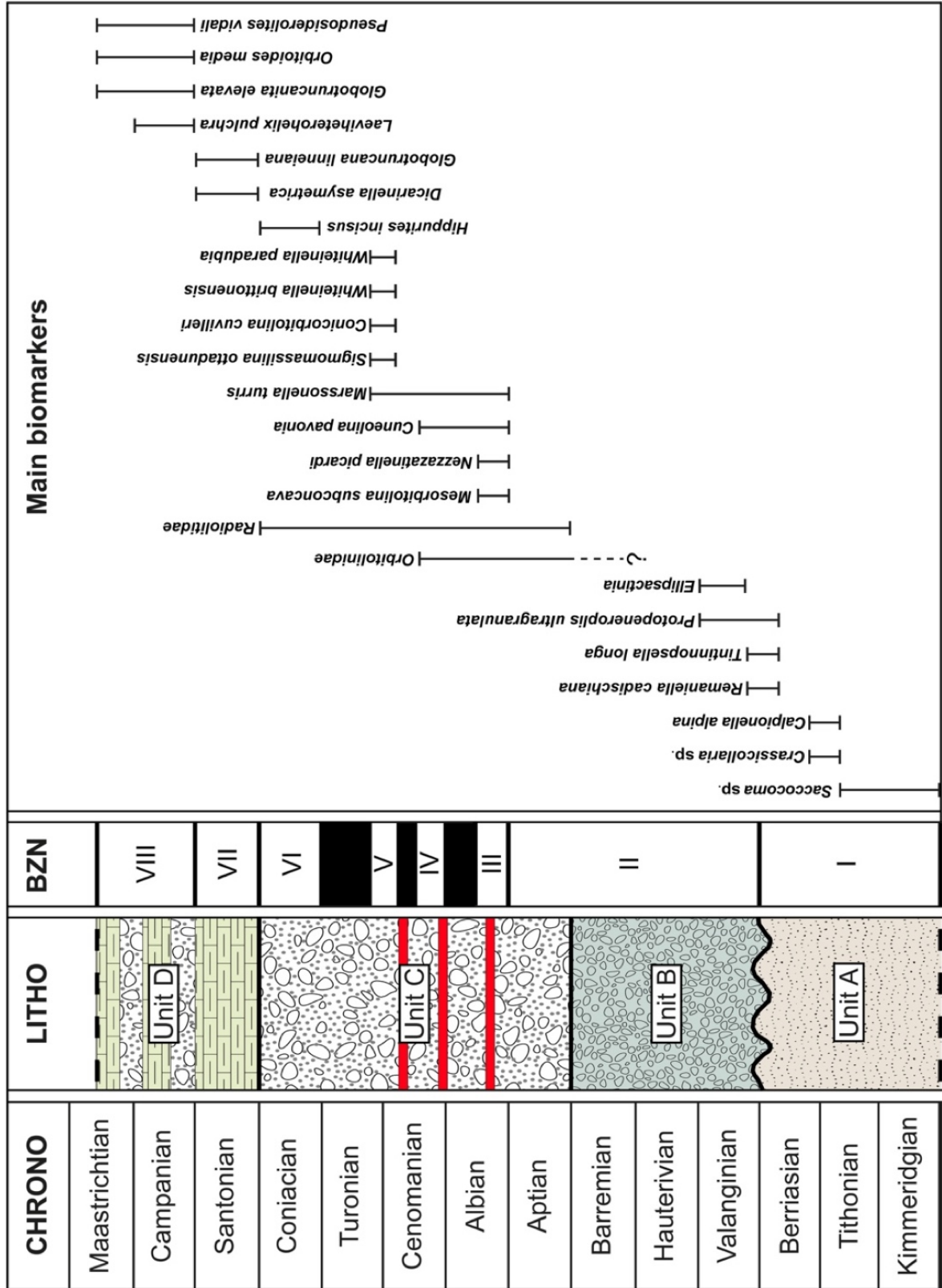


Fig. 6. A) Field photograph of Unit D showing the alternation of calcilutites (1) and calcidebrites (2). Locality Rocca Rumena. B) Microfacies of the calcidebrite matrix showing *Orbitoides* sp. (green arrow) and rudist fragments (white arrows), sample N121, locality Rocca Rumena. C) Microfacies of the calcilutites rich in planktonic foraminifers (e.g. *Globotruncanita stuartiformis*, green arrow), sample N120, locality Rocca Rumena.

5. Biostratigraphy and microfacies analysis

Eight biozones have been defined on the base of biotas belonging to different systematic groups (e.g. tintinnids, rudists, calcareous algae, benthonic and planktonic foraminifers). The identified biozones, numbered from 1 to 8, cover the uppermost Jurassic and almost the whole Cretaceous system (Fig. 7). Biozone 3 and 4 show good matches respectively with *Mesorbitolina subconcava* taxon-range zone and *Conicorbitolina conical/Conicorbitolina cuvillieri* partial-range zone, both by Velić (2007). Biozone 7 coincides with *Dicarinella asymetrica* zone by Petrizzo et al. (2017).

Fig. 7. Composite stratigraphic column of the WSC-E showing the informal lithostratigraphic and biozonal subdivisions and the stratigraphic distribution of selected biomarkers. CHRONO stands for chronostratigraphy, LITHO for lithostratigraphy and BZN for (informal) biozonation.



5.1 Biozone 1

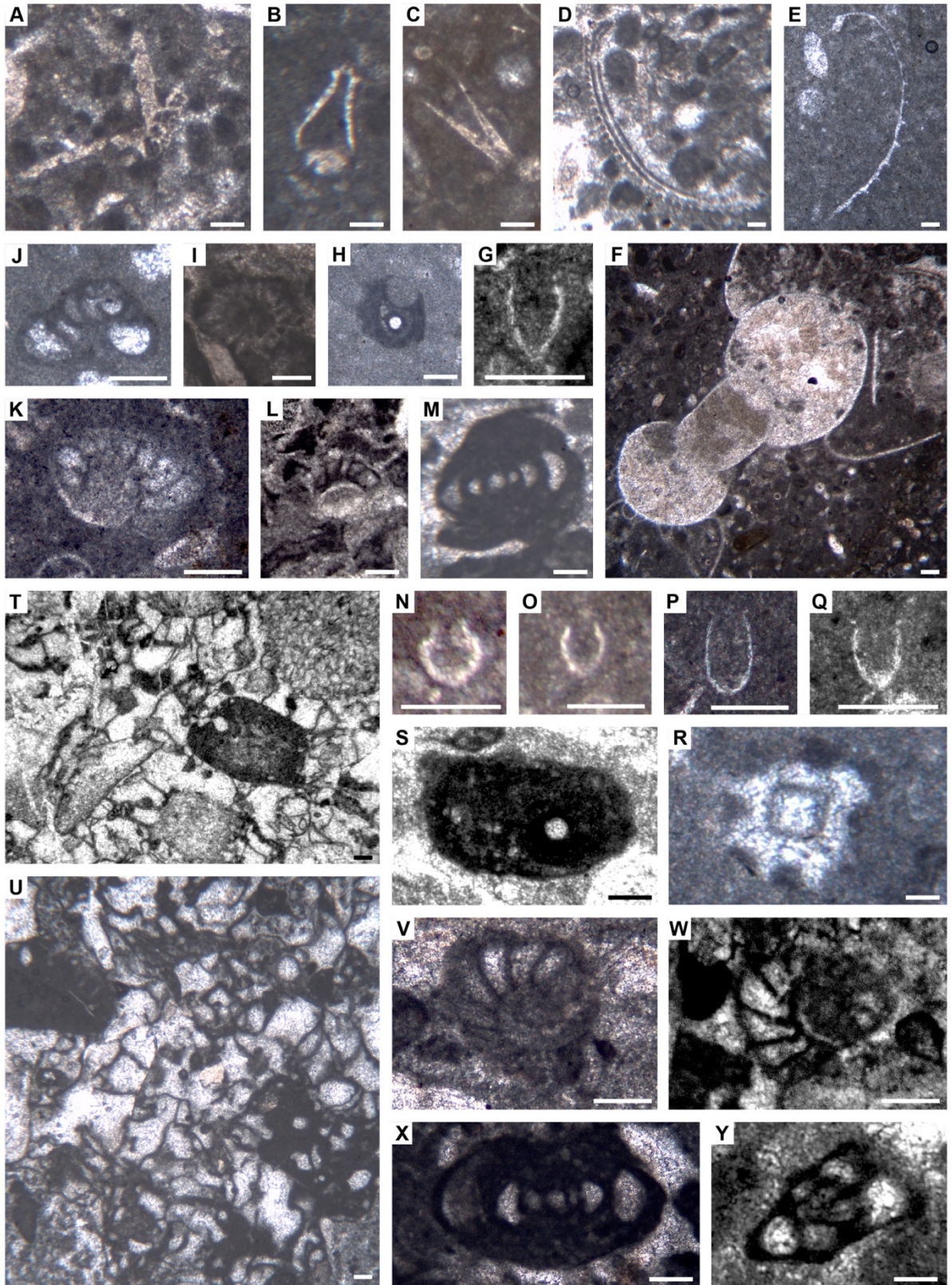
This biozone corresponds to Unit A, the observed taxa are listed below. Biomarkers and the most representative microfossils are shown in Fig. 8. Abundant *Saccocoma* sp. (Fig. 8A-C) fragments characterize lower samples of this unit. Echinoids spines, calcispheres, sponges spiculae, *Globochaete* sp., aptychi and ammonites (Fig. 8D-F) also occur frequently. Upper samples firstly show the occurrence of calpionellids such as *Crassicollaria* sp. (Fig. 8G). Shallow water skeletal grains such as *Crescentiella morronensis* (Fig. 8H), calcareous algae *Salpingoporella pigmea* (GÜMBEL) (Fig. 8I), and benthic foraminifers *Dobrogeolina ovidi* NEAGU (Fig. 8J), *Protopenneroplis ultragranulata* (GORBATCHIK) (Fig. 8K and L), *Nautiloculina* sp., (Fig. 8M) and *Lenticulina* sp. are present as well. The uppermost samples of Unit A still record the concomitant occurrence of pelagic and shallow-water skeletal grains. The assemblage consists of calpionellids [e.g. *Calpionellopsis* sp., *Calpionella alpina* LORENZ (Fig. 8N and O), *Tintinopsella longa* COLOM (Fig. 8P), *Remaniella cadischiana* (COLOM) (Fig. 8Q)], calcispheres, abundant and heavy recrystallized radiolarians, and rare benthic foraminifers (e.g. *Protopenneroplis ultragranulata*, *Nautiloculina* sp., *Lenticulina* sp., *Marssonella* sp., Textularidae and Lituolidae) echinoid spines and crinoids ossicles.

5.2 Biozone 2

This biozone corresponds to Unit B and the observed taxa are listed below. The most representative ones and the biomarkers as well are shown in Fig. 8. *Incertae saedis* such as *Coptocompylodon* sp. have been observed (Fig. 8R) and large bryozoan fragments are abundant both in the matrix and in the lithoclasts. Sometimes the latter may consist in clay chips rich in calpionellids and calcispheres coming from the underlying Unit A and belonging to Biozone 1. *Ellipsactinia*, *Crescentiella morronensis* and the pervasive presence of encrusting organisms such as *Bacinella irregularis* ELLIOT and *Lithocodium aggregatum* RADOIČIĆ characterize Biozone 2 (Fig. 8S-U). Benthic foraminifers are rare and often

recrystallized [e.g. *Protopeneroplis ultragranulata* (Fig. 8V and W), *Nautiloculina broennimanni* ARNAUD VANNEAU and PEYBERNES (Fig. 8X) and *Moesiloculina danubiana* NEAGU (Fig. 8Y)]. Rare planktonic foraminifera such as *Hedbergella* sp. may occur in the matrix.

Fig. 8. Biozone 1 (A to R) and Biozone 2 (S to Z). (A, B, C) *Saccocoma* sp., samples FM2, FM3, FM5, locality Pizzo Noce. (D, E) Ammonite aptychi, samples FM1, FM7, locality Pizzo Noce. (F) Ammonite transverse cross section, sample FM4, locality Pizzo Noce. (G) *Crassicollaria* sp., sample PSb2, locality Piano di Sopra. (H) *Crescentiella morronensis*, sample PSN100, locality Piano di Sopra. (I) *Salpingoporella pygmaea*, sample FM4, locality Pizzo Noce. (J) cfr. *Dobrogeolina ovidi*, sample FM102c, locality Rocca Rumena. (K, L) *Protopeneroplis ultragranulata*, samples FM12, FM9, locality Pizzo Noce. (M) *Nautiloculina broennimanni*, samples FM4, locality Rocca Rumena. (N, O) *Calpionella alpina*, samples FM7, FM8, locality Pizzo Noce. (P) *Tintinnopsella longa*, sample FM101, locality Rocca Rumena. (Q) *Remaniella cadischiana*, sample N115, locality Pizzo Noce. (R) *Coptocompylodon* sp., sample PSN100, locality Piano di Sopra. (S) *Crescentiella morronensis*, sample FM101, locality Rocca Rumena. (T) pervasive *Bacinella/Lithocodium* encrustation, *Crescentiella morronensis* and bryozoan fragment, sample N113, locality Pizzo Noce. (U) *Bacinella irregularis* and *Lithocodium aggregatum*, sample FM102d, locality Rocca Rumena. (V, W) *Protopeneroplis ultragranulata*, samples FM102c, PS[^], localities Rocca Rumena and Piano di Sopra. (X) *Nautiloculina broennimanni*, sample FM102c, locality Rocca Rumena. (Y) cfr. *Moesiloculina danubiana*, sample N112, locality Pizzo Noce. Scale bar 100 μ m.



5.3 Biozone 3

This biozone corresponds to the lower part of Unit C and the observed taxa are listed below. The most representative ones and the biomarkers as well are shown in Fig. 9. The first occurrence of rudists characterizes Biozone 3. Rudists become dominant and, as well as echinoids fragments, are the most abundant skeletal grains in this assemblage. Some well-preserved specimens and fragments were ascribed to the family Radiolitidae on the base of the typical cellular network in the outer layer of the shells. Sometimes, an intense microboring affects the rudist fragments, especially in the samples coming from the northern sector of the study area. The benthic foraminiferal assemblage is particularly rich and well diversified with *Nezzazatinella picardi* (HENSON) (Fig. 9A and B), *Nezzazata isabellae* ARNAUD VANNEAU and SLITER (Fig. 9C and D) and Orbitolinidae (e.g. *Mesorbitolina* sp., Fig. 9E; *Mesorbitolina subconcava* LEYMERIE, Fig. 9F and *Mesorbitolina texana* (ROEMER), Fig. 9G) as the most abundant taxa. *Marssonella turris* (D'ORBIGNY), *Lenticulina* sp., *Nezzazata* sp., cfr. *Nezzazata simplex* OMARA, *Istriloculina eliptica* (YOVCHEVA), *Rumanoloculina robusta* NEAGU, cfr. *Pseudonummoloculina aurigerica* CALVEZ and *Cuneolina* sp. D'ORBIGNY complete the benthic foraminiferal assemblage. Dasycladacean algae such as *Neomeris cretacea* STEINMANN (Fig. 9H), *Zittelina* aff. *massei* BUCUR, GRANIER, SASARAN (Fig. 9I) and ?*Pseudocymopolia* sp. (Fig. 9J) are also present in this biozone. Clay chips bearing planktonic foraminifera such as *Globigerinelloides* sp. and *Ticinella roberti* (GANDOLFI) (Fig. 9K) are scattered in the skeletal matrix. Bryozoans, gastropods, crinoid ossicles, red algae (*Solenopora* sp. and *Lithothamnium* sp.) and problematics such as *Bacinella irregularis* and *Lithocodium aggregatum*, *Mercierella dacica* DRAGASTAN, *Crescentiella morronensis* and *Coptocompylodon* sp. (Fig. 9L) are often present.

5.4 Biozone 4

This biozone corresponds to the upper part of Unit C. The observed taxa are listed below. The most representative ones and the biomarkers as well are shown in Fig. 9. Rudist fragments mainly related to the Radiolitidae family are the most common constituents of the fossil assemblage. Abundant and often well-preserved Orbitolinidae characterize Biozone 5. In particular, the analysis of the embryonic apparatus allowed referring some specimens to *Conicorbitolina cuvillieri* (MOULLADE) (Fig. 9M and N). *Pseudocyclamina* aff. *sphaeroidea* GENDROT (Fig. 9O-Q), *Cuneolina pavonia* (Fig. 9R), *Marssonella turris* (D'ORBIGNY), *Pseudolituonella reicheli* MARIE, and *Trinocladus tripolitanus* RAINERI (Fig. 9S) also define the microfossil assemblage. In the Mt. Monaco area (Fig.1), the assemblage is dominated by Orbitolinidae and *Caprina schiosensis* (Fig. 9T).

5.5 Biozone 5

This biozone occurs in the upper part of Unit C. The observed taxa are listed below. The most representative ones and the biomarkers as well are shown in Fig. 9. The biozone mainly differs from the preceding one as it lacks in Orbitolinidae while rudist fragments, mainly referred to Radiolitidae family, are the most abundant skeletal grains. The observed specimens were ascribed to the genus *Whiteinella*. In particular, the identified species are *Whiteinella paradubia* (SIGAL) and *Whiteinella brittonensis* LOEBLICH and TAPPAN (Fig. 9U and V). Small imperforate taxa such as *Sigmomassilina ottadunensis* CHIOCCHINI, (Fig. 9W and X) *Pseudolituonella reicheli* MARIE and *Marssonella turris* (D'ORBIGNY) (Fig. 9Y) constitute the benthic foraminifer assemblage. Calcispheres such as *Pithonella ovalis* (KAUFMANN) and “*Stomiosphaera*” *sphaerica* (KAUFMANN) (Fig. 9Z) are pretty abundant as well.

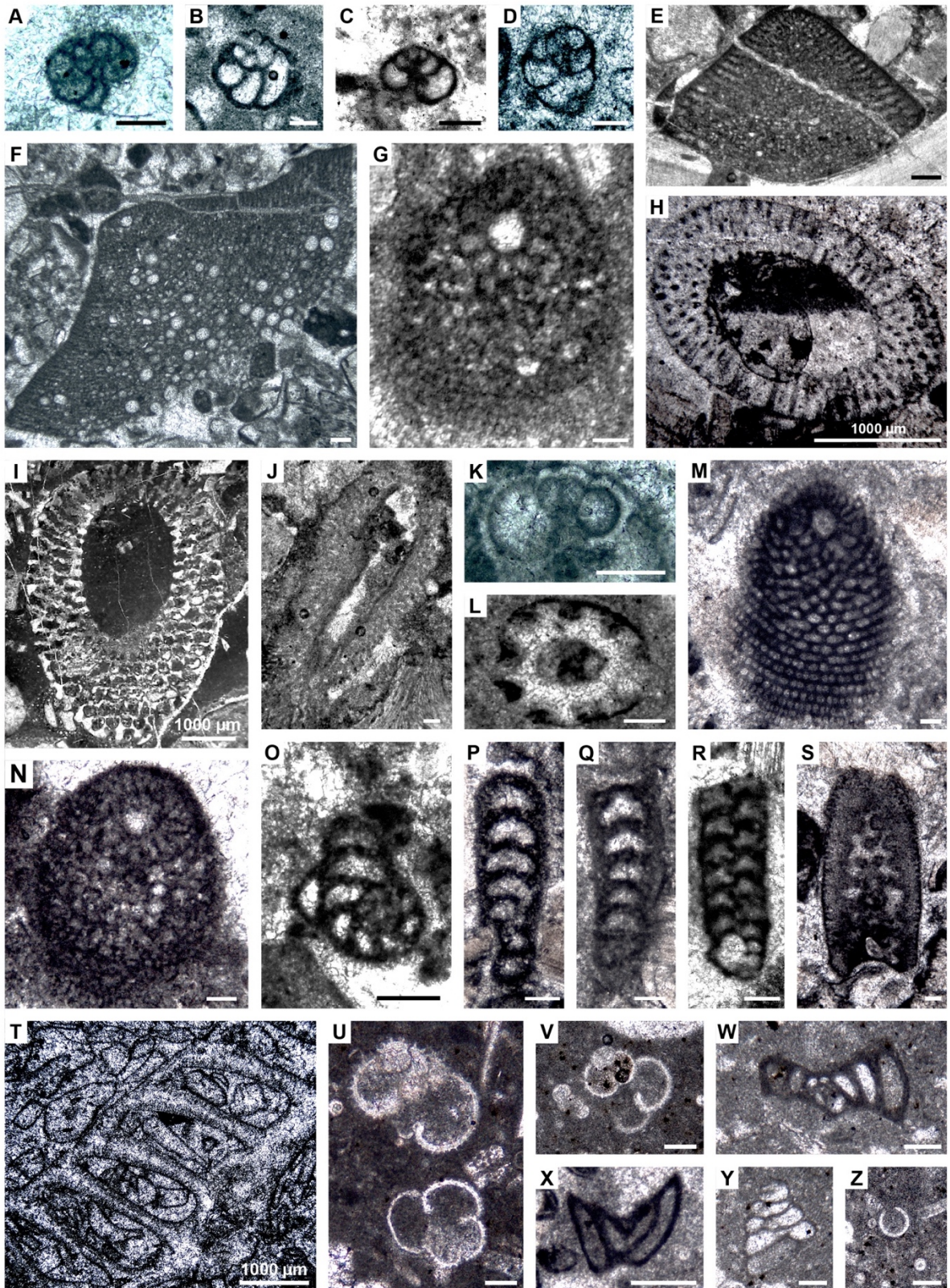


Fig. 9. Biozone 3 (A to M), 4 (N to T) and 5 (U to Z). (A, B) *Nezzazatinella picardi*, samples N1, N102, locality Pizzo Noce. (C, D) *Nezzazata isabellae*, samples N100, N103, locality Pizzo Noce. (E) *Mesorbitolina* sp., sample NQ4, locality Pizzo Noce. (F) *Mesorbitolina subconcava*, sample N106, locality Pizzo Noce. (G) *Mesorbitolina texana* sp., sample Nq3, locality Pizzo Noce. (H) *Neomeris cretacea*, sample N4, locality Pizzo Noce. (I) *Zittelina* aff. *massei*, sample NQ3, locality Pizzo Noce. (J) ?*Pseudocymopolia* sp., sample N2, locality Pizzo Noce. (K) *Ticinella* cfr. *roberti*, sample N1, locality Pizzo Noce. (L) *Coptocompylodon* sp., sample N1, locality Pizzo Noce. (M-N) *Conicorbitolina cuvilleri*, samples CvS1, Cms3, locality Pizzo Noce. (O-Q) *Pseudocyclammina* aff. *sphaeroidea*, samples CvS4, CvS8, MSp4, localities Pizzo Noce and Mt. Sparagio. (R) *Cuneolina pavonia*, MSp4, locality Mt. Sparagio. (S) *Trinocladus tripolitanus*, sample Cms1, locality Pizzo Noce. (T) *Caprina schiosensis*, sample CM3, locality Mt. Monaco. (U, V) *Whiteinella* cfr. *paradubia* cfr. *brittonensis*, samples RR1, RR2, locality Rocca Rumena. (W) *Sigmomassilina ottadunensis*, sample RR1, locality Rocca Rumena. (X) *Nezzazata* sp., sample RR1, locality Rocca Rumena. (Y) *Marssonella turris*, sample RR1, locality Rocca Rumena. (Z) cfr. *Stomiosphaera sphaerica*, sample RR2, locality Rocca Rumena. Scale bar 100 μm (when not differently specified).

5.6 Biozone 6

This biozone corresponds to the uppermost part of Unit C. The observed taxa are listed below. The most representative ones and the biomarkers are shown in Fig. 10. The skeletal content mainly consists of rudists and undetermined benthic and planktonic foraminifera. The latter are often heavily recrystallized preventing the identification. Echinoderms debris with syntaxial overgrowth are abundant as well as *Bacinella irregularis*, *Lithocodium aggregatum* and *Crescentiella morronensis*. Large loose and well-preserved specimens of large rudists characterizes Biozone 6. An abundant taxon in the foramol assemblage exhibits in transversal section a peculiar star-shaped external ornamentation and well-developed pillars. The observed features allow to refer these specimens to *Hippurites incisus* DOUVILLÉ (Fig. 10A-C). Other rudists, belonging to the genus *Biradiolites* (Fig. 10D), are present as well. Some specimens exhibit an internal whitish matrix different from the light grey matrix surrounding the shells.

5.7 Biozone 7

This biozone corresponds to the lower part of Unit D. The observed taxa are listed below. The most representative ones and the biomarkers as well are shown in Fig. 10. The assemblage strongly differs from the previous ones as being dominated by planktonic foraminifers [i.e. *Globotruncana linneiana* (D'ORBIGNY) (Fig. 10E), *Marginotruncana schneegansi* (SIGAL) (Fig. 10F), *Marginotruncana coronata* (BOLLI) (Fig. 10G), *Marginotruncana marginata* (REUSS) (Fig. 10H), *Marginotruncana pseudolinneiana* PESSAGNO, *Dicarinella hagni* (SCHEIBNEROVA), *Dicarinella asymetrica* (SIGAL) (Fig. 10I, J). Rudists occur just as comminuted fragments while benthic foraminifers are completely lacking.

5.8 Biozone 8

This biozone matches the upper part of Unit D. The observed taxa are listed below. The most representative ones and the biomarkers are shown in Fig. 10. Main constituents of the assemblage are large hyaline foraminifers such as *Orbitoides media* (D'ARCHIAC) (Fig. 10 K), *Orbitoides* sp. (Fig. 10 L and M), *Pseudosiderolites vidali* DOUVILLÉ (Fig. 10N) in addition to smaller microgranular foraminifers, cfr. *Fleuryana adriatica* DE CASTRO, DROBNE and GUŠIĆ (Fig. 10O and P) and undetermined rudists. The assemblage also exhibits a rich and diversified planktonic foraminifer assemblage [i.e. *Globotruncanita stuartiformis* (DALBIEZ) (Fig. 10Q), *Globotruncanita elevata* (BROTZEN) (Fig. 10R), *Laeviheterohelix pulchra* (BROTZEN) (Fig. 10S), *Globigerinelloides prairiehillensis* PESSAGNO, *Globigerinelloides messinae* (BRÖNNIMANN) (Fig. 10T), *Heterohelix reussi* (CUSHMAN), *Heterohelix carinata* (CUSHMAN), *Marginotruncana marginata* (Fig. 10U), *Globotruncana bulloides* VOGLER and *Globotruncana linneiana* (Fig. 10V)].

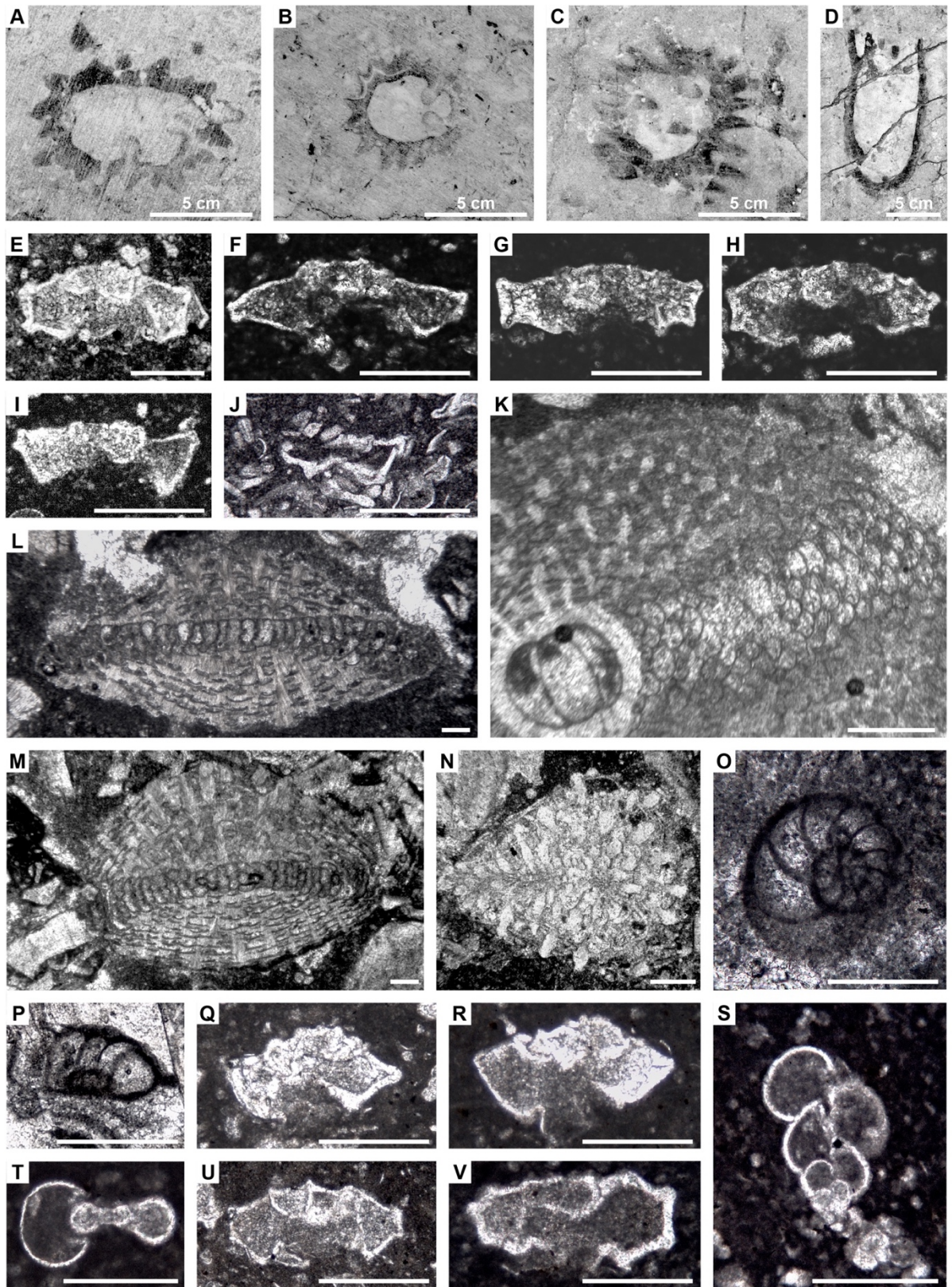


Fig. 10. Biozone 6 (A to D), 7 (E to J) and 8 (K to V). (A, B, C) *Hippurites incisus*, locality Segala. (D) *Biradiolites* sp., locality Segala. (E) *Globotruncana linneiana*, sample Mj10, locality Segala. (F) *Marginotruncana schneegansi*, sample Mj10, locality Segala. (G) *Marginotruncana coronata*, sample Mj9, locality Segala. (H) *Marginotruncana marginata*, sample Mj9, locality Segala. (I, J) *Dicarinella asymerica*, samples Mj10, Sgm1, locality Segala. (K) *Orbitoides media*, sample N121, locality Rocca Rumena. (L, M) *Orbitoides* sp., sample N121, locality Rocca Rumena. (N) *Pseudosiderolites vidali*, sample N121, locality Rocca Rumena. (O, P) cfr. *Fleuryana adriatica*, sample N121, locality Rocca Rumena. (Q) *Globotruncanita stuartiformis*, sample N120, locality Rocca Rumena. (R) *Globotruncanita elevata*, sample N121, locality Rocca Rumena. (S) *Laeviheterohelix pulchra*, sample N121, locality Rocca Rumena. (T) *Globigerinelloides messinae*, sample N121, locality Rocca Rumena. (U) *Marginotruncana marginata*, sample N121, locality Rocca Rumena. (V) *Globotruncana linneiana* sample N121, locality Rocca Rumena. Scale bar 300 μm (when not differently specified).

6. Discussion

There is no doubt that the depositional system of the WSCE is typical of a tectonic escarpment that was fed both by allochthonous extraclasts coming from the footwall sequences, mixed to huge amounts of skeletal grains produced throughout the Cretaceous in the adjacent platform margin (i.e. the matrix of the gravity-flow deposits). The dominant tectonic control of this escarpment is witnessed by repeated magmatic intercalations of basaltic tuffites and pillow lavas (Bellia et al., 1981) related to active crustal faults. A careful sedimentological analysis of the WSCE goes beyond the purposes of the present contribution, as it has been already performed (Randazzo et al., *in press*). Hereafter we discuss the most peculiar characters of the different biozones identified in the skeletal matrices of the gravity-flow deposits and their chronostratigraphic attribution.

6.1 Biozone 1 (Kimmeridgian-Berriasian)

The high abundance in *Saccocoma* sp. allows to refer the base of this biozone to the early Kimmeridgian-late Tithonian interval (Chiocchini et al., 2008). Dinoflagellate cysts constituted an important food source for *Saccocoma* sp. and the other Triassic and Cretaceous

roveacrinids as well (see Hughes, 2019 and reference therein). Most of the Jurassic and Cretaceous calcispheres are interpreted as calcareous dinoflagellate cysts that flourished in response to a nutrient enrichment in the seawater (Flügel, 2004). Therefore, as put forward for some Cretaceous assemblages (Ferrè et al., 2019; Hughes, 2019), the abundance in roveacrinids (i.e. *Saccocoma* sp.) and calcispheres at the base of Biozone 1 may have been triggered by an episode of high productivity occurred during the early Kimmeridgian-late Tithonian interval. The presence of *Crassicollaria* sp. and cfr. *Calpionella alpina* ascribes the lowermost part of this biozone to the late Tithonian-earliest Berriasian interval (Andreini et al., 2007). A faunal turnover in the calpionellid assemblage follows, in particular, the occurrences of *Remaniella cadischiana* and *Tintinopsella longa* suggest a late Berriasian-early Valanginian age (Andreini et al., 2007). Furthermore, these chronostratigraphic constraints would be confirmed by the presence of *Protopeneroplis ultragranulata*, cfr. *Dobrogeolina ovidi* and cfr. *Nautiloculina broennimanni* (Chiocchini et al., 2008; Ivanova et al., 2015, and references therein). The ramp deposits constituting Unit A can be thus constrained to the early Kimmeridgian-early Valanginian interval.

6.2 Biozone 2 (Valanginian-Aptian?)

This biozone totally lacks in calpionellids and the corresponding microfacies from Unit 2 show pervasive encrustations of *Bacinella irregularis* and *Lithocodium aggregatum*. *Protopeneroplis ultragranulata* and *Nautiloculina broennimanni* are the main biomarkers suggesting a Valanginian age for the lower part of Biozone 2 (Chiocchini et al., 2008; Ivanova et al., 2015). The occurrence of *Ellipsactinia* supports this interpretation being very abundant in the Italian sedimentary record from Late Jurassic to Valanginian times (Russo and Morsilli, 2007). Upward the aforementioned biomarkers disappear and the biostratigraphic resolution decreases. The upper boundary of the biozone that matches the top of Unit 2 could be assigned to the early Aptian on the base of the presence of cfr. *Moesiloculina danubiana* (Chiocchini

et al., 2008). However only few specimens can't support such hypothesis with confidence. Notwithstanding, the collected biostratigraphic data allow to constrain the abrupt evolution from Unit A (low-angle carbonate ramp) to Unit B (steep and tectonically-controlled slope) to the Berriasian-Valanginian interval.

The biostratigraphic resolution is still poor; however, the first occurrence of representatives of the Radiolitidae rudist family would support an Aptian age (Chiocchini et al., 2008) for Biozone 2 and the corresponding megabreccia body at the base of Unit C.

6.3 Biozone 3 (lower Albian)

This biozone corresponds to the lower part of Unit C where the first volcanic intercalation occurs. In particular, the Biozone 3 has been observed in the matrices of the megabreccias in which these volcanics are intercalated. The well-diversified assemblage (e.g. *Cuneolina pavonia*, *Nezzazata isabellae*, *Nezzazatinella picardi*, *Rumanoloculina robusta*, *Ticinella roberti* and Orbitolinidae) and the occurrence of the biomarker *Mesorbitolina subconcava*, allowed to refer this biozone to the early Albian (Chiocchini et al., 2008). The occurrence of dasycladacean algae such as *Zittelina aff. massei* (upper Aptian-middle Albian; Bucur et al., 2010) and *Neomeris cretacea* (Barremian-Albian; Sokač, 2004) furtherly characterize the association. On the base of these biostratigraphic data, the same age is proposed for the first volcanic intercalation.

6.4 Biozone 4 (upper Cenomanian p.p.)

Just above the second documented volcanic intercalation a thick megabreccia body related to Unit C follows in the western Mt. Sparagio ridge. The corresponding biozone exhibits an assemblage particularly rich in large and grain-to-grain resedimented Orbitolinidae. In particular, the occurrence of the biomarker *Conicorbitolina cuvilleri* allowed to refer Biozone 4 to the upper Cenomanian p.p. (Velić et al., 2007). Other taxa constituting

the assemblage (e.g. *Pseudolituonella reicheli*, *Pseudorhapydionina dubia*) seldom occur and confirm the same age as well. *Trinocladus tripolitanus* Raineri is known from upper Albian-Coniacian (Schlagntweit, 1992, and references therein). The top of megabreccias corresponding to Biozone 4 is truncated in the western part of the Mt. Sparagio ridge by Miocene calcarenites, thus the following biozones were analyzed in other sectors of the study area.

6.5 Biozone 5 (uppermost Cenomanian/lowermost Turonian)

This biozone corresponds to the megabreccias following the the third documented volcanic intercalation and related to Unit C. Several specimens belonging to the genus *Whiteinella* characterizes the biozone. In particular, the identified species (i.e. *Whiteinella paradubia* and *Whiteinella brittonensis*) would suggest an uppermost Cenomanian-Turonian age (Premoli Silva and Verga, 2004). On the other hand, the upper boundary of *Marssonella turris* and *Sigmomassilina ottadunensis* stratigraphic ranges occurs in the lower part of the upper Cenomanian, as observed in the type locality (l'Ottaduna stratigraphic section, southeastern side of the Mt. Cairo, southern Latium, central Italy) and in other localities of the southern Latium (Chiocchini, 2008). In addition, *Sigmomassilina ottadunensis* was identified also in the lowermost Cenomanian of Val D'Agri, Basilicata, southern Italy (Chiocchini, 2008). However, the absence of Orbitolinidae, whom last occurrence is referred to the lower part of the upper Cenomanian and usually associated with the aforementioned biomarker (Chiocchini, 2008; Chiocchini et al., 2008), would support an uppermost Cenomanian-Turonian age.

6.6 Biozone 6 (Coniacian)

This biozone corresponds to a thick pile of megabreccia beds and calciturbidites constituting the uppermost part of Unit C. Rare and heavy recrystallized biomarkers do not

allow a biostratigraphic characterization based on foraminifers (both benthic and planktonic). However, a number of well-preserved star-shaped (in transversal section) rudists attributable to *Hippurites incisus* occur. This taxon is reported in Coniacian limestones of France (Sénesse, 1937; Toucas, 1904), Austria (Götz, 2003) and Spain (Troya, 2015). Therefore, Biozone 6 has been assigned to the Coniacian in the absence of other biostratigraphic evidences.

6.7 Biozone 7 (Santonian)

This biozone corresponds to the lower part of Unit D mainly consisting of pelagic calcilutites. These limestones exhibit a well-diversified planktonic foraminifers assemblage characterized by keeled and double keeled taxa (e.g. *Dicarinella asymetrica*, *Dicarinella hagni*, *Marginotruncana pseudolinneiana*, *Marginotruncana coronata*, *Marginotruncana schneegansi*, *Marginotruncana marginata*, *Globotruncana linneiana*). This assemblage and, in particular, the occurrence of *Globotruncana linneiana* suggest a Santonian age (*Dicarinella asymetrica* zone, Petrizzo et al., 2011; Petrizzo et al., 2017) for Biozone 7.

6.8 Biozone 8 (Campanian-Maastrichtian)

This biozone corresponds to the upper part of Unit D mainly consisting in alternating calcidebrites and calcilutites. The concomitant occurrences of *Globotruncana linneiana*, *Globigerinelloides prairiehillensis*, *Laeviheterohelix pulchra*, *Globotruncana bulloides*, *Globotruncanita stuartiformis*, *Globotruncanita elevata* and *Orbitoides media* and *Pseudosiderolites vidali* would ascribe Biozone 9 to the early Campanian-middle Maastrichtian interval (Chiocchini et al., 2008; Petrizzo et al., 2011). *Fleuryana adriatica* upper Maastrichtian. However, although rare, the presence of *Laeviheterohelix pulchra* could limit the chronostratigraphic attribution of this biozone to the Campanian.

6.9 Age of extraclasts occurring in the allocthonous carbonate deposits

Besides the skeletal supply, the gravity-flow deposits of the WSCE consist of a huge amount of extraclasts, obviously older than the matrix. Repeated collapses of sedimentary successions exposed along the footwalls of several extensional faults between Platform and escarpment triggered the extraclastic supply. Evidence of the slope failures is the presence of metre-scale slump scars in several studied sections (Fig. 11).

In the Unit A no lithoclasts are observed. Facies associations in the upper part of this unit are wackestone with both pelagic (calpionellids) and platform-margin-derived biotas (*Crescentiella morronensis*, *Protopenneroplis ultragranulata*). Randazzo et al. (*in press*) have interpreted the upper part of this unit as typical of a ramp setting.

The Unit B records the beginning of the extraclastic supply along the WSCE. This unit consists of parallel bedded, clast- to matrix-supported and poorly sorted, thin to very thick-bedded breccias (FC1 in Randazzo et al., *in press*). The lithoclastic supply in this unit mostly consists of angular and sub-angular coral/*Ellipsactinia*/sponge boundstones of Tithonian age, associated to a minor amount of wackestones with ammonites and filaments derived from the Rosso Ammonitico and gray laminated peloidal packstones coming from the Upper Triassic-lowermost Jurassic peritidal cycles. This extraclastic content supports a submarine exposure of the sedimentary substrate of at least 100 metres, considering the stratigraphic thickness between the Cretaceous sediments and the top of the underlying carbonate platform.

Rudist floatstone/rudstone and skeletal grainstones are the main extraclastic constituents in the Unit C. However, the lithoclastic supply from Tithonian reefs is still present in the lower part of this unit, as observed in the Pizzo Noce and Piano di Sopra areas (Fig. 12A, B, C, D). Besides the stromatoporoids, this is confirmed also by the occurrence of Upper Jurassic biotas in some lithoclasts, such as calpionellids, *Saccocoma* sp. (Fig. 12E, F, G, H, I) and benthic foraminifers (e.g. *Haghimashella arcuata*, Fig. 12J). Extraclasts with *Coscinoconus campanellus* (Fig. 12K), *Charentia cuvillieri* (Fig. 12L) and *Salpingoporella dinarica* (Fig.

12M), biomarker for the Aptian stage (Chiocchini et al., 2008) confirm the involvement in the resedimentation phenomena of the pre-Albian sedimentary substrate down to the Upper Jurassic succession.

On the base of the stratigraphic distribution of the volcanic intercalations, it is fair to imagine that the tectonic influence and associated seismicity still played a major role during the late Albian-Cenomanian p.p. However, no older lithoclasts were found in the megabreccias corresponding to this biozone, in contrast to what is observed in Biozone 2, 3 and 4. In addition, the megabreccias corresponding to Biozone 5 show early-lithification features suggesting that the gravity-flows acting along the slope did not involve the hard and older substratum. Upward, Orbitolinidae and older taxa such as *Ticinella* sp. still occur in some lithoclasts of the megabreccias corresponding to Biozone 6. In particular, *Ticinella* sp. points to the Albian substratum exposure and the ongoing extensional tectonic phase in the uppermost Cenomanian-Turonian.

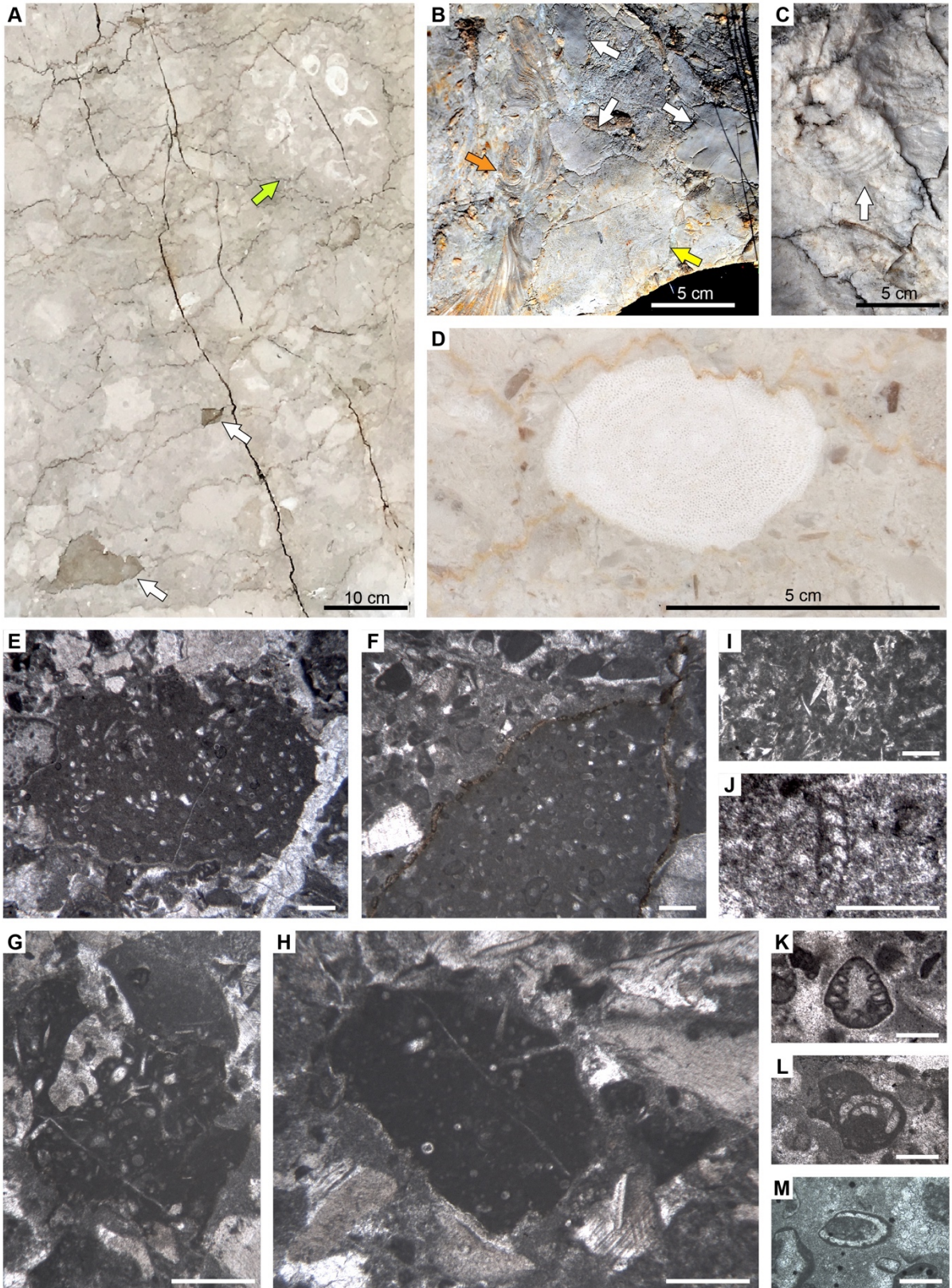
The matrix in these megabreccias consists of very abundant loose silt- to pebble-sized skeletal debris as compared to the Lower Cretaceous limestones. This increasing productivity may have favoured by warmer climatic conditions as recorded along the north Gondwana margin (Deaf et al. 2020 and ref. therein), coupled to the Tethyan late Albian-early Cenomanian sea level rise (Haq, 2014).



Fig. 11. Examples of slump scars affecting the WSCE limestones. Detachment surfaces have been highlighted for purpose of clearance.

The increasing carbonate productivity during late Aptian and Cenomanian is well documented in the Panormide Platform, where up to 200 m of rudist limestones record a great variability of facies influenced by sea-level fluctuations (Di Stefano and Ruberti, 2000). However tectonic activity is still ongoing during Cenomanian in the southern Tethys since, despite the eustatic sea-level rise, some carbonate platforms record drastic facies changes coupled to subaerial exposures (e.g. Apennine and Apulia carbonate platforms, Carannante et al., 2007; Carannante et al., 2009). In the eastern sector of the Mt. Sparagio ridge, platform margin limestones of Cenomanian age are overlapped by Turonian/Coniacian calcidebrites and Santonian Scaglia-type calcilutites related to Unit D. This deepening of the facies environments, coupled with the dismemberment of the Panormide Platform in isolated patch reefs recorded in the uppermost Cretaceous of Mt. Pellegrino (Montanari, 1964; Camoin; 1982), may account for the tectonic backstepping of this Cretaceous carbonate system.

Fig. 12. Resedimented lithoclasts and bioclasts in the WSCE MTDs. A) Rosso Ammonitico lithoclasts (white arrows) and rudist boundstone (yellow arrow) reworked in a megabreccia body of Aptian age, locality Pizzo Noce. B) Rosso Ammonitico lithoclasts (white arrows), *Ellipsactinia* (yellow arrow) and bryozoan (orange arrow) in a breccia of Aptian age, locality Piano di Sopra. C, D) *Ellipsactinia* in rudist breccias of Albian-Cenomanian age, locality Pizzo Noce. E, F) Calpionellid bearing lithoclasts in rudist breccias of Albian-Cenomanian age, samples FM101, FM102d, locality Rocca Rumena. G, H) *Saccocoma* sp. bearing lithoclast in rudist breccias of Albian-Cenomanian age, sample Nq3, locality Pizzo Noce. I) *Saccocoma* sp., sample FM16, locality Pizzo Noce. J) *Haghimashella arcuata*, sample PSbS2, locality Piano di Sopra. K) *Coscinoconus campanellus*, sample Bfr14, locality Rocca Rumena. L) *Charentia cuvillieri*, sample Bfr14, locality Rocca Rumena. M) *Salpingoporella dinarica*, sample N1, locality Pizzo Noce.



7. Conclusions

A new integrated study of the stratigraphic, micropaleontological and microfacies features of the Cretaceous carbonate slope succession from the Capo San Vito Peninsula (Western Sicily, Italy) allows to constrain the chronostratigraphic distribution of the facies associations recognized along the slope and the evolution of the slope and of the inferred adjacent carbonate platform throughout the Cretaceous.

The detailed study and correlation of a number of well exposed sections allowed to differentiate four informal lithostratigraphic units and eight informal biozones. Hemipelagic facies, containing both pelagic and platform margin biota (Biozone 1) suggest the presence of a gentle ramp during the Kimmeridgian-Valanginian interval (Unit A, *Calpionellid/Crescentiella* limestones). The Valanginian-Aptian interval shows the onset of the calciclastic sedimentation and the tectonic exposure of older sedimentary sequences along footwall blocks (Unit B, *Ellipsactinia* breccias). The sedimentary change from muddy ramp facies to coarse calcidebrites is very sharp and could be dated as old as Berriasian p.p.-Valanginian. The occurrence of stromatoporoids coming from the platform-margin (e.g. *Ellipsactinia*) and pervasive *Bacinella/Lithocodium* encrustations characterize the biostratigraphic content (Biozone 2). The calciclastic sedimentation continues during the Aptian-Coniacian interval (Unit C). The rise of rudists as the most abundant constituent characterizes these calciclastic deposits. In particular, the biostratigraphic content is represented by the upper part of Biozone 2 and by the following four biozones (Biozone 3, 4, 5, 6), well-constrained by several biomarkers. This time interval records three submarine eruptions that account for an anorogenic magmatism related to deep rooted extensional faults and, in turn, for a dominant tectonic control for the WSCE evolution. The supply of gravity-flow deposits and skeletal shedding lasts until the Maastrichtian, though interrupted by periods of quiescence favoring the background pelagic sedimentation (Unit D). Planktonic foraminifers dominate the biostratigraphic content (Biozone 7) in the lower part of this unit.

The co-occurrence of benthic and planktonic foraminifers (Biozone 8) characterizes the upper part of Unit D made of the alternation of breccias beds and lime mudstones. The sharp decrease in the platform skeletal supply precedes the shut-down of the carbonate factory (i.e. Panormide Platform) during late Maastrichtian times. The tectonic backstepping of this Cretaceous carbonate system is documented by the overlap of slope deposits on Cenomanian facies associations typical of the platform edge. These stratigraphic relationships may account for the progressive fragmentation of the Panormide Platform into smaller and isolated highs before their definitive demise. The evolution of the WSCE is well tuned to the Cretaceous geodynamic context of the Southern Tethys. As widely supported by previous studies, this last sector suffered an extensional stress field related to the tectonic subsidence in the Sirt Basin and the convergence between Africa and Europe.

Acknowledgements

The data presented in this paper are part of a larger stratigraphic and sedimentological study presented by one of the authors (V.R.) as part of his PhD thesis at the University of Palermo. The PhD grant was supported by the FSE SICILIA 2020 via University of Palermo. Research granted by PD project R4D14-P5F5RISS_MARGINE (University of Palermo). We warmly thank the representatives of the marble industry of the Capo San Vito Peninsula and in particular Pellegrino, Bova, Maiorana, Santoro, Bellanova and Miceli companies for allowing the access to their quarries and marble sawmills. We are grateful to journal editor Eduardo Koutsoukos and two anonymous reviewers for constructive comments and suggestions that improved an early version of this paper.

References

- Abate, B., Di Maggio, C., Incandela, A., Renda, P.,** 1991. Carta geologica dei Monti di Capo San Vito, scala 1 : 25.000. Dipartimento di Geologia e Geodesia dell'Università di Palermo.
- Abate, B., Di Maggio, C., Incandela, A., Renda, P.,** 1993. Nuovi dati sulla geologia della Penisola di Capo San Vito (Sicilia Nord-Occidentale). Mem. Soc. Geol. Ital. Mem., 47, 15-25.
- Andreini, G., Caracuel, J.E., Parisi, G.,** 2007. Calpionellid biostratigraphy of the Upper Tithonian–Upper Valanginian interval in Western Sicily (Italy). *Swiss Journal of Geosciences* 100, 179–198.
- Bellanca, A.,** 1969. Marmi di Sicilia. Istituto regionale per il finanziamento alle industrie in Sicilia. IRFIS, 167 pp.
- Bellia, S., Lucido, G., Nuccio, P.M., Valenza, M.,** 1981. Magmatismo in area trapanese in relazione all'evoluzione geodinamica della Tetide. *Rendiconti - Società Italiana di Mineralogia e Petrologia* 38, 163–174.
- Bucur, I.I., Granier, B., Sășăran, E.,** 2010. *Zittelina massei* n. sp., a new dasycladacean alga from the Lower Cretaceous strata of Pădurea Craiului (Apuseni Mountains, Romania). *Facies* 56, 445–457.
- Bucur, I.I., Senowbari-Daryan, B., Abate, B.,** 1996. Remarks on some foraminifera from the Upper Jurassic (Tithonian) reef limestone of Madonie Mountains (Sicily). *Bollettino della Società Paleontologica Italiana* 35(1), 65-80.
- Camoin, G.,** 1982. Plats-formes carbonatées et récifs à rudistes du Crétacé de Sicile. Phd Thesis, Univ. Provence, Marseille, 244 pp.
- Carannante, G., Ruberti, D., Simone, L., Vigliotti, M.,** 2007. Cenomanian carbonate depositional settings: case histories from the central-southern Apennines (Italy). *SEPM special publication* 87, 11-25.
- Carannante, G., Pugliese, A., Ruberti, D., Simone, L., Vigliotti, M., Vigorito, M.,** 2009. Evoluzione cretacea di un settore della piattaforma apula da dati di sottosuolo e di affioramento (Appennino campano-molisano). *Italian Journal of Geosciences* 128(1), 3-31.
- Catalano, R., Agate, M., Basilone, L., Di Maggio, C., Mancuso, M., Sulli, A., Di Stefano, E., Gasparo Morticelli, M., Avellone, G., Abate, B.,** 2011. Foglio 593, “Castellammare del Golfo” e carta geologica allegata. Regione Siciliana - Ispra.
- Catalano, R., D'Argenio, B.,** 1982. Guida alla geologia della Sicilia occidentale. *Guide Geologiche Regionali. Società Geologica Italiana*, 1-155.
- Catalano, R., Di Stefano, P., Sulli, A., Vitale, F. P.,** 1996. Paleogeography and structure of the central Mediterranean: Sicily and its offshore area. *Tectonophysics*, 260(4), 291-323.
- Cestari, R., Sartorio, D.,** 1995. Rudists and facies of the periadriatic domain. *Agip San Donato Milanese*, 207 pp.
- Chiocchini, M.,** 2008. New benthic foraminifera (Miliolacea and Soritacea) from the Cenomanian and upper Turonian of the Monte Cairo (southern Latium, central Italy). *Memorie Descrittive Carta Geologica d'Italia*, 84, 171-202.
- Chiocchini, M., Chiocchini, R.A., Didaskalou, P., Potetti, M.,** 2008. Micropaleontological and biostratigraphical researches on the Mesozoic of the Latium-Abruzzi carbonate platforms (Central Italy).

Memorie Descrittive della Carta Geologica d'Italia 84, 63 pp.

Di Stefano, G., 1898. Studi stratigrafici e paleontologici sul sistema cretaceo della Sicilia. I calcari con *Polyconites* di Termini-Imerese. *Palaeontographia Italica* 4, 1–46.

Di Stefano, P., Gullo, M., 1997. Late Paleozoic- Early Mesozoic stratigraphy and paleogeography of Sicily, in: Catalano Raimondo (Ed.), *Time Scales and Basin Dynamics. Sicily, the Adjacent Mediterranean and Other Natural Laboratories. VIII ILP Workshop in Western Sicily, Guidebook*. Offset Studio, Palermo, pp. 87–99.

Di Stefano, P., Ruberti, D., 2000. Cenomanian rudist-dominated shelf-margin limestones from the Panormide carbonate platform (Sicily, Italy): Facies analysis and sequence stratigraphy. *Facies* 42, 133–160.

Deaf, A.S., Harding, I.C., Marshall, J., E.A., 2020. Cretaceous (Hauterivian-Cenomanian) palaeoceanographic conditions in southeastern Tethys (Matruh Basin, Egypt): Implications for the Cretaceous climate of northeastern Gondwana. *Cretaceous Research* 106, 1-35.

Dunham, R.J., 1962. Classification of carbonate rocks according to depositional texture. In: *Classification of Carbonate Rocks* (Eds W.E. Ham), 1, AAPG Mem., 108-121.

Embry III, A.F., Klován, J.E., 1971. A late Devonian reef tract on northeastern Banks Island, NWT. *Bulletin of Canadian petroleum geology* 19, 730–781.

Ferré, B., Monier-Castillo, A., López-Palomino, I., Aguilera-Franco, N., Palma-Ramírez, A., Contreras-Cruz, D. Romo-Ramírez, J. R., Muñoz-Jaramillo, C. R., 2019. Roveacrinoidal assemblages (Crinoidea, Roveacrinida, saccocomidae) from the Albian carbonate microfacies of Sierra Azul (Sabinas Basin, Coahuila, Mexico). *Revista Brasileira de Paleontologia*, 22, 3–14.

Flügel, E., 2004. *Microfacies of carbonate rocks. Analysis, interpretation and application*. Springer. 984 pp.

Gemmellaro, G.G., 1865. Sulle Caprinellidi dell'Ippuritano dei dintorni di Palermo. *Atti Accademia Gioenia* 2, 187–238.

Giunta, G. and Liguori, V., 1972. Geologia della estremità Nord-Occidentale della Sicilia. *Riv. Min. Sicil.*, 136-138, 165-226.

Giunta, G., Liguori, V., 1973. Evoluzione paleotettonica della Sicilia nord-occidentale. *Bollettino della Società Geologica Italiana* 92, 903–924.

Götz, S., 2003. Biotic interaction and synecology in a Late Cretaceous coral–rudist biostrome of southeastern Spain. *Palaeogeography, Palaeoclimatology, Palaeoecology* 193, 125–138.

Haq, B.U., 2014. Cretaceous eustasy revisited. *Global and Planetary Change* 113, 44-58.

Hughes, W.G., 2019. Turonian microcrinoids from the lower Aruma Formation of Saudi Arabia. *Micropaleontology*, 65(4), 357–377.

Ivanova, D., Bonev, N., Chatalov, A., 2015. Biostratigraphy and tectonic significance of lowermost Cretaceous carbonate rocks of the Circum-Rhodope Belt (Chalkidiki Peninsula and Thrace region, NE Greece). *Cretaceous Research* 52, 25–63.

Montanari, L., 1964. Geologia del Monte Pellegrino (Palermo). Parte 1. Stratigrafia e tettonica. *Rivista Mineraria Siciliana* 15, 173–197.

Nigro, F., Renda, P., 2002. From Mesozoic extension to Tertiary collision: deformation patterns in the units of

the North-Western Sicilian chain. *Bollettino della Società Geologica Italiana* 121, 87–97.

Oldow, J. S., Channell, J. E. T., Catalano, R., D'argenio, B., 1990. Contemporaneous thrusting and large-scale rotations in the western Sicilian fold and thrust belt. *Tectonics*, 9(4), 661–681.

Pepe, F., Bertotti, G., Cella, F., Marsella, E., 2000. Rifted margin formation in the south Tyrrhenian Sea: A high-resolution seismic profile across the north Sicily passive continental margin. *Tectonics* 19, 241–257.

Petrizzo, M.R., Falzoni, F., Silva, I.P., 2011. Identification of the base of the lower-to-middle Campanian Globotruncana ventricosa Zone: comments on reliability and global correlations. *Cretaceous Research* 32, 387–405.

Petrizzo, M.R., Jiménez Berrocoso, Á., Falzoni, F., Huber, B.T., Macleod, K.G., 2017. The Coniacian–Santonian sedimentary record in southern Tanzania (Ruvuma Basin, East Africa): Planktonic foraminiferal evolutionary, geochemical and palaeoceanographic patterns. *Sedimentology* 64, 252–285.

Premoli Silva, I., Verga, D. 2004. Practical manual of Cretaceous planktonic foraminifera. In: International School on Planktonic Foraminifera: 3rd Course (Eds D. Verga and R. Rettori), Perugia, Italy, Universities of Perugia and Milan, pp. 283.

Randazzo, V., Le Goff, J., Di Stefano, P., Reijmer, J., Todaro, S., Cacciatore, M. S., *in press*. Carbonate slope re-sedimentation in a tectonically-active setting (Western Sicily Cretaceous Escarpment, Italy). *Sedimentology*.

Russo, A., Morsilli, M., 2007. New insight on architecture and microstructure of Ellipsactinia and Sphaeractinia (Demosponges) from the Gargano Promontory (Southern Italy). *Geologica Romana* 40, 215–225.

Scandone, P., Radoičič, R., Giunta, G., Liguori, V., 1972. Sul significato delle dolomie Fanusi e dei calcari ad Ellipsactinie della Sicilia settentrionale. *Rivista mineraria Siciliana* 133–135, 51–61.

Schlagintweit, F., 1992. Further record of calcareous algae (dasycladaceae, udoteaceae, solenoporaceae) from the Upper Cretaceous of the Northern Calcareous Alps (Gosau Formation, Branderfleck Formation). *Revue de Paléobiologie* 11, 1–12.

Schmidt di Friedberg, P., 1965. Litostratigrafia petrolifera della Sicilia. *Rivista mineraria Siciliana* 15, 3–43.

Sénesse, P., 1937. Contribution à l'étude du crétacé supérieur des Corbières méridionales. Toulouse, Les freres Douladoure imprimerie 182 pp.

Senowbari-Daryan, B., Bucur, I.I., Abate, B., 1994. Upper Jurassic calcareous algae from the Madonie Mountains, Sicily. *Beiträge zur Paläontologie* 19, 227–259.

Sirna, G., 1982. Quelques Rudistes cénomaniens du Monte Pellegrino (Palermo, Sicile). *Geologica Romana* 12, 79–87.

Sokač, B., 2004. On some peri-Mediterranean Lower Cretaceous Dasyclad species (calcareous algae; Dasycladales) previously assigned to different genera. *Geologia Croatica* 57, 15–53.

Speranza, F., Maniscalco, R., Mattei, M., Funicello, R., 2000. Paleomagnetism in the Sicilian Maghrebides: review of the data and implications for the tectonic styles and shortening estimates. *Memorie della Società Geologica Italiana* 55, 95–102.

Speziale, S., 1997. Il magmastismo mesozoico-paleogenico della Sicilia occidentale. PhD Thesis, Università

degli Studi di Catania, 241 pp.

Todaro, S., Di Stefano, P., Zarcone, G., Randazzo, V., 2017. Facies stacking and extinctions across the Triassic–Jurassic boundary in a peritidal succession from western Sicily. *Facies* 63, 1–20. <https://doi.org/10.1007/s10347-017-0500-5>

Todaro, S., Rigo, M., Randazzo, V., Di Stefano, P., 2018. The end-Triassic mass extinction: A new correlation between extinction events and $\delta^{13}\text{C}$ fluctuations from a Triassic–Jurassic peritidal succession in western Sicily. *Sedimentary Geology* 368, 105–113. <https://doi.org/10.1016/j.sedgeo.2018.03.008>

Toucas, A., 1904. Études sur la classification et l'évolution des Hippurites, deuxième partie. *Mémoire de la Société géologique de France*, 30(12), 65–128.

Troya Garcia L., 2015. Rudistas (Hippuritida bivalvia) del Cenomaniense-Coniacense (Cretácico Superior) del Pirineo meridional-central. PhD Thesis, Universitat Autònoma de Barcelona, 519 pp.

Velić, I., 2007. Stratigraphy and Palaeobiogeography of Mesozoic Benthic Foraminifera of the Karst Dinarides (SE Europe)-PART 1. *Geologia Croatica* 60, 1–60.

Zappaterra, E., 1990. Carbonate paleogeographic sequences of the Periadriatic Region. *Boll. Soc. Geol. It.* 109, 5–20.

Zarcone, G., Di Stefano, P., 2010. La Piattaforma Carbonatica Panormide: Un caso anomalo nell'evoluzione dei bacini della Tetide Giurassica. *Italian Journal of Geosciences* 129, 188–194. <https://doi.org/10.3301/IJG.2010.01>

4. General conclusions

The PhD study aimed to reconstruct the stratigraphic architecture of a Cretaceous carbonate escarpment and its evolutionary history in the frame of the geodynamic scenario of the south-western Tethys. The study was based on an integrated sedimentological and biostratigraphic analysis of the Cretaceous limestones cropping out in the Capo San Vito Peninsula (western Sicily, southern Italy) and it represents an original attempt to relate the Cretaceous deposits to specific sedimentary environments, through a careful facies analysis, and to a reliable chronostratigraphic frame. The studied Cretaceous limestones originally pertaining to the reconstructed Western Sicily Cretaceous Escarpment (WSCE) belong to different tectonic units of the Maghrebian fold and thrust belt that are piled up in the Capo San Vito Peninsula. Following orogenic tectonics, the tectonic units of the area were affected by extensional and transtensional deformations during the Plio-Pleistocene. The lateral relationships with the inferred source area of the slope sediments, the Panormide Carbonate Platform, are nowadays obscured by tectonic deformations. This notwithstanding, a good match between the stratigraphic events recorded by the WSCE and the coeval stratigraphy of the Panormide Carbonate Platform can be observed.

The main achievements of the PhD study can be summarized by four main outputs: 1) the implementation of a 3D model showing the facies distribution along the WSCE; 2) the definition of eleven facies types as the expression of specific gravity-flow mechanisms in relation to a dominant seismo-tectonic activity; 3) the definition of eight informal biozones that allow to time constrain the main events which took place along the WSCE throughout the Cretaceous; 4) the characterization of a crustal shear phase affecting the WSCE and the Panormide Platform in the frame of the Cretaceous geodynamic context of south-western Tethys .

1) Thanks to the outstanding exposures provided by hundreds of quarries extracting ornamental stones, detailed macro- and micro-facies analyses were performed. The obtained dataset of sedimentological features allowed to recognize comparable slope facies in different tectonic units, and to reconstruct their lateral distribution across the sedimentary system (carbonate ramp, platform margin, upper slope and toe-of-slope to basin). Furthermore, this research allowed to relate the different slope facies to specific gravity-flow deposits and to the factors governing their initiation, duration, and emplacement. In particular, calcidebrites are the predominant type of slope deposits in the WSCE debris-dominated slope architecture.

2) Factors that have contributed to gravitational instabilities in the shelf edge and upper slope include earthquakes related to a severe extensional tectonic phase affecting the WSCE during the Cretaceous. Volcanic intercalations alternate with the carbonate gravity-flow deposits, representing a specific feature of the studied depositional system. These volcanic intercalations consist of tuffites and pillow lavas, with a high TiO_2 content suggesting a deep-seated origin of the magma. Moreover, the occurrence of older lithoclasts embedded in younger gravity-flow deposits account for the exposure of older sedimentary sequences along the footwall of normal faults. These evidences, along with (i) thick megabreccia bodies occurring above or below volcanic intercalations; (ii) decametre-scale slump scars, (iii) extensional synsedimentary faults, all suggest that repeated seismic shocks are the most likely trigger mechanism for the emplacement of the gravity-flow deposits constituting the WSCE, whilst not excluding a possible contribution of the sea-level fluctuations in the redistribution of the slope sediments.

3) The detailed biostratigraphic analysis and correlation of a number of well-exposed sections allowed to differentiate eight informal biozones and to place the different studied sections, either from a single tectonic unit or from different ones, within a reliable chronostratigraphic frame. The integration of sedimentological and biostratigraphic data allowed in turn to time-constrain the main WSCE events, being: i) the abrupt transformation

from a carbonate ramp to a tectonically-controlled escarpment during the Berriasian-Valanginian; ii) the peak of tectonic instability leading to the emplacement of thick megabreccia bodies and repeated submarine volcanic emissions during the Aptian-Cenomanian; iii) the almost coeval increase in the skeletal supply in response to the highstand shedding occurred during the Albian-Cenomanian; iv) the tectonic backstepping of the carbonate depositional system during the Senonian, ending with the definitive shutdown of the carbonate factory in the late Maastrichtian. The acquired biostratigraphic dataset is in large part new for the Cretaceous of Sicily. It is based on different systematic groups and provides information on the associations that populated a south-western Tethyan carbonate platform during the Cretaceous.

4) This study provides new regional insights on the paleogeographic evolution of the Central Mediterranean area and, in particular, of the Panormide Carbonate Platform during Cretaceous times. The latter represents a key area for the south-western Tethys, since it may have acted as a continental bridge between Africa and Adria during the Early Cretaceous allowing the migration of Gondwanian dinosaurs toward Laurasia. The deep-seated anorogenic magmatism points to a major role of extensional crustal shears affecting the WSCE, that led to the progressive backstepping of the platform culminating with its definitive demise. The extensional stress field is well tuned to the extensional tectonic phase affecting the whole south-western Tethyan domain during Cretaceous times, as well documented by the tectonic subsidence of the Sirt Basin and the evolution of the Apulia and Apennine platforms.

References

- Abate, B., Catalano, R., D'Argenio, B., Di Stefano, E., Di Stefano, P., Lo Cicero, G., Montanari, L., Pecoraro, C., Renda, P.** (1982) Evoluzione delle zone di cerniera tra Piattaforme carbonatiche e Bacini nel Mesozoico e nel Paleogene nella Sicilia Occidentale. In: *Guida alla geologia della Sicilia occidentale. Guide Geologiche Regionali della S.G.I, Palermo*, (Eds. R. Catalano, B. D'Argenio), pp. 53-81.
- Abate, B., Di Maggio, C., Incandela, A., Renda, P.** (1991) Nuovi dati sulla geologia della Penisola di Capo San Vito (Sicilia Nord-Occidentale). *Soc. Geol. Ital. Mem.*, 47, 15-25.
- Abate, B., Di Maggio, C., Incandela, A., Renda, P.** (1993) Carta geologica dei Monti di Capo San Vito, scala 1: 25.000. Dipartimento di Geologia e Geodesia dell'Università di Palermo.
- Adams, E.W., Kenter, J.A.M.** (2013) So different, yet so similar: comparing and contrasting siliciclastic and carbonate slopes. In: *Deposits, Architecture and Controls of Carbonate Margin, Slope and Basinal Settings*. (Eds. Verwer, K., Playton, T.E., Harris, P.M.), *SEPM Spec. Publ.*, 14-25.
- Allen, J.R.L.** (1985) *Principles of Physical Sedimentology*. George Allen and Unwin, London.
- Amore, C., Carveni, P., Scribano, V., Sturiale, C.** (1988) Facies ed età del vulcanismo nella fascia sud-orientale della Sicilia (Pachino-Capo Passero). *Boll. Soc. Geol. It.*, 107, 11 pp.
- Artoni, A., Bernini, M., Papani, G., Rizzini, F., Barbacini, G., Rossi, M., Rogledi, S., Ghielmi, M.** (2010) Mass-transport deposits in confined wedge-top basins: surficial processes shaping the Messinian orogenic wedge of Northern Apennine of Italy. *Ital. J. Geosci.*, 129 (1) (2010), pp. 101-118.
- Artoni, A., Polonia, A., Carlini, M., Torelli, L., Mussoni, P., Gasperini, L.** (2019) Mass Transport Deposits and geo-hazard assessment in the Bradano Foredeep (Southern Apennines, Ionian Sea). *Mar. Geol.*, 407, 275-298.
- Basilone, L., Sulli, A.** (2018) Basin analysis in the Southern Tethyan margin: Facies sequences, stratal pattern and subsidence history highlight extension-to-inversion processes in the Cretaceous Panormide carbonate platform (NW Sicily). *Sedim. Geol.*, 363, 235- 251.
- Basilone, L., Sulli, A., Gasparo Morticelli, M.** (2016) Integrating facies and structural analyses with subsidence history in a Jurassic–Cretaceous intraplateau basin: outcome for paleogeography of the Panormide Southern Tethyan margin (NW Sicily, Italy). *Sed. Geol.*, 339, 258–272.
- Bates, R.L., Jackson, J.A.** (1980) *Glossary of Geology*. Am. Geol. Inst., Falls Church, Va., 749 pp.
- Bates, R.L., Jackson, J.A.** (1984) *Dictionary of Geological Terms*, 3rd edn: American Geological Institute, Anchor Books, New York, 571 pp.
- Beckett, D., Jagiello, K., Gilchris, R., Wilson, E., Nelson, R., Wilkes, M., Fretwell, N., Rigo, G., Minelli, G., Sellwood, B., Barchi, M.**, (1996) A Study of the Reservoir Potential of an Outcrop Analogue for the Apulian Platform Oilfields in the Southern Apennines. Southern Apennines Joint Venture Study Report (British Gas/Amoco/Lasmo Internal Report).
- Bianchi, F., Carbone, S., Grasso, M., Invernizzi, G., Lentini, F., Longaretti, G., Merlini, S., Mostardini, F.** (1987) Sicilia orientale: profilo geologico Nebrodi-Iblei. *Mem. Soc. Geol. Ital.*, 38, 429-458.

- Bosellini, A.** (1992) Sequence stratigraphy in carbonate successions: some Italian examples. Proc. Conf. Sequence Stratigraphy of European Basins, Dijon, 18-20 May, Abstr., 1, p. 30.
- Broquet P.** (1968) Étude géologique de la région des Madonies (Sicile). Phd thèse, Fac. Sc., Lille, 797 pp.
- Broquet, P., Mascle, G.** (1972) Les grands traits stratigraphiques et structuraux des Monts de Trapani (Sicile occidentale), Ann. Soc. Geol. Nord., 92, 139-146.
- Bouma, A.H.** (1962) Sedimentology of Some Flysch Deposits: A Graphic Approach to Facies Interpretation. Elsevier, Amsterdam, The Netherlands, 16 pp.
- Caffisch, L.** (1966) La geologia dei Monti di Palermo. Riv. It. Paleont. e Strat., mem. XII, 108 pp., Milano.
- Camoin, G.** (1982) Plats-formes carbonates et récifs à rudistes du Crétacé de Sicile. Phd Thesis, Univ. Provence, Marseille, 244 pp.
- Canudo, J.A., Barco, J.L., Pereda-Superbiola, X., Ruiz-Omeñaca, J.J., Salgado, L., Torcida Fernández-Baldor, F., Gasulla, J.M.** (2009) What Iberian dinosaur reveal about the bridge said to exist between Gondwana and Laurasia in Early Cretaceous. Bull. Soc. Géol. Fr. 180, 5-11.
- Carter, L., Milliman, J.D., Talling, P.J., Gavey, R., Wynn, R.B.** (2012) Near-synchronous and delayed initiation of long run-out submarine sediment flows from a record-breaking river flood, offshore Taiwan. Geophys. Res. Lett. 39, L12603.
- Casabianca, D., Bosence, D., Beckett, D.** (2002) Reservoir potential of Cretaceous platform-margin breccias, Central Italian Apennines. J. Petrol. Geol., 25(2), 179-202.
- Catalano, R., D'Argenio, B.** (1982) Schema Geologico della Sicilia. In: Guida alla Geologia della Sicilia Occidentale (Eds R. Catalano and B. D'Argenio), Soc. Geol. Ital., guide geologiche regionali, 9-41.
- Catalano, R., Agate, M., Basilone, L., Di Maggio, C., Mancuso, M., Sulli, A.** (2011) Note illustrative della Carta Geologica d'Italia alla scala 1: 50.000, Foglio n. 593 "Castellammare del Golfo" e carta geologica allegata. Regione Siciliana - Ispra.
- Ciofalo, S.** (1869) Descrizione dei fossili di Termini Imerese. Termini Imerese, 13 pp.
- Ciofalo, S.** (1878) Enumerazione dei principali fossili che si rinvennero nella serie delle rocce stratificate dei dintorni di Termini Imerese. Atti. Acc. Gioenia Sc. Nat., 12, 115-122.
- Cook, H.E., McDaniel, P.N., Mountjoy, E.W., Pray, L.C.** (1972) Allochthonous carbonate debris flows at Devonian Bank ("Reef") margins Alberta, Canada. Bull. Canad. Petrol. Geol. 20, 439-497.
- Cook, H.E., Enos, P.** (1977) Deep-water carbonate environments - an introduction. Soc. Econ. Paleontol. Mineral. Spec. Publ., 25, 1-3.
- Cook, H.E., Mullins, H.T.** (1983) Basin margin. In: *Carbonate Depositional Environments* (Eds D.G. Bebout and C.H. Moore), AAPG Spec. Publ., 539-618.
- Corrado, S.** (1996) Evoluzione termica e carico tettonico di alcune successioni sedimentarie dell'Appennino centrale: un esempio nelle aree di piattaforma carbonatica e di scarpata. Mem. Soc. Geol. Ital. 51, 527-541 Atti della 77a Riunione estiva.

- Crevello, P.D., Schlager, W.** (1980) Carbonate debris sheets and turbidites, Exuma Sound, Bahamas. *J. Sed. Petrol.* 50 (4), 1121-1148.
- D'Argenio, A.** (1999) Analisi stratigrafica delle successioni Mesozoiche e Terziarie dell'offshore della Sicilia nord-occidentale. *Natural. Sicil.*, 23 (1-2), 43-61.
- Dasgupta, P.** (2003) Sediment gravity flow - the conceptual problems. *Ear. Sci. Rev.*, 62, 265-281.
- De Stefani, T.** (1949) Correzioni da apportare al foglio di Palermo della carta dell'Ufficio Geologico e relative considerazioni stratigrafico-tettoniche. Estratto da "Plinia", 2, fasc. 1.
- Di Stefano, G.** (1888) Studi stratigrafici e paleontologici sul Sistema Cretaceo della Sicilia; I calcari con Polyconites di Termini Imerese. *Atti del Real. Accad. di Sc. Lett. e Bell. Art. di Palermo*, X, 66 pp.
- Di Stefano, G.** (1889) Gli stati con *Caprotina*. *Atti del Real. Accad. di Sc. Lett. e bell. Art. di Palermo*, X, 66 pp.
- Di Stefano, G.** (1908) I calcari cretacei con Orbitoidi dei dintorni di Termini Imerese e di Bagheria. *Giorn. Sc. Nat. ed Ec. di Palermo*, XXVI, 11 pp.
- Di Stefano, P., Ruberti, D.** (2000) Cenomanian rudist-dominated shelf- margin limestones from the Panormide Carbonate Platform (Sicily, Italy): facies analysis and sequence stratigraphy. *Facies*, 42, 133-160.
- Droxler, A.W., Schlager, W.** (1985) Glacial vs interglacial sedimentation rates and turbidity frequency in the Bahamas. *Geology* 13, 799-802.
- Eberli, G.P., Ginsburg, R.N.** (1989) Cenozoic progradation of northwestern Great Bahama Bank, a record of lateral platform growth and sea level fluctuations. In: *Controls on Carbonate Platform to Basin Development* (Eds. P. Crevello, J.L., Wilson, J.F. Sarg, J.F. Read) *SEPM Spec. Publ.*, 44, 339-352.
- Eberli, G.P., Bernoulli, D., Sanders, D., Vecsei, A.** (1993) From aggradation to progradation: the Maiella Platform, Abruzzi, Italy. In: *Cretaceous Carbonate Platforms* (Eds T. Simo, R.W. Scott and J.P. Masse), *AAPG Mem.*, 56, 213-232.
- Enos, P.** (1977) Tamahra limestone of the Poza Rica trend, Cretaceous, Mexico. In: *Deep-Water Carbonate Environments* (Eds H.E. Cook, E Enos) *Soc. Econ. Paleontol. Mineral. Spec. Publ.* 25, 273-314.
- Enos, P.** (1985) Cretaceous debris reservoirs, Poza Rica field, Veracruz, Mexico. In: *Carbonate Petroleum Reservoirs* (Eds P.O. Roehl, P.W. Choquette, New York, Springer-Verlag) 455-469.
- Enos, P., Moore, C.H.** (1983) Fore-reef slope. In: *Carbonate Depositional Environments* (Eds. P.A. Scholle, D.G. Bebout, C.H. Moore) *Mem. Am. Ass. Pet. Geol.* 33, 507-537.
- Enos, P., Stephens, B.P.** (1993) Mid-Cretaceous basin margin carbonates, east-central Mexico. *Sedimentology*, 40, 539-556.
- Everts, A.-J.W.** (1991) Interpreting compositional variations of calciturbidites in relation to platform stratigraphy: an example from the Paleogene of SE Spain. *Sed. Geol.* 71, 231-242.
- Finetti, I.** (2005) CROP Project: Deep Seismic Exploration of the Central Mediterranean and Italy. In: *Atlases in Geoscience 1* (Eds Finetti, I., Elsevier, Amsterdam), 779.

- Fisher, M.A., Normark, W.R., Greene, H.G., Lee, H.J., Sliter, R.W.** (2005) Geology and tsunamigenic potential of submarine landslides in Santa Barbara Channel, Southern California, *Mar. Geol.*, 224, 1-22.
- Floquet, M., Hennuy, J.** (2003) Evolutionary gravity flow in the middle Turonian - early Coniacian Southern Provence basin (SE France): origins and depositional processes. In: *Submarine Mass Movements and their Consequences* (Eds: J. Lcat and J. Minert), Kluwer Academic Publishers, pp. 417 - 424.
- Floquet, M., Gari, J., Hennuy, J., Léonide, P., Philip, J.** (2005) Sédimentations gravitaires carbonatées et silicoclastiques dans un bassin en transtension, séries d'âge Cénomanién à Coniacien moyen du Bassin Sud-Provençal. 10ème Congrès Français de Sédimentologie 52. Publ ASF, Paris, Giens, 80 pp.
- Gamberi, F., Rovere, M., Marani, M.** (2011) Mass-transport complex evolution in a tectonically active margin (Gioia Basin, southeastern Tyrrhenian Sea). *Mar. Geol.*, 279, 98-110.
- Garilli, V., Klein, N., Buffetaut, E., Sander, P.M., Pollina, F., Galletti, L., Cillari, A., Guzzetta, D.** (2009) First dinosaur bone from Sicily identified by histology and its paleobiogeographical implications. *N. Jb. Geol. Paläont. Abh.*, 25 (2), 207-216.
- Gattacceca, J., Speranza, F.** (2002) Paleomagnetism of Jurassic to Miocene sediments from the Apenninic carbonate platform (southern Apennines, Italy): evidence for a 60° counterclockwise Miocene rotation. *Earth Planet. Sci. Lett.*, 201, 19-34.
- Gattacceca, J., Speranza, F.** (2007) Paleomagnetism constraints for the tectonic evolution of the southern Apennines belt (Italy). *Boll. Soc. Geol. It. Spec.* 7, 39-46.
- Gemmellaro, C.** (1860) Sopra varie conchiglie fossili del Cretaceo Superiore e nummulitico di Pachino. *Att. Ac. Gioenia Sc. Nat.*, 2(15), 269-284.
- Gemmellaro, G.G.** (1865) Sulle Caprinellidi dell'Ippuritico dei dintorni di Palermo. *Att. Ac. Gioenia*, 2(20), 187-238.
- Gemmellaro, G.G.** (1868-1876) Studi paleontologici sulla fauna del calcare a *Terebratula janitor* del Nord di Sicilia. *P.I.*, 8(56), Palermo.
- Genesseeux, M., Mauffret, A., Pautot, G.** (1980) Les glissements sous-marins de la pente continentale niçoise et la rupture de câbles en mer Ligure (Méditerranée occidentale): *Comptes Rendus de l'Académie des Sciences de Paris*, 290(D), 959-962.
- Ginsburg, R.N., Harris, P.M., Eberli, G.P., and Swart, P.K.** (1991) The growth potential of a bypass margin, Great Bahama Bank. *J. Sed. Petrol.*, 61(6), 976-987.
- Giunta, G. and Liguori, V.** (1972) Geologia della estremità Nord-Occidentale della Sicilia. *Riv. Min. Sicil.*, 136-138, 165-226.
- Giunta, G. and Liguori, V.** (1973) Evoluzione paleotettonica della Sicilia nord-occidentale. *Boll. Soc. Geol. Ital.*, 92, 903-924.
- Gorsline, D.S.** (1978) Anatomy of margin basins. *J. Sed. Petrol.*, 48, 1055-1068.
- Grasso, M., Lentini, F.** (1982) Sedimentary and tectonic evolution of eastern Hyblean Plateau (southeastern Sicily) during the Late Cretaceous to Quaternary time. *Palaeogeogr. Palaeoclimat. Palaeocol.*, 39, 261-280.

- Grasso, M., Lentini, F., Vezzani, L.** (1978) Lineamenti stratigrafico-strutturali delle Madonie (Sicilia centro-settentrionale). *Geol. Rom.*, XVII, 45-69.
- Grasso, M., Lentini, F., Nairn, A.E.M., Vigliotti, L.** (1983) A geologic and paleomagnetic study of the Hyblean volcanic rocks, Sicily. *Tectonophysics*, 98, 271-295.
- Graziano, R.** (2000) The Aptian-Albian of the Apulia Carbonate Platform (Gargano Promontory, Southern Italy): evidence of palaeoceanographic and tectonic controls on the stratigraphic architecture of the platform margin. *Cretaceous Res.*, 21, 106-127.
- Haak, A.B., Schlager, W.** (1989) Compositional variations in calciturbidites due to sea-level fluctuations, late Quaternary, Bahamas. *Geol. Rund.*, 78 (2), 477-486.
- Hairabian, A., Borgomano, J., Masse, J.P., Nardon, S.** (2015) 3-D stratigraphic architecture, sedimentary processes and controlling factors of Cretaceous deep-water resedimented carbonates (Gargano Peninsula, SE Italy). *Sed. Geol.*, 317, 116-136.
- Hampton, M.A.** (1972) The role of subaqueous debris flows in generating turbidity currents. *J. Sed. Petrol.* 42, 775-793.
- Haq, B.U., Hardenbol, J., Vail, P.R.** (1987) Chronology of fluctuating sea-levels since the Triassic. *Science* 35, 1156-1167.
- Haq, B.U., Hardenbol, J., Vail, P.R.** (1988) Mesozoic and Cenozoic chronostratigraphy and eustatic cycles. In: *Sea-Level Changes: An Integrated Approach*. (Eds C.K. Wilgus, B.S. Hastings, C.G.St.C. Kendall, H.W. Posamentier, C.A. Ross, J.C. Van Wagoner), Soc. Econ. Paleontol. Mineral., Spec. Publ. 42, 71-108.
- Hennuy, J.** (2003) Sedimentation carbonatée et silicoclastique sous contrôle tectonique, le bassin sud-provençal et sa plate-forme carbonatée du Turonien moyen au Coniacien moyen. Evolution séquentielle, diagenétique, paléogéographique. Unpubl. PhD Thesis, Univ. Provence, Marseille. 252 pp.
- Hine, A.C., Neumann, A.C.** (1977) Shallow carbonate- bank-margin growth and structure, Little Bahama Bank, Bahamas. *AAPG Bull.*, 61, 376-406.
- Hine, A.C., Wilber, R.J., Neumann, A.C.** (1981) Carbonate sand bodies along contrasting shallow bank margins facing open seaways: Northern Bahamas. *AAPG Bull.*, 65, 261-290.
- Ineson, J.R., Surlyk, F.** (1995) Carbonate slope aprons in the Cambrian of North Greenland: geometry, stratal patterns and facies, In: *Atlas of Deep-Water Environments; Architectural Style in Turbidite Systems*: London, Chapman and Hall (Eds. K.T. Pickering, R.N. Hiscott, N.H. Kenyon, F. Ricci Lucchi, R.D. Smith) 56–62.
- Jagiello, K., Beckett, D., Fretwell, N. and Bencini, R.** (1996) Fracture analysis and reservoir development: Tempa Rossa Core Report. Southern Apennines Joint Venture (Amoco, British Gas, Lasmò) Internal Report.
- Jo, A., Eberli, G.P., Grasmueck, M.** (2015) Margin collapse and slope failure along southwestern Great Bahama Bank. *Sed. Geol.*, 317, 43-52.
- Kenter, J.A.M.** (1990) Carbonate platform flanks, slope angle and sediment fabric. *Sedimentology*, 37(5), 777-794.
- Kenter, J.A.M., Schlager, W.** (1989) A comparison of shear strength in calcareous and siliciclastic marine sediments. *Mar. Geol.*, 88, 145-152.

- Kenter, J.A.M., Harris, P.M., Della Porta, G.** (2005) Steep microbial boundstone-dominated platform margins: examples and implications: *Sed. Geol.*, 178, 5-30.
- Kopf, A., Kasten, S., Bles, J.** (2011) Geochemical evidence for groundwater-charging of slope sediments: the Nice airport 1979 landslide and tsunami revisited. In: *Submarine mass movements and their consequences* (Eds D. Mosher, R.C. Shipp, L. Moscardelli, J.D. Chaytor, C.D.P. Baxter, H.J. Lee, R. Urgeles, Springer, Dordrecht).
- Kuenen, P.H., Migliorini, C.I.** (1950) Turbidity currents as a cause of graded bedding. *J. Geol.*, 58, 91-127.
- Lamarche, G., Mountjoy, J., Bull, S., Hubble, T., Krastel, S., Lane, E., Micallef, A., Moscardelli, L., Mueller, C., Pecher, I., Woelz, S.** (2016) Submarine mass movements and their consequences. 7th International Symposium. *Advances in Natural and Technological Research*, 41, 621 pp.
- Le Goff, J., Cerepi, A., Swennen, R., Loisy, C., Caron, M., Muska, K., El Desouky, H.** (2015) Contribution to the understanding of the Ionian Basin sedimentary evolution along the eastern edge of Apulia during the Late Cretaceous in Albania. *Sed. Geol.*, 317, 87-101.
- Le Goff, J., Reijmer, J.J.G., Cerepi, A., Loisy, C., Swennen, R., Heba, G., Cavailhes, T., De Graaf, S.** (2019) The dismantling of the Apulian carbonate platform during the late Campanian-early Maastrichtian in Albania. *Cretaceous Res.*, 96, 83-106.
- Locat, J.** (2001) Instabilities along ocean margins: a geomorphological and geotechnical perspective. *Mar. Petrol. Geol.*, 18(4), 503-512.
- Locat, J., Lee, H.J.** (2002) Submarine landslides: advances and challenges. *Canad. Geotech. J.*, 39, 193-212.
- Lowe, D.R.** (1982) Sediment gravity flows: II. Depositional models with special reference to the deposits of high density turbidity currents. *J. Sed. Petrol.*, 52, 279-297.
- Loucks, R.G., Kerans, C., Janson X., Marhx Rajano, M. A.** (2010) Lithofacies analysis and stratigraphic architecture of a deep-water carbonate debris apron: Lower Cretaceous (latest Aptian to latest Albian) Tamabra Formation, Poza Rica Field Area, Mexico. In: *Mass-Transport Deposits in Deepwater Settings, SEPM Spec. Publ.* 95, 1-23.
- Marr, J.G., Harff, P.A., Shanmugam, G., Parker, G.** (2001) Experiments on subaqueous sandy gravity flows: the role of clay and water content in flow dynamics and depositional structures. *Geol. Soc. Am. Bull.*, 113, 1377-1386.
- McLean, D.J., Mountjoy, E.W.** (1993) Upper Devonian buildup- margin and slope development in the southern Canadian Rocky Mountains: *Geol. Soc. Am. Bull.*, 105, 1263- 1283.
- Meckel, T.** (2010) Classifying and characterizing sand-prone submarine mass-transport deposits. In: *AAPG Annual Convention and Exhibition, New Orleans, LA, April 11-14, 2010.*
- Meckel III, L.D.** (2011) Reservoir characteristics and classification of sand-prone submarine mass- transport deposits, *SEPM Special Publication* 96, 432-452.
- Mezga, A., Cvetko Tešović, B., Bajraktarević, Z.** (2007) First record of dinosaurs in the late Jurassic of the Adriatic–Dinaric Carbonate Platform (Croatia). *Palaios* 22 (2), 188-199.
- Middleton, G.V., Hampton, M.A.** (1973) Sediment gravity flows: mechanics of flow and deposition. In: *Turbidites and Deep-Water Sedimentation.* (Eds G.V. Middleton, A.H. Bouma) *Soc. Econ. Paleontol. Mineral., Pac. Sect., Short Course*, 1-38.

- Minisini, D., Trincardi, F., Asioli, A., Canu, M., and Fogliani, F.** (2007) Morphologic variability of exposed mass-transport deposits on the eastern slope of Gela Basin (Sicily channel). *Bas. Res.*, 19, 217-240.
- Montanari, L.** (1964) Geologia dei Monti di Trabia. *Riv. Min. Sic.* 17, 97-99.
- Montanari, L.** (1966) Geologia del Monte Pellegrino (Palermo). *Riv. Min. Sic.* 15/88-90, 1-64, 20 tab.
- Morsilli, M., Bosellini, A., Rusciadelli, G.** (2004) The Apulia carbonate platform margin and slope, Late Jurassic to Eocene of the Maiella and Gargano Promontory: physical stratigraphy and architecture. In: 32nd International Geological Congress - Field Trip Guidebook (Eds APAT), Roma, 1-44.
- Mosher, D.C., Shipp, R.C., Moscardelli, L., Chaytor, J.D., Baxter, C.D.P., Lee, H.J., Urgeles, R.** (2010) Submarine mass movements and their consequences – 4th International Symposium. In: *Advances in natural and technological hazards research*. Springer, Dordrecht.
- Mosher, D., Laberg, J.S., Murphy, A.** (2016) The role of submarine landslides in the Law of the Sea. In: *Submarine mass movements and their consequences* (Eds G. Lamarche, J. Mountjoy, Springer, Dordrecht), 15-26.
- Mountjoy, E.W., Cook, H.E., Pray, L.C., McDaniel, P.M.** (1972) Allochthonous carbonate debris flows – worldwide indicators of reef complexes, banks, or shelf margins. *International Geol. Congress, 24th, Proc., Sect. 6*, 172-189.
- Mountjoy, E.W., Becker, S.** (2000) Frasnian to Famennian sea-level changes and the Sassenach Formation, Jasper Basin, Alberta Rocky Mountains. In: *Genetic Stratigraphy on the Exploration and Production Scales: Case Studies from the Pennsylvanian of the Paradox Basin and the Upper Devonian of Alberta* (Eds. P.W. Homewood, G.P. Eberli), Bull. des Centres de Recherches Elf Exploration Production, Mem. 24: Pau, Elf Expl. and Prod. Ed.s, 181-201.
- Mulder, T., Cochonat, P.** (1996) Classification of offshore mass movements. *J. Sed. Res.*, 66(1), 43-57.
- Mulder, T., Alexander, J.** (2001) The physical character of sedimentary density currents and their deposits. *Sedimentology* 48, 269-299.
- Mulder, T., Joumes, M., Hanquiez, V., Gillet, H., Reijmer, J.J.G., Tournadour, E., Chabaud, L., Principaud, M., Schnyder, J.S.D., Borgomano, J., Fauquembergue, K., Ducassou, E., Busson, J.** (2017) Carbonate slope morphology revealing sediment transfer from bank-to-slope (Little Bahama Bank, Bahamas). *Mar. Petrol. Geol.* 83, 26-34.
- Mullins, H.T.** (1983) Comments and reply on “eustatic control of turbidites and winnowed turbidites”. *Geology* 11, 57-58.
- Mullins, H.T., Heath, K.C., Van Buren, H.M., Newton, C.R.** (1984) Anatomy of modern open-ocean carbonate slope: Northern Little Bahama Bank. *Sedimentology*, 31, 141-168.
- Mullins, H.T., Cook, H.E.**, (1986) Carbonate apron models: alternatives to the submarine fan model for paleoenvironmental analysis and hydrocarbon exploration. *Sedimentary Geology*, 48, 37-79.
- Mutti, E.** (1992) Turbidite Sandstones. Agip Societa' per Azioni, Istituto di Geologia, Universita' di Parma, San Donato Milanese (Milan), Italy, 27 pp.
- Mutti, E., Ricci Lucchi, F.** (1972) Le torbiditi dell'Appennino settentrionale: introduzione all'analisi di facies. *Soc. Geol. Ital. Mem.*, 11, 161-199.

- Nardin, T.R., Hein, F.J., Gorsline, D.S., Edwards, B.D.** (1979) A review of mass movement processes, sediments and acoustic characteristics, and contrast in slope and base-of-slope systems versus canyon-fan-basin floor systems. In: *Geology of Continental Slopes*. (Eds L.J. Doyle, O.H. Pilkey), Spec. Publ. - Soc. Econ. Paleontol. Mineral., 27, 61-73.
- Nelson, C.H.** (1983) Modern submarine fans and debris aprons: an update of the first half century. In: *Revolution in the Earth Sciences: advances in the past half-century* (Ed. J.S. Boardman, Kendall/Hunte, Dubuque, Iowa), 148-166.
- Neri, C.** (1993) Stratigraphy and sedimentology of the Monte Acuto Formation (Upper Cretaceous-Lower Paleocene, Gargano Promontory, Southern Italy). *Ann. Univ. Ferrara, Sezione Scienze della Terra*, 4, 13-44.
- Neri, C., Luciani, V.** (1994) The Monte S. Angelo Sequence (Late Cretaceous-Paleocene, Gargano Promontory, Southern Italy): physical stratigraphy and biostratigraphy. *Giorn. Geol.*, 56, 149-165.
- Nigro, F., Renda, P.** (1999) Evoluzione geologica ed assetto strutturale della Sicilia centro-settentrionale. *Boll. Soc. Geol. It.*, 118 (2), 375-388.
- Ogniben, L.** (1960) Note illustrative dello schema geologico della Sicilia Nord-Orientale. *Riv. Min. Sic.*, 64-65, 183-212, 2 tav. di sez. geol. 1:200.000. Palermo.
- Nicosia, U., Petti, F.M., Perugini, G., D'Orazi, Porchetti S., Sacchi, E., Conti, M.A., Mariotti, N., Zarattini, A.** (2007) Dinosaur tracks as paleogeographic constraints: new scenarios for the Cretaceous geography of the Periadriatic region. *Ichnos* 14, 69-90.
- Pepe, F., Bertotti, G., Cloething, S.** (2004) Tectono-stratigraphic modelling of the North Sicily continental margin (southern Tyrrhenian Sea). *Tectonophysics* 384, 257-273.
- Pereda-Superbiola, X.** (2009) Biogeographical affinities of Late Cretaceous continental tetrapods of Europe: a review. *Bull. Soc. Géol. Fr.* 180, 57-71.
- Patacca, E., Scandone P., Giunta G., Liguori, V.** (1979) Mesozoic paleo- tectonic evolution of the Ragusa zone (Southeastern Sicily). *Geol. Rom.*, 18, 331-369.
- Payros, A., Pujalte, V.** (2008) Calciclastic submarine fans: an integrated overview. *Earth Sci. Rev.* 86, 203–246.
- Petti, F.M.** (2006) Orme dinosauriane nelle piattaforme carbonati che mesozoiche italiane: sistematica e paleo biogeografia. Ph.D. Thesis. Università degli Studi di Modena e Reggio Emilia, 219 pp.
- Platania, G.** (1909) Il maremoto dello Stretto di Messina del 28 dicembre 1908. *Bollettino della Società Sismologica Italiana*, n. 13.
- Playton, T.E., Janson, X., Kerans, C.** (2010) Carbonate slopes. In: *Facies Models 4* (Eds N.P. James and R.W. Dalrymple). *GEOtext 6: Geological Association of Canada*, St John's, Newfoundland. 449-476.
- Posamentier, H.W., Kolla, V.** (2003) Seismic geomorphology and stratigraphy of depositional elements in deep-water settings. *J. Sed. Res.* 73(3), 367-388.
- Posamentier, H.W., Vail, P.R.** (1988) Eustatic controls on clastic deposition II - Sequence and systems tract models. In: *Sea-Level Changes: An Integrated Approach*. (Eds C.K. Wilgus, B.S. Hastings, C.G.St.C. Kendal, H.W. Posamentier, C.A. Ross and J.C. Van Wagoner), *Soc. Econ. Paleontol. Mineral. Spec. Publ.* 42, 125-154.

- Postma, G.** (1986) Classification of sediment gravity flow deposits based on flow conditions during sedimentation. *Geology*, 14, 291-294.
- Principaud, M., Mulder, T., Gillet, H., Borgomano, J.** (2015) Large-scale carbonate sub- marine mass-wasting along the northwestern slope of the Great Bahama Bank (Bahamas): morphology, architecture, and mechanisms. *Sed. Geol.*, 317, 27-42.
- Stampfli, G.M., Mosar, J.** (1999) The making and becoming of Apulia: Mem. Sci. Geol. (Univ. Padova) spec. vol. 3rd workshop Alpine geology, 51(1), 141-154.
- Reijmer, J.J.G., Schlager, W., Bosscher, H., Beets, C.J., McNeill, D.F.** (1992) Pliocene/ Pleistocene platform facies transition recorded in calciturbidites (Exuma Sound, Bahamas). *Sed. Geol.* 78, 171-179.
- Reijmer, J.J.G., Swart, P.K., Bauch, T., Otto, R., Reuning, L., Roth, S., Zechel, S.** (2009) A re-evaluation of facies on Great Bahama Bank I: new facies maps of Western Great Bahama Bank. *Perspectives in Carbonate Geology: a Tribute to the Career of Robert Nathan Ginsburg*. Int. Assoc. Sedimentol. Spec. Publ., 98, 29-46.
- Reijmer, J.J.G., Palmieri, P., Groen, R.** (2012) Compositional variations in calciturbidites and calcidebrites in response to sea-level fluctuations (Exuma Sound, Bahamas). *Facies*, 58 (4), 493-507.
- Reijmer, J.J.G., Mulder, T., Borgomano, J.** (2015a) Carbonate slopes and gravity deposits. *Sed. Geol.*, 317, 1-8.
- Reijmer, J.J.G., Palmieri, P., Groen, R., Floquet, M.** (2015b) Calciturbidites and calcidebrites: sea-level variations or tectonic processes? *Sed. Geol.*, 317, 53-70.
- Rusciadelli, G.** (2005) The Maiella escarpment (Apulia platform, Italy): geology and modeling of an Upper Cretaceous scalloped erosional platform margin. *Boll. Soc. Geol. Ital.*, 124, 661–673.
- Rusciadelli, G., Sciarra, N., Mangifesta, M.** (2003) 2D modelling of large-scale platform margin collapses along an ancient carbonate platform edge (Maiella Mt., Central Apennines, Italy): geological model and conceptual framework. *Palaeogeogr., Palaeoclimatol., Palaeoecol.*, 200, 189-203.
- Rustichelli, A., Iannace, A., Tondi, E., Di Celma, C., Cilona, A., Giorgioni, M., Parente, M., Girundo, M., Invernizzi, C.** (2017) Fault-controlled dolomite bodies as palaeotectonic indicators and geofluid reservoirs: new insights from Gargano Promontory outcrops. *Sedimentology*, 64, 1871-1900.
- Ryan, W.B.F., Heezen B.F.** (1965) Ionian Sea submarine canyons and the 1908 Messina turbidity current. *Geol. Soc. Am. Bull.*, 76.
- Sarkar, S., Marfurt, K.J., Hodgson, B.F., Slatt, R.M.** (2008) Attribute Expression of Mass Transport Deposits in an Intraslope Basin - A Case Study. SEG Las Vegas Annual Meeting, 958-962.
- Schlager, W.** (1991) Depositional bias and environmental change - important factors in sequence stratigraphy. *Sedimentology* 70, 109-130.
- Schlager, W.** (1992) Stratigraphic responses of a carbonate platform to relative sea-level change: Broken Ridge, S.E. Indian Ocean: Discussion. *Am. Assoc. Pet. Geol. Bull.* 76, 1034- 1037.
- Schlager, W., Ginsburg, R.N.** (1981) Bahama carbonate platform - the deep and the past. *Mar. Geol.*, 44, 1-24.
- Schlager, W., Camber, O.** (1986) Submarine slope angles, drowning unconformities and self erosion of limestone escarpments. *Geology* 14, 762-765.

- Schlager, W., Chermak, A.** (1979) Sediment facies of platform- basin transition, Tongue of the Ocean, Bahamas. In: *Geology of Continental Slopes* (Eds L.J. Doyle, O.H. Pilkey) Soc. Econ. Paleontol. Mineral. Spec. Publ. 27, 193-208.
- Schlager, W., Ginsburg, R.N.** (1981) Bahama carbonate platforms - the deep and the past: *Marine Geology*, 44, 1-24.
- Schlager, W., Reijmer, J.J.G., Droxler, A.** (1994) Highstand shedding of carbonate platforms. *J. Sed. Res.; Section B - Stratigraphy and Global Studies* 64 (3), 270-281.
- Schmidt di Friedberg, P., Barbieri, F. Giannini, G.** (1960): La Geologia del gruppo montuoso delle Madonie (Sicilia centro- settentrionale). *Boll. Soc. Geol. It.*, 81(1), 73-140.
- Spence, G.H., Tucker, M.E.** (1997) Genesis of limestone megabreccias and their significance in carbonate sequence stratigraphic models: a review. *Sed. Geol.* 112(3-4), 163-193.
- Stampfli, G.M., Mosar, J.** (1999) The making and becoming of Apulia: *Mem. Sci. Geol. (Univ. Padova) spec. vol. 3rd workshop Alpine geology*, 51(1), pp. 141–154.
- Surlyk, F., Ineson, J.R.** (1987) Aspects of Franklinian shelf, slope and trough evolution and stratigraphy in North Greenland: *Grønlands Geologiske Undersøgelse*, 133, 41-58.
- Surlyk, F., Ineson, J.R.** (1992) Carbonate gravity flow deposition along a platform margin scarp (Silurian, North Greenland): *J. Sed. Petrol.*, 62, p. 400–410.
- Talling, P.J., Wynn, R.B., Masson, D.G., Frenz, M., Cronin, B.T., Schiebel, R., Akhmetzhanov, A.M., Dallmeier-Ties- sen, S., Benetti, S., Weaver, P.P.E., Georgiopoulou, A., Zuhlsdorff, C., Amy, L.A.** (2007) Onset of submarine debris flow deposition far from original giant landslide. *Nature*, 450, 541-544.
- Talling, P.J., Masson, D.G., Sumner, E.J., Malgesini, G.** (2012) Subaqueous sediment density flows: depositional processes and deposit types. *Sedimentology* 59: 1937–2003.
- Tappin, D.R., Watts, P., McMurtry, G.M.** (2001) The Sissano, Papua New Guinea tsunami of July 1998: offshore evidence on the source mechanism. *Mar. Geol.* 175, 1-23.
- Tournadour, E., Mulder, T., Borgomano, J., Hanquiez, V., Ducassou, E., Gillet, H.** (2015) Origin and architecture of a Mass Transport Complex on the northwest slope of Little Bahama Bank (Bahamas): relations between off-bank transport, bottom current sedimentation and submarine landslides. *Sed. Geol.*, 317, 9-26.
- Turco, E., Schettino, A., Nicosia, U., Santantonio, M., Di Stefano, P., Iannace, A., Cannata, D., Conti, M.A., Deiana, G., D'Orazi Porchetti, S., Felici, F., Liotta, D., Mariotti, M., Milia, A., Petti, F.M., Pierantoni, P.P., Sacchi, E., Sbrescia, V., Tommasetti, K., Valentini, M., Zamparelli, V., Zarcone, G.** (2007) Mesozoic Paleogeography of the Central Mediterranean Region. *Geitalia*, VI Forum Italiano di Scienze della Terra. Epitome 2, 108.
- Vail, P.R., Audemard, F., Bowman, S.A., Eisner, P.N., Perez-Cruz, G.** (1991) The stratigraphic signatures of tectonics, eustasy and sedimentology. In: *Cycles and Events in Sedimentology*. (Eds G. Einsele, W. Ricken, A. Seilacher, Springer-Verlag, Berlin), 617-659.
- Walker, R.G.** (1966) Shale Grit and Grindslow shales: transition from turbidite to shallow-water sediments in the Upper Carboniferous of northern England. *J. Sed. Petrol.*, 36, 90-114.

- Weber, L.J., Francis, B.P., Harris, P.M., Clark, M.** (2003) Stratigraphy, lithofacies, and reservoir distribution, Tengiz Field, Kazakhstan. In: *Permo-Carboniferous Carbonate Platforms and Reefs* (Eds. W.M. Ahr, P.M. Harris, W.A. Morgan, I.D. Somerville) SEPM, Spec. Publ. 78, 351-394.
- Weirich, F.H.** (1988) Field evidence for hydraulic jumps in subaqueous sediment gravity flows. *Nature*, 332, 626-629.
- Whalen, M.T., Eberli, G.P., Van Buchem, F.S.P., Mountjoy, E.W., Homewood, P.W.** (2000) Bypass margins, basin-restricted wedges, and platform-to-basin correlation, Upper Devonian, Canadian Rocky Mountains: Implications for sequence stratigraphy of carbonate platform systems: *J. Sed. Res.*, 70, 913-936.
- Wilson, C.K., Long, D., Bulat, J.** (2004) The morphology, setting and processes of the Afen Slide. *Mar. Geol.*, 213, 149-167.
- Wunsch, M., Betzler, C., Lindhorst, S., Lüdmann, T., Eberli, G.P.** (2016) Sedimentary dynamics along carbonate slopes (Bahamas archipelago). *Sedimentology*, 64, 631-657.
- Zarcone, G.** (2008) Analisi delle discontinuità stratigrafiche mesozoiche della Piattaforma Carbonatica Panormide: vincoli per l'assetto paleogeografico dell'area Centro Mediterranea. PhD Thesis, Università di Palermo, pp.122.
- Zarcone, G., Di Stefano, P.** (2008) Mesozoic discontinuities in the Panormide Carbonate Platform: constraints on the palaeogeography of the central Mediterranean: *Rend. online SGI*, 2, pp. 191-194. www.socgeol.it.
- Zarcone, G., Di Stefano, P.** (2010) La Piattaforma Carbonatica Panormide: un caso anomalo nell'evoluzione dei bacini della Tetide giurassica. *Boll. Soc. Geol. It.*, 129, 188-194.
- Zarcone, G., Petti, F.M., Cillari, A., Di Stefano, P., Guzzetta, D., Nicosia, U.** (2010) A possible bridge between Adria and Africa: new palaeobiogeographic and stratigraphic constraints on the Mesozoic palaeogeography of the Central Mediterranean area. *Earth-Sci. Rev.*, 103(3-4), 154-162.